Mechanical behaviour of structures subjected to travelling fire

Author: Arian Loli

Supervisor: Ing. Kamila Horová

University: Czech Technical University in Prague

University: Czech Technical University in Prague
Date: 19.12.2014

CZECH TECHNICAL UNIVERSITY IN PRAGUE
Faculty of Civil Engineering
Thákurova 7, 166 29 Prague 6, Czech Republic

MASTER'S THESIS PROPOSAL

study programme: Civil Engineering
study branch: SUSCOS
academic year: 2014/2015

Student's name and surname: Arian Loli
Department: Department of steel and timber structures
Thesis supervisor: Ing. Kamila Horová
Thesis title: Mechanical behaviour of structures subjected to travelling fire
Thesis title in English: Mechanical behaviour of structures subjected to travelling fire

Framework content: State of the art of design fire models including models of travelling fire; overview of structural fire design methodology including heat transfer and modelling of structural behaviour; application of a travelling fire model to structures of different geometrical and material arrangements; analysis of structural behaviour; parametrical study; verification and validation; final recommendation for modelling of structures exposed to horizontal travelling fire.

Assignment date: 1/10/2014 Submission date: 19/12/2014

If the student fails to submit the Master's thesis on time, they are obliged to justify this fact in advance in writing, if this request (submitted through the Student Registrar) is granted by the Dean, the Dean will assign the student a substitute date for holding the final graduation examination (2 attempts for FGE remain). If this fact is not appropriately excused or if the request is not granted by the Dean, the Dean will assign the student a date for retaking the final graduation examination, FGE can be retaken only once. (Study and Examination Code, Art 22, Par 3, 4.)

The student takes notice of the obligation of working out the Master's thesis on their own, without any outside help, except for consultation. The list of references, other sources and names of consultants must be included in the Master's thesis.

.....
Master's thesis supervisor

.....
Head of department

Date of Master's thesis proposal take over: 1/10/2014

.....
Student

This form must be completed in 3 copies – 1x department, 1x student, 1x Student Registrar (sent by department)

No later than by the end of the 2nd week of instruction in the semester, the department shall send one copy of BT Proposal to the Student Registrar and enter data into the faculty information system KOS. (Dean's Instruction for Implementation of Study Programmes and FGE at FCE CTU Art. 5, Par. 7)

DECLARATION OF HONOUR

I hereby declare that I worked out the presented thesis independently and I quoted all used sources of information in accord with Methodical instructions about ethical principles for writing academic thesis.

I grant permission to Czech Technical University in Prague to reproduce and distribute copies of this thesis document in whole or in part.

Prague, December 19th, 2014 _____

(signature of the student)

ACKNOWLEDGMENT

I would like to express my deepest gratitude to my supervisor Ing. Kamila Horová for her full support, expert guidance, understanding and encouragement throughout my work. This master thesis would not be completed without her help, overview of my work as progresses, as well as approval to go on the next stage when the previous one was successfully done. I would like to thank her for thorough and careful reading of the thesis and all the suggestions which were more than welcome.

Special acknowledgements are addressed to Board of Directors of SUSCOS_M Erasmus Mundus Master Programme and to all lecturers that I had during this excellent experience. In addition I am very grateful to European Commission for giving me the scholarship which made it easier for me to focus on my studies.

I would like to thank all my friends of this master programme for their contribution throughout my study. I was very blessed to share wonderful moments with these incredible people.

Finally, I would like to thank my family for their love and encouragement over the years. Your continuous support has given me the strength to do it all.

ABSTRACT

Observations of accidental fires and real-scale experiments have shown that large and even middle size compartments do not burn simultaneously but flames tend to travel, burning a specific area at a certain time. During these observations, difference of temperature up to 400°C has been measured inside the compartment while traditional methods of design use the approach of homogenous temperature in the entire compartment at the same time. Therefore studies regarding travelling fire express high interest as they tend to give results closer to the real situations.

To study the effect of the spreading flames on the structural behaviour of a building, a simple 3D structure has been conceived and modelled in the software Vulcan. Traditional methods described in design codes and several travelling fire scenarios with different direction of the flames have been applied to the structure. All models of travelling fire have their root on shifted parametrical fire curves which are based on the rate of heat release, the so-called iBMB fire curves. Mechanical behaviour of the structure has been evaluated in the terms of deflection and axial force obtained in the beams. Results of the analysis have been showed for each thermal load case and also comparisons have been done among the fire scenarios.

Comparison of the results has provided important conclusions. Travelling fire models gives the most severe cases for fire resistance requested for long period of time. On the contrary, traditional methods provide worse results for short requested period of fire resistance. All travelling fire scenarios should be taken into account to determine the most severe fire conditions.

KEYWORDS

Structural fire design, heterogeneous temperature, design fire models, travelling fire, structural behaviour

TABLE OF CONTENTS

LIST OF FIGURES

LIST OF TABLES

1. INTRODUCTION

1.1. Overview

Architectural demands are increasing rapidly as a result of significant developments in the technology of construction and computers. Complex challenges are getting out of the bonds of traditional structural engineering methods and have been subject of many researches and innovative studies. These researches and studies have also influenced the fire engineering field where in most of the cases, traditional design methods cannot fulfil the new architectural criteria, for example in storey height, compartment size or ventilation conditions.

Investigations of real accidental fires in large compartments such as in Windsor Tower in Madrid and TU Delft in the Netherlands or full scale compartment tests executed in the United Kingdom and Czech Republic show that large and even middle open-plan compartment sizes do not burn uniformly throughout the entire area but the fire tends to travel across the area of the compartment as flames spread. Because of this characteristic, these fires have been named as *travelling fires*.

Figure 1.1. Photo of the fire test executed in Veselí nad Lužnicí, Czech Republic [1]

On the other hand, traditional fire models used in structural fire design like standard temperature-time curve (which is developed more than one century before) or parametric temperature-time curve (which is specified in Eurocode), do not take into account the effect of heterogeneous temperature throughout the compartment. Also more advanced zone models are based on the principle of constant burning temperature for each zone. The above mentioned methods are based on the assumption of uniform burning and homogenous temperature conditions; furthermore they have limitations regarding their applications for large or middle enclosures.

For all the above-mentioned reasons, the application of travelling fire expresses high interest of study as it has a significant impact on the mechanical response of the structure.

1.2. Objective of the thesis

Structural fire design has an important role in overall building design and construction. For this reason, it is necessary to apply the right thermal load to structural elements in order to have a better estimation of the mechanical behaviour of the structure. This master thesis gives a brief description of possible design fire models used in structural engineering and tends to emphasise that modern method of travelling fire is more advanced in comparison with traditional methods and aims to determine better the performance of a structure exposed to fire. More specifically, the objectives of this thesis are as follows:

- Understand the structural fire design procedure by describing different fire models and providing characteristics and limitations for each of them; from traditional models to advanced computational ones, with particular importance given to travelling fire models;
- Examine and compare the mechanical response of a structure by using different thermal inputs, including both uniform burning and travelling fires, in order to determine the appropriate fire model to be applied to the structures;
- Investigate the effect of travelling fire on the mechanical behaviour of a structure with different materials (steel and composite) and geometrical arrangements.

Following the scope of the present thesis, particular importance is given to travelling fire models; the advantages and the achieved results of these models are emphasised. The comparative studies are done with the help of Vulcan which is suitable software for thermal analysis.

1.3. Layout of the thesis

The structure of the thesis is composed from five chapters which include the theoretical background of fire design methods and their application in a single storey building. To attain the objectives of the thesis, both theoretical and applicative examples are mainly based on design procedures defined by Eurocode and innovative studies in the field of travelling fire.

Second chapter presents a literature review of fire science and fire structural design. It starts in the first paragraph with stages of a compartment fire during a burning process. In the second one, the heat transfer mechanism in structures is explained, with main focus to the heat transfer in steel and concrete structures. The third paragraph presents various traditional

fire models which are developed and published in design codes. This paragraph gives a brief description of different fire models, starting with nominal temperature-time curves, parametric fire curves and in the end, advanced fire models like zone models and Computational Fluid Dynamics (CDF) are described. Special attention is given to the fourth paragraph where the innovative method of travelling fire is described since it early origins and particular researches and conclusions regarding the influence of travelling fire in structural response of steel and concrete structures are presented.

Third chapter tends to underline the advantages of travelling fire method in comparison with uniform burning through an applicative example. At the beginning of the chapter, the mechanical and thermal properties of steel and concrete at elevated temperatures are given. Before presenting the structure that is subject of studies in this thesis, the software used for thermal analysis is described shortly. Afterwards, three analytical fire curves applied in the structure including the creation of travelling fire curve are presented. The first case of study shows the effect of different thermal inputs in the mechanical behaviour of the structure with steel beams while the second case studies the effect of fire models by applying in the structure with composite beams. Mechanical behaviour is studied in terms of axial forces and deflections of the elements which are displayed in diagrams.

Fourth chapter is a summary of the conclusions of this thesis by the work undertaken. Recommendations and possible future work are also highlighted here.

2. STATE OF ART

2.1. Modelling of fire

2.1.1. Compartment fires

Compartment fires are defined as fires in enclosed spaces which can occur in rooms, offices of buildings but also can include other spaces like transportation vehicles such as trains, planes, etc. [2] In general, the development of compartment fires can be divided in three main phases: growth period which is also known as pre-flashover, burning period which is also known as post-flashover (often referred to as 'fully developed fire') and the decay period (Fig. 2.1). [3] Additionally, all fires include an ignition phase but from different suppression activities, they may fail to grow before going through all the above phases. [2]

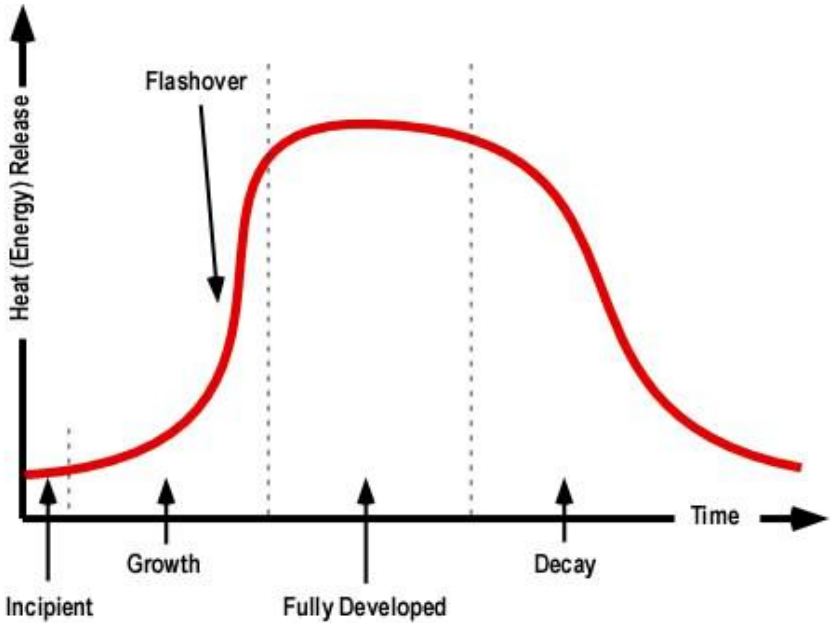

Figure 2.1. Phases of fire development in a compartment [4]

Pre-flashover fires imply mostly life safety while post-flashover fires imply the integrity of the structure. The temperature reached in the compartment during a post-flashover fire must be taken into account for fire structural design but also both the growth and decay phase should be considered. [2]

2.1.1.1. *Pre-flashover period*

Following ignition, the fire starts to grow from the fuel itself, without any significant influence from the conditions of the compartment. Many of the accidental fires stay on this phase since there may be neither enough fire load nor sufficient ventilation to lead the fire to other phases. In most of the cases it is human action that grows the load of the fire and causes flashover by increasing air supply from opening of a door or a window.

The general effect of this phase of fire in the compartment is small in comparison with other stages; therefore in most of the cases this phase is not taken into account in fire structural calculations. [3]

Flashover is defined as the transition from a growing fire to a fully developed fire as the fire consumes all the available fuel within the compartment. Flashover is not a precise term and several definitions can be found in the literature but in most of them it is connected with gas temperatures between 500 and 600°C. [2]

2.1.1.2. *Post-flashover period*

In post-flashover period, the heat release rate of the fire is the greatest; thereby the rate of the temperature rises throughout the compartment is high. Typically for this period, the air available in the compartment is not enough to burn all the materials being pyrolyzed. In this case, the fire is said to be *ventilation controlled*. In compartment fires, the temperature over 1000°C is possible to get reached. This rate of the temperature rise continues until the amount of fuel consumption in the compartment starts to decrease. [3]

During the post-flashover period structural elements are facing the worst effects of fire and structural integrity of the structure can highly be affected. As a result, this is the phase which should lead the structural fire design of the structure. After the rate of the temperature rise reaches a peak, the decay phase begins. [3]

2.1.1.3. *Decay period*

As it can be understandable from the name, in the decay period fuel becomes consumed and therefore the compartment temperature starts to decrease. It should be taken into account that due to ventilation, the fire may change to *fuel controlled* where the amount of air is sufficient for combustion. [3]

2.2. Heat transfer in structures

Heat can be transferred from one location to another through three different means: conduction, convection and radiation. In following subparagraphs it is given a brief introduction for each of the ways and also some explanations how heat transfer influences the temperature of steel and concrete structures subjected to fire.

2.2.1. Conduction

Conduction is the heat transferred within solids. It can also happen in liquids but this case is considered as part of convection. There are three important facts that come through conduction:

- Heat will flow from a hotter part to a colder one.
- Heat flow is proportional to the temperature gradient.
- Heat flow is proportional to the thermal conductivity of a material *k*.

There are two types of conduction: steady-state conduction where temperature does not change with time and transient conduction where temperature depends on the time. [5]

2.2.1.1. *Steady-state conduction*

The steady-state expression of an insulated bar (Figure 2.2a) with temperatures at the sides T_1 and T_2, which has reached thermal equilibrium, is given by the Fourier Law of Conduction:

$$\dot{h} = -\lambda \frac{dT}{dx} \tag{2.1}$$

where $\dot{h}$ is heat flux per unit area [W/m^2],

T is the temperature [K],

x is the distance along the bar length [m],

λ is the thermal conductivity of the material [W/(m·K)].

For a bar with cross-section area A, the total heat flow will be $A \cdot \dot{h}$. The negative sign shows the direction of the heat flow from the hotter side to the colder one. [5]

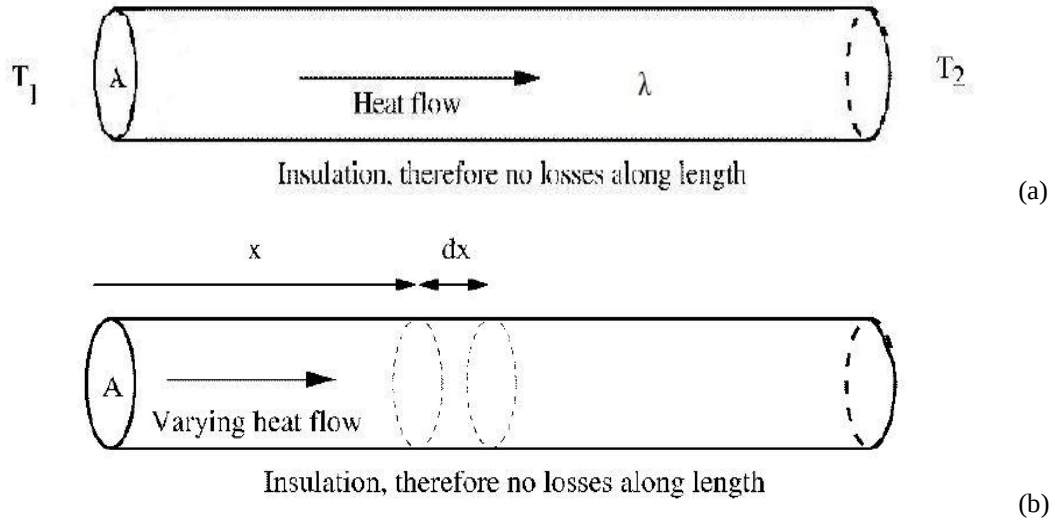

Figure 2.2. (a) Idealisation one-dimensional steady-state conduction, (b) Idealisation one-dimensional transient conduction [5]

2.2.1.2. *Transient conduction*

In fire engineering, transient conduction is the typical way of transferring conductive heat flow as the temperature increases quickly during a fire. To determine the expression it is considered the same one-dimensional bar as in the paragraph above but with temperature at its sides changing with time (Figure 2.2b). It is also considered no loss of energy along the length due to insulation. The energy needed to change the temperature is equal to the difference between the heat flow into the system and the heat flow out of it, till temperature at each point no longer changes. This principle is given by the following expression:

$$\underbrace{\rho c A\, dx\, \partial T}_{\text{Energy change}} = \underbrace{+\lambda A dt\left(\frac{\partial T}{\partial x}+\frac{\partial^2 T}{\partial x^2}dx\right)}_{\text{Energy flowing in}} - \underbrace{\lambda A dt \frac{\partial T}{\partial x}}_{\text{Energy flowing out}} \tag{2.2}$$

where c is the specific heat capacity of the material [J/(kg·K)].

When no change of temperature is detected, the above equation derives to a steady-state one. The solution of transient heat equations is difficult thus usually numerical solutions are used. [5]

2.2.2. Convection

Convection is the heat transferred from a fluid to a solid or vice versa. There are two types of convection: free (natural) and forced. Free convection occurs when a fluid adjacent to a solid changes its density as a result of the heat transfer and starts to flow, for example the plume of gases above a fire which have less density because of the heat and rise. Forced convection occurs when a fluid driven by external forces flows a solid, for example a fan cooling a computer chip.

The heat transferred by convection per unit area is given by the following Newton equation:

$$\dot{h}_c = \alpha_c \left(T_s - T_f\right) \tag{2.3}$$

where $\dot{h}_c$ is the rate of heat transferred per unit area [W/m^2],

T_s and T_f are the solid and fluid temperatures respectively [K],

α_c is the convective heat transfer coefficient [W/(m^2·K)].

The convective heat transfer coefficient α_c depends on many factors like conductivity, viscosity and density of the fluid, geometry of the surface from which convection is taking place, type of convection (free or forced), and nature of fluid (turbulent or laminar). In reality it is difficult to determine this coefficient but in some design codes suggestions are given for the values to be used in fire engineering. [5]

2.2.3. Radiation

Radiation is the heat released by a body solely on account of its temperature. The electromagnetic spectrum that transfers heat has a small range but visible and infra-red light are also included. Unlike the previous forms of heat transfer, thermal radiation can be concentrated in a small spot and this is the principle used to produce energy by solar plants.

Radiation released by a body is proportional to the fourth power of its temperature (in Kelvin). Hence, it is unimportant for heat transferred at low temperature (θ < 200°C) but is determinant at high temperature (θ > 400°C). The expression that calculates the heat released from a hot body to the ambient by radiation is:

$$\dot{h}_r = \varepsilon\sigma\left(T_2^4 - T_1^4\right) \tag{2.4}$$

where $\dot{h}_r$ is rate of heat transferred per unit area [W/m^2],

ε is the surface emissivity (compared to the radiation of heat from an ideal "black body" with the emissivity coefficient ε = 1)

σ is Stephan-Boltzmann constant [$\sigma = 5.67\times10^{-8}$ W/(m^2·K^4)],

T_1 and T_2 are respectively the ambient and hot body temperatures [K].

Radiation is important in fire engineering because the heat can be transferred through a flame, gas or hot surface to other objects. For example, when a fire occurs in one building, the heat can be transferred by radiation through an opening to ignite an adjacent building. [5]

2.2.4. Heat transfer to steel structures

Heat transfer in steel structures depends whether the steel is insulated or uninsulated. The transfer in uninsulated steel structures is easier to explain and it will be described first.

2.2.4.1. *Uninsulated steel structures*

As the majority of the steel sections are thin, usually the assumption of homogenous temperature within the cross-section is made. Due to this, a simple equation of energy balance can be used to determine the heat transfer.

In Figure 2.3 is shown a cross-section at temperature T_m, with cross-section area A_m, volume of the element V, which is surrounded by hot gases with temperature T_g. The heat flowed into the section at the time Δt, is calculated as the sum of radiative and conductive heat transfer:

$$A_m\left[\alpha_c\left(T_g - T_m\right) + \varepsilon\sigma\left(T_g^4 - T_m^4\right)\right]\Delta t \tag{2.5}$$

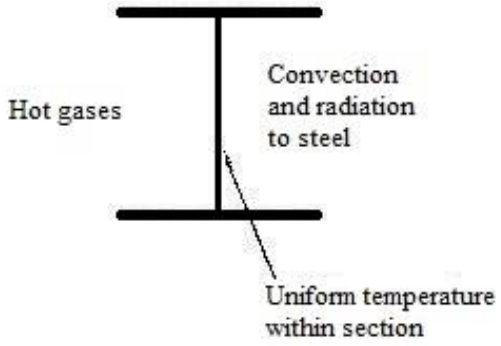

Figure 2.3. Heat transfer of an uninsulated steel element [5]

The heat that enters in the section will raise its temperature with $\Delta\theta_{a,t}$ and it requires an amount of energy equal to:

$$\rho_a c_a \Delta\theta_{a,t} V \tag{2.6}$$

where c_a is the specific heat capacity [J/(kg·K)] and ρ_a is the density of the steel [kg/m^3].

The energy expressions showed in equations 2.5 and 2.6 should be equal and after some transformations, the increase of the section's temperature will be:

$$\Delta\theta_{a,t} = \frac{A_m}{V}\frac{\Delta t}{\rho_a c_a}\left[h\left(T_g - T_m\right) + \varepsilon\sigma\left(T_g^4 - T_m^4\right)\right] \tag{2.7}$$

The ratio A_m/V is a typical value of steel sections known as the section factor and it can be calculated directly or taken from section tables. The perimeter to be considered depends on the contact of the section with fire or other elements. For example in a steel beam that holds a concrete slab as shown in the right side of Figure 2.4, the perimeter value should not take into account the side connected with concrete as no heat will be transferred through it.

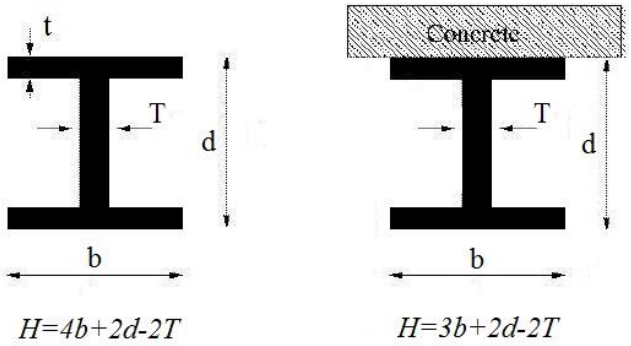

Figure 2.4. Values of perimeter for calculation of section factor [5]

The equation 2.7 can be used to calculate the temperature of uninsulated steel elements subjected to fire using gas temperatures taken from standard or parametric fire curves as input. [5]

2.2.4.2. *Insulated steel structures*

The way to calculate the steel temperature of an insulated steel member is the same as for uninsulated element by equating the energy stored in the steel in a small time Δt to the heat flowed from the hot gases to the steel. As the radiation component is not considered due to insulation, the equation of energy balance is:

$$\dot{h}_c A_m \Delta t = \rho_a c_a \Delta\theta_{a,t} V_m \tag{2.8}$$

The rate of heat transfer can be expressed in the terms of conduction considering the temperature of the insulation the same with the temperature of the steel:

$$\dot{h} = \frac{\lambda}{d}\left(T_g - T_m\right) \tag{2.9}$$

where λ is the thermal conductivity of a material [W/(m·K)],

d is the thickness of the insulation [m].

After replacing equation 2.9 to 2.8 we can determine the temperature rise of the section:

$$\Delta\theta_{a,t} = \left[\frac{A_m}{V}\frac{\lambda}{d\rho_a c_a}\left(T_g - T_m\right)\right]\Delta t \tag{2.10}$$

In a similar way to uninsulated elements, equation 2.10 can be used to calculate the temperature of protected steel elements during fire. [5]

2.2.5. Heat transfer to concrete structures

Heat transfer to concrete elements is more complex than to steel ones. Concrete sections are massive in comparison with steel and the temperature among the cross-section is not uniform. Also in normal state, concrete contains water in the pores that vaporises when the section is heated. For these reasons, it is difficult to determine the temperature of a heated concrete element using analytical formulas. The calculation of the section temperatures can be done using finite elements methods or using graphs which can be found in design codes to calculate the temperature of concrete elements exposed to fire in simple cases.

In reinforced concrete elements, the temperature of the steel bars is assumed to be the same as the temperature of the concrete surrounding them. [5]

2.3. Traditional models of fire

2.3.1. Standard fire curves

Design methods using standard fire curves are the first described methods that have been used to determine the fire resistance capacity of structural members. Check criteria for standard fire curves is based on the basic principle of exposing a single structural member or an assembly to a standard fire with specified load and intensity and determining if this element collapses or not to the peak temperature. [6]

The most common structural elements that can be designed with this method are columns, beams and floors. Usually, standard fire curves are not used for elements like connections or joints. [7]

Standard design fire curves can be found in various codes such as American Society for Testing and Materials (ASTM), Eurocode, etc. These curves are used for fully developed fires and the temperature is assumed homogenous within the compartment. A brief description of these curves in different codes is given below.

2.3.1.1. *ASTM E119*

The ASTM E119 fire curve [8] equation has been one of the first to be published and fire curves of other standards are derived from it. The fire curve represents a fully developed fire in a compartment and it is defined from the following equation:

$$T = 750\left(1 - e^{-3.79553\sqrt{t}} + 170.41\sqrt{t}\right) + T_0 \tag{2.11}$$

where:

T is the gas temperature in the fire compartment [°C],

T_0 is the initial compartment temperature (in normal conditions T_0 = 20°C),

t is the time [hours].

2.3.1.2. *ISO 834*

The ISO 834 curve [9] shows that temperature increases with time at a constant rate and it is defined by the following expression:

$$T = T_0 + 345\log_{10}(8t + 1) \tag{2.12}$$

where:

T is the gas temperature in the fire compartment at time t [°C],

T_0 is the initial compartment temperature [°C],

t is the time [minutes].

Figure 2.5 shows the comparison between ASTM E119 and ISO 834 fire curves.

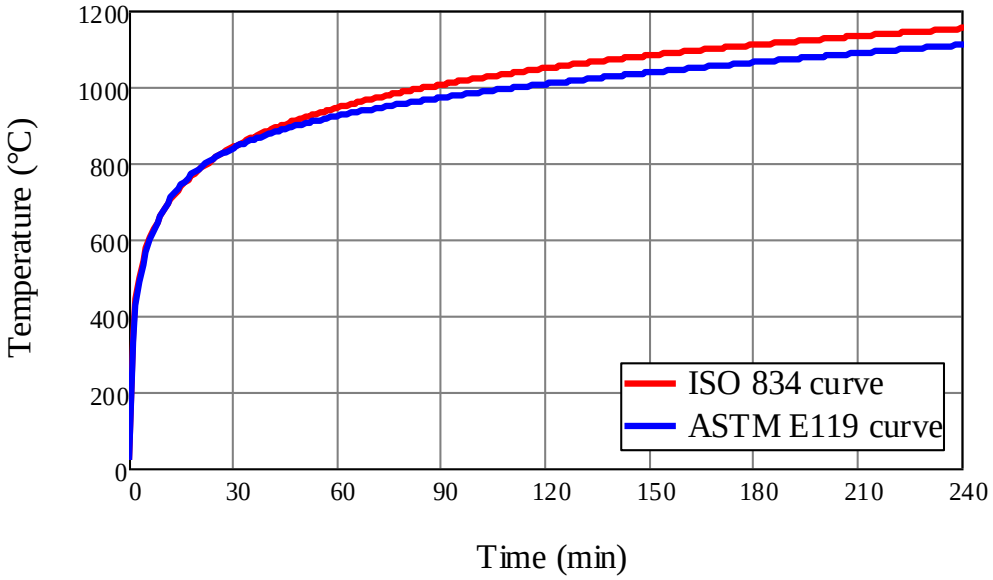

Figure 2.5. Comparison between ASTM E119 and ISO 834 fire curves

2.3.1.3. *Eurocode nominal fires*

Eurocode 1, Part 1-2 gives fire design procedure using both standard (nominal) and parametric fire curves. Nominal temperature-time curves are provided for three different fire curves: standard, external and hydrocarbon. [10] Standard temperature-time curve given in Eurocode is equal to ISO 834 fire curve described in the paragraph above.

- The standard temperature-time curve is given by equation below:

$$\Theta_g = 20 + 345\log_{10}(8t+1) \tag{2.13}$$

where:

Θ_g is the gas temperature in the compartment [°C],

t is the time [minutes].

- The external temperature-time curve is intended for the outside of external walls which are exposed to the fire coming from different directions from outside. The equation that gives the external fire curve is:

$$\Theta_g = 660\left(1 - 0.687e^{-0.32t} - 0.313e^{-3.8t}\right) + 20 \tag{2.14}$$

- For a hydrocarbon fire, the hydrocarbon temperature-time curve is given by:

$$\Theta_g = 1080\left(1 - 0.325e^{-0.167t} - 0.675e^{-2.5t}\right) + 20 \tag{2.15}$$

Three types of nominal temperature-time curves prescribed by Eurocode are shown in Figure 2.6.

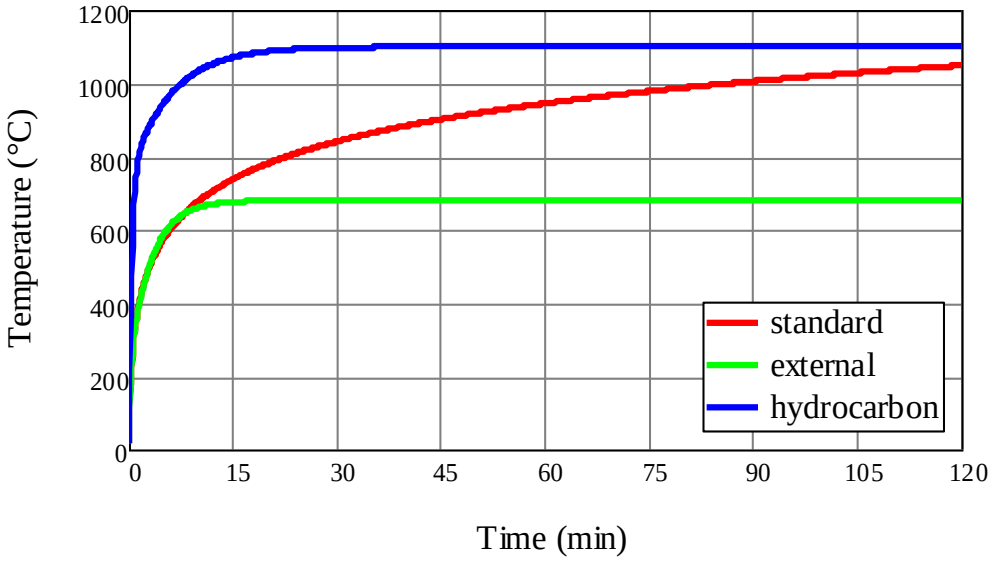

Figure 2.6. Comparison of Eurocode nominal fire curves

2.3.2. Parametric fire curves

Many codes and standards are now using parametric fire curves together with nominal fire curves. The advantage of a parametric fire curve is that it takes into account the compartment size, opening factor, fire load and the boundary properties; therefore it provides a more realistic estimation of the compartment conditions to be used in the structural fire design of structural members in comparison with the standard fire curve. [6]

The same as nominal fire curve, parametric fire curve is used for post-flashover compartment fires. Parametric analyses also assume that the temperature is uniform within the fire compartment; hence this assumption may lead in non-realistic results after comparison with real fire tests.

Parametric curves are developed empirically, based on the results obtained from fire tests. The procedure of design using parametric fire curves is published in many codes and standards. Below this procedure is shown for Eurocode parametric curve, iBMB parametric fire curve which is based on rate of heat release and BFD curves used in Australia.

2.3.2.1. *Eurocode parametric model*

The Eurocode parametric fire model (Annex A in EN 1991-1-2:2002) has been derived from Swedish curves which have been first published by Magnusson and Thelandersson (1970). As it can be seen from Figure 2.7, the curve is typically composed from an exponential part (heating phase) until the temperature in compartment reaches Θ_{max} and a linear part (cooling phase) till the temperature reaches a residual temperature. [7]

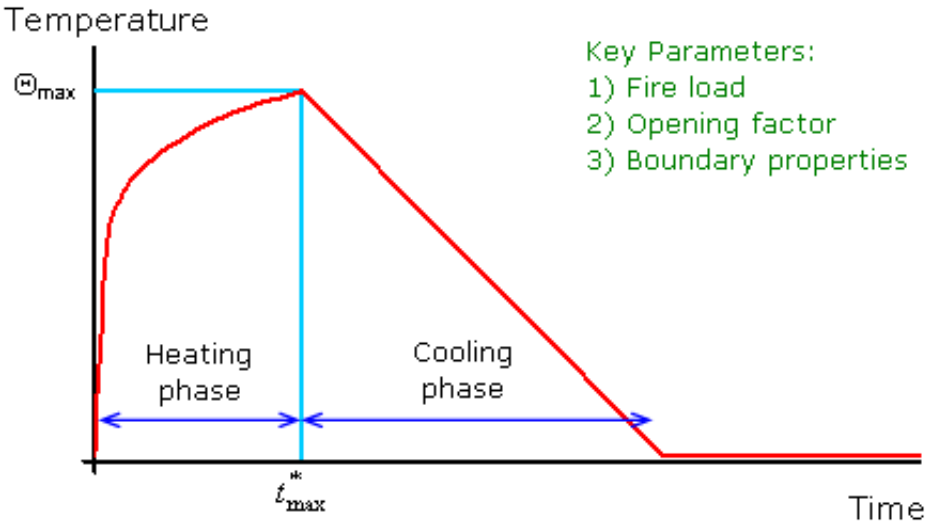

Figure 2.7. Typical graph of a parametric fire curve [11]

The conditions to be fulfilled in order to use this design method are specified in Annex A of EN 1991-1-2:2002 [10] as listed below:

- The following temperature-time curve description is valid for fire compartments up to 500 m^2 of floor area, without openings in the roof and for a maximum compartment height of 4 m. It is assumed that the fire load of the compartment is completely burnt out.
- If fire load densities are specified without specific consideration to the combustion behaviour, then this approach should be limited to fire compartments with mainly cellulosic type fire loads.

The temperature-time curve in the heating phase is given by the following equation:

$$\Theta_g = 20 + 1325\left(1 - 0.324e^{-0.2t^*} - 0.204e^{-1.7t^*} - 0.472e^{-19t^*}\right) \tag{2.16}$$

where:

Θ_g is the gas temperature in the compartment [°C] and

$$t^* = t \cdot \Gamma \ \text{[h]} \tag{2.17}$$

Γ is time factor function given by:

$$\Gamma = \left[O/b\right]^2 / \left(0.04/1160\right)^2 \tag{2.18}$$

The opening factor O has the limits $0.02 \le O \le 0.20$ and is calculated by:

$$O = A_v \sqrt{h_{eq}} \,/\, A_t \tag{2.19}$$

The thermal absorptivity b has the limits $100 \le b \le 2200$ and is calculated by:

$$b = \sqrt{(pc\lambda)} \tag{2.20}$$

All the parameters used to build the heating phase curve are defined in Annex A of Eurocode EN 1991-1-2:2002.

The temperature-time curve in the cooling phase is given by:

$$\Theta_g = \begin{cases} \Theta_{\max} - 625\left(t^* - t^*_{\max} \cdot x\right) & \text{for } t^*_{\max} \le 0.05 \\ \Theta_{\max} - 250\left(3 - t^*_{\max}\right)\left(t^* - t^*_{\max} \cdot x\right) & \text{for } 0.05 < t^*_{\max} < 2 \\ \Theta_{\max} - 250\left(t^* - t^*_{\max} \cdot x\right) & \text{for } t^*_{\max} \ge 2 \end{cases} \tag{2.21}$$

where:

$$t^*_{\max} = \left(0.2 \cdot 10^{-3} \cdot q_{t,d} \,/\, O\right) \cdot \Gamma \tag{2.22}$$

and

$$x = \begin{cases} 1.0 & \text{for } t_{\max} > t_{\lim} \\ t_{\lim} \cdot \Gamma \,/\, t^*_{\max} & \text{for } t_{\max} = t_{\lim} \end{cases} \tag{2.23}$$

The opening factor O is the most determinant factor in the parametric fire curve. This can be seen from the diagrams in Figures 2.8, 2.9 and 2.10 that show the effect of opening factor O, fire load q and thermal absorptivity b in temperature of the compartment.

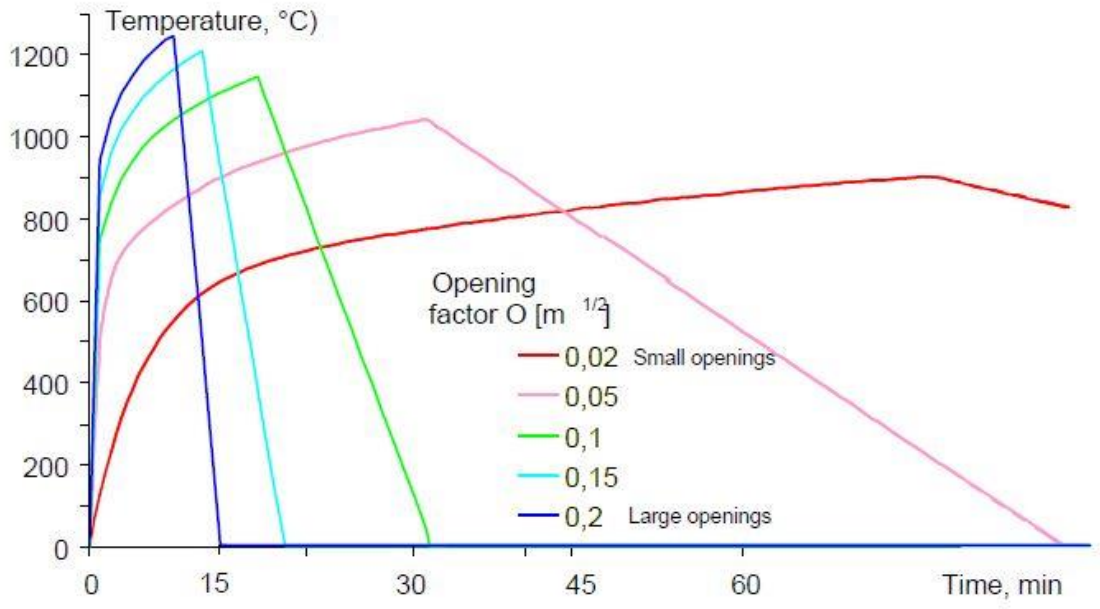

Figure 2.8. Impact of the opening factor *O* in the compartment temperature [12]

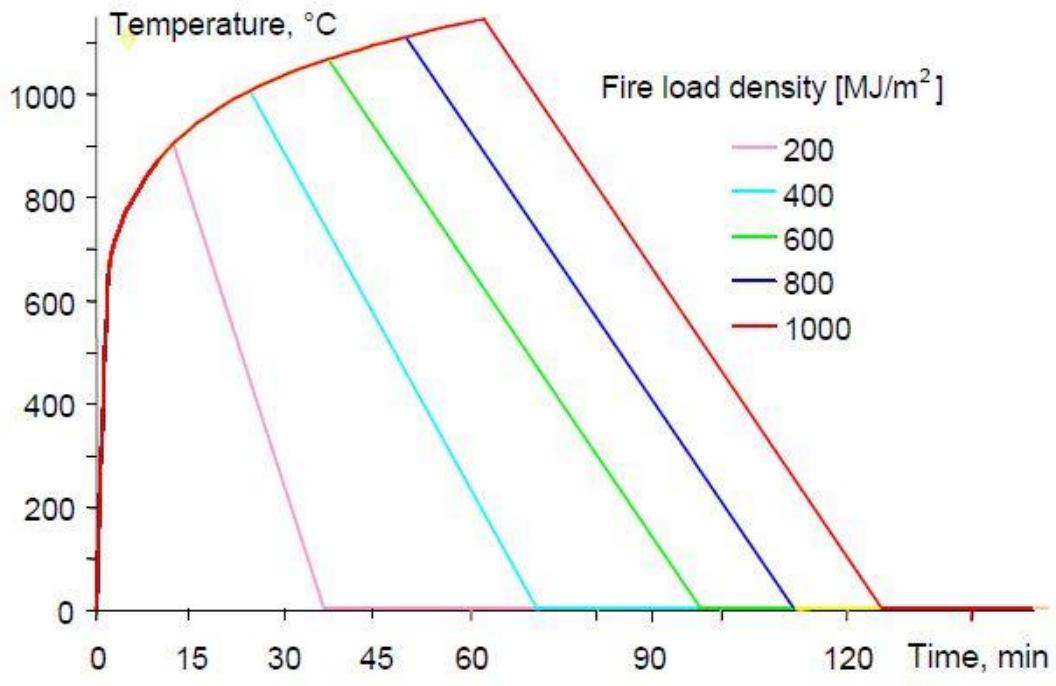

Figure 2.9. Impact of the fire load density *q* in the compartment temperature [12]

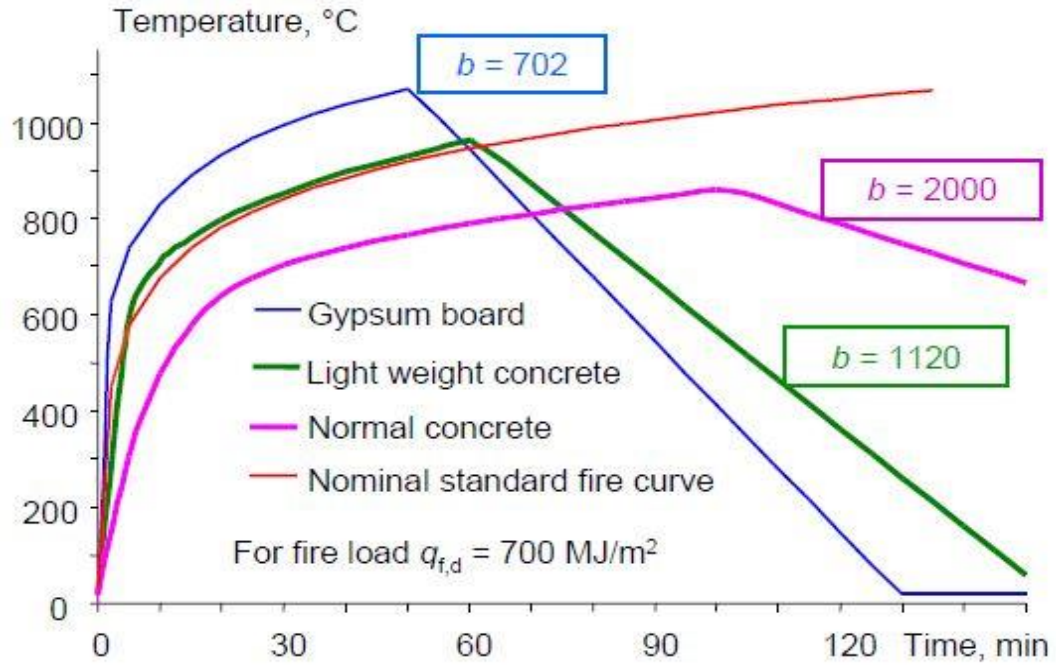

Figure 2.10. Impact of the thermal absorptivity *b* in the compartment temperature [12]

2.3.2.2. *iBMB parametric fire curve*

The so-called iBMB parametric fire curve has been presented by German researchers Zehfuss and Hosser [13] in 2003. Contrary to Eurocode parametric fire curve, this curve is directly derived from the rate of heat release that defines the design fire taking also into account boundary conditions of the fire compartment like fire load, ventilation conditions, geometry and thermal properties of the enclosure. The rate of heat release curve is obtained from Annex E of EN 1991-1-2:2002 [10] and by comparing this curve together with temperature-time curve of a natural fire, the researchers concluded that both curves are characterised by three distinctive points at the times t_1, t_2, t_3, where the slope of both curves is changing. Figure 2.11 shows the connection between rate of heat release and the temperature of a natural fire.

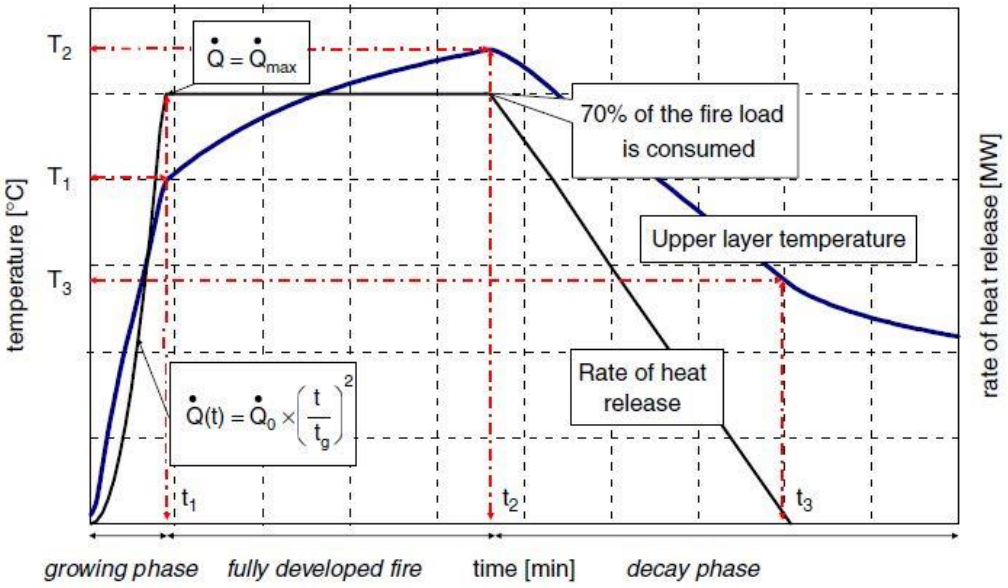

Figure 2.11. Relationship between rate of heat release and upper layer temperature [13]

As it can be seen from the start of the fire until time t_1, the heat release rate and the temperature increase rapidly. At time t_1 the rate of heat release reaches the maximum and it stays constant until t_2. From time t_1 to time t_2, the temperature increases moderately. As 70% of the fire load is consumed at t_2, the rate of heat release drops off linearly until time t_3 when the whole fire load is consumed and the rate of heat release goes to value 0. After reaching its peak value at t_2 also the temperature starts to decrease.

The values of t_1, t_2, t_3 can be determined from rate of heat release curve and afterwards, the expressions of calculating T_1, T_2 and T_3 were given in the study for two cases; when rate of heat release is determined by the ventilation conditions and by the fire load.

For *ventilation-controlled* fires, temperature development depends on the opening factor O and surface factor b. The expressions to calculate T_1, T_2 and T_3 for the reference fire load density of $q = 1300\ MJ/m^2$ are given below:

$$T_1 = -8.75 \cdot 1/O - 0.1 \cdot b + 1175^{\circ}C \tag{2.24}$$

$$T_2 = (0.004 \cdot b - 17) \cdot 1/O - 0.4 \cdot b + 2175^{\circ}C \leq 1175^{\circ}C \tag{2.25}$$

$$T_3 = -5.0 \cdot 1/O - 0.16 \cdot b + 1060^{\circ}C \tag{2.26}$$

with the opening factor: $O = A_w \sqrt{h_w} / A_t \quad [m^{1/2}]$ (2.27)

where:

A_w is the area of the ventilation opening [m^2],

h_w is the average height of the ventilation openings [m],

A_t is the enclosure surface without openings [m^2], and

b is the average thermal property of the enclosure linings [$J/m^2s^{1/2}K$].

For *fuel-controlled* fires, temperature development depends mainly on the heat released by the fire source and the expressions to calculate T_1, T_2 and T_3 for the reference fire load density of $q = 1300\ MJ/m^2$ are given below:

$$T_1 = \begin{cases} 24000 \cdot k + 20^{\circ}C & \text{for } k \leq 0.04 \\ 980^{\circ}C & \text{for } k > 0.04 \end{cases} \tag{2.28}$$

$$T_2 = \begin{cases} 33000 \cdot k + 20^{\circ}C & \text{for } k \leq 0.04 \\ 1340^{\circ}C & \text{for } k > 0.04 \end{cases} \tag{2.29}$$

$$T_3 = \begin{cases} 16000 \cdot k + 20^{\circ}C & \text{for } k \leq 0.04 \\ 660^{\circ}C & \text{for } k > 0.04 \end{cases} \tag{2.30}$$

with $$k = \left(\frac{\dot{Q}^2}{A_w \sqrt{h_w} A_t \ b} \right)^{1/3} \tag{2.31}$$

where:

$\dot{Q}$ is the maximum rate of heat release [MW].

After defining the three characteristic points of time and temperature, the next step is to determine the functional law of the curve that connects these points. As a result, the curve is composed by three parts and the function for each part is given in the expression below:

$$T = \begin{cases} \dfrac{T_1 - T_0}{t_1^2} t^2 + T_0 & \text{for } 0 \leq t \leq t_1 \\ (T_2 - T_1) \sqrt{(t - t_1)/(t_2 - t_1)} + T_1 & \text{for } t_1 < t \leq t_2 \\ (T_3 - T_2) \sqrt{(t - t_2)/(t_3 - t_2)} + T_2 & \text{for } t > t_2 \end{cases} \tag{2.32}$$

In the first section of the curve the temperature rises quadratically until reaching the value T_1. Afterwards, the second part of the slope increases moderately and the function is built following a square root law until it reaches T_2. The same principle is also used to describe the function of third part of the curve till T_3.

The iBMB parametric fire curve was built for fire load density of $q = 1300\ MJ/m^2$. With the same principles, the study shows how to build the curve for fire load density q_x smaller than the reference one. In this case the fire load Q is decreased to $Q_x = q_x \times A_f$ and value of $t_{2,x}$ is calculated instead of t_2.

$$t_{2,x} = t_1 + \frac{(0.7Q_x) - \dot{Q}_0\left(t_1^3/3t_g^2\right)}{\dot{Q}_{\max}} \tag{2.33}$$

The associated temperature $T_{2,x}$ is determined by replacing $t_{2,x}$ instead of t in equation.

$$T_{2,x} = (T_2 - T_1)\sqrt{(t_{2,x} - t_1)/(t_2 - t_1)} + T_1 \tag{2.34}$$

For different values of q_x, the temperature $T_{3,x}$ at time $t_{3,x}$ is in line with a logarithmic function through two points; ($t_0=0$; $T_0=20°C$) and (t_3; T_3):

$$T_{3,x} = \left(T_3/\log_{10}(t_3+1)\right)\log_{10}(t_{3,x}+1) \tag{2.35}$$

The functional law that describes the decreasing part of the iBMB curve is given by the expression below:

$$T = (T_{3,x} - T_{2,x})\sqrt{(t - t_{2,x})/(t_{3,x} - t_{2,x})} + T_{2,x} \tag{2.36}$$

Two iBMB parametric curves for reference fire load density $q=1300\ MJ/m^2$ and $q_x < q$ are shown in Figure 2.12.

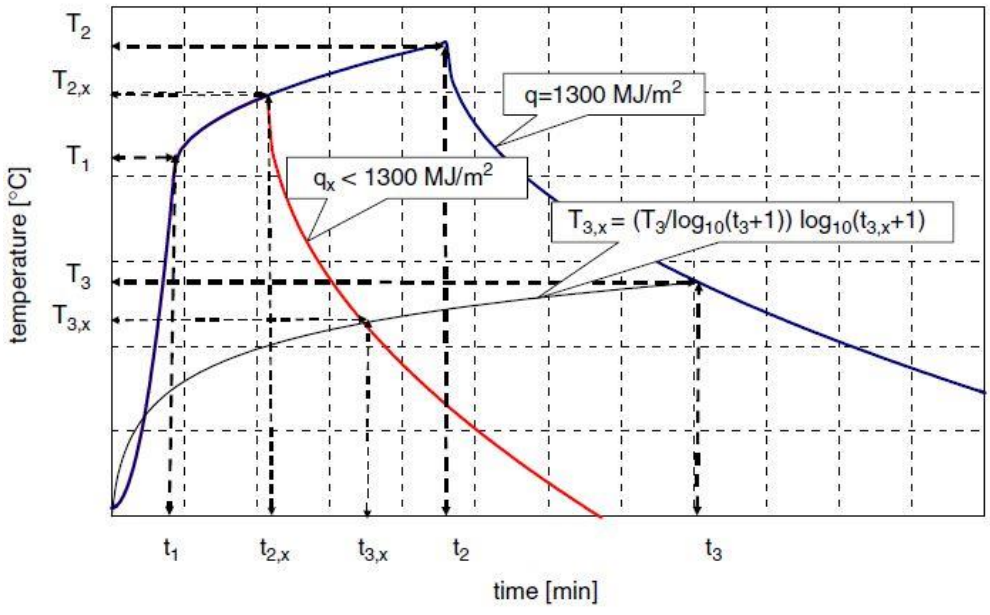

Figure 2.12. Description of iBMB parametric curves for different fire load densities [13]

2.3.2.3. *BFD curves*

As it can be seen from the paragraph 2.3.2.1, the creation of parametric fire curve according to Eurocode for both heating and cooling phases needs multiple formulas and variables to be determined. As a result, it is a complex and inefficient curve to be used in fire engineering design. To avoid this complexity, researchers have developed a new simplified curve named BFD curve, based on data achieved from more than 142 natural fire tests. [6]

The development of BFD curve is described in details by Barnett and Clifton [14] in their studies. In difference from European parametric, BFD curve is represented by two basic equations:

$$T_g = T_a + T_m \cdot e^{-z} \tag{2.37}$$

and

$$z = \left(\log_e t - \log_e t_m\right)^2 / S_c \tag{2.38}$$

where:

T_g is the gas temperature in the compartment at time t [°C],

T_a is the ambient temperature [°C],

T_m is the maximum gas temperature generated above T_a [°C],

t is the time from start of fire [minutes],

t_m is the time at which T_m occurs [minutes],

S_c is the shape constant for the temperature-time curve.

From the above equations it can be noticed that the input parameters to determine the curve are maximum gas temperature T_m, time in which maximum gas temperature occurs t_m and a shape constant of the curve S_c.

Figure 2.13 shows the effect of the time in which maximum gas temperature t_m occurs as a variable parameter.

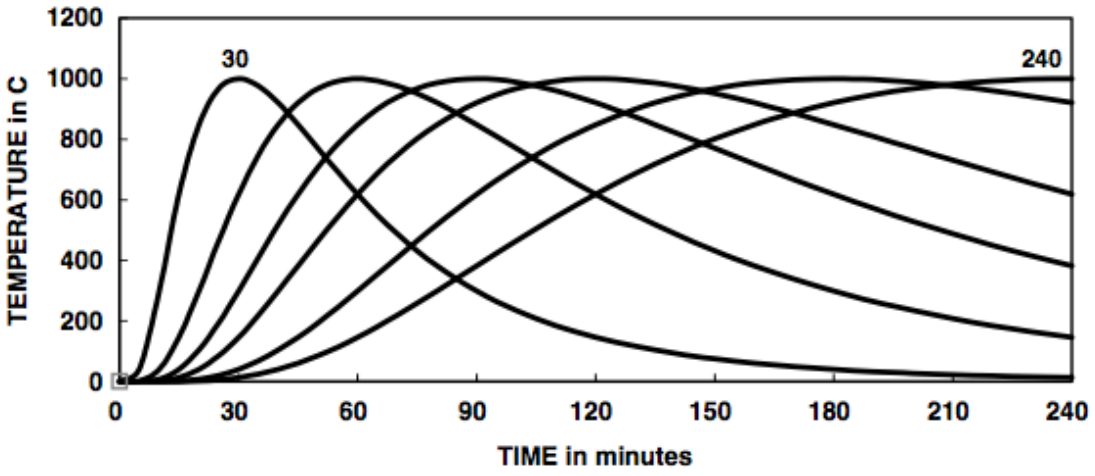

Figure 2.13. Impact of the time to maximum gas temperature t_m in the BFD curve [14]

In Figure 2.14 it is shown the impact of different maximum gas temperatures T_m while keeping the time to maximum temperature and shape factor constant. When the maximum gas temperature increases, the intensity of the fire curve is higher.

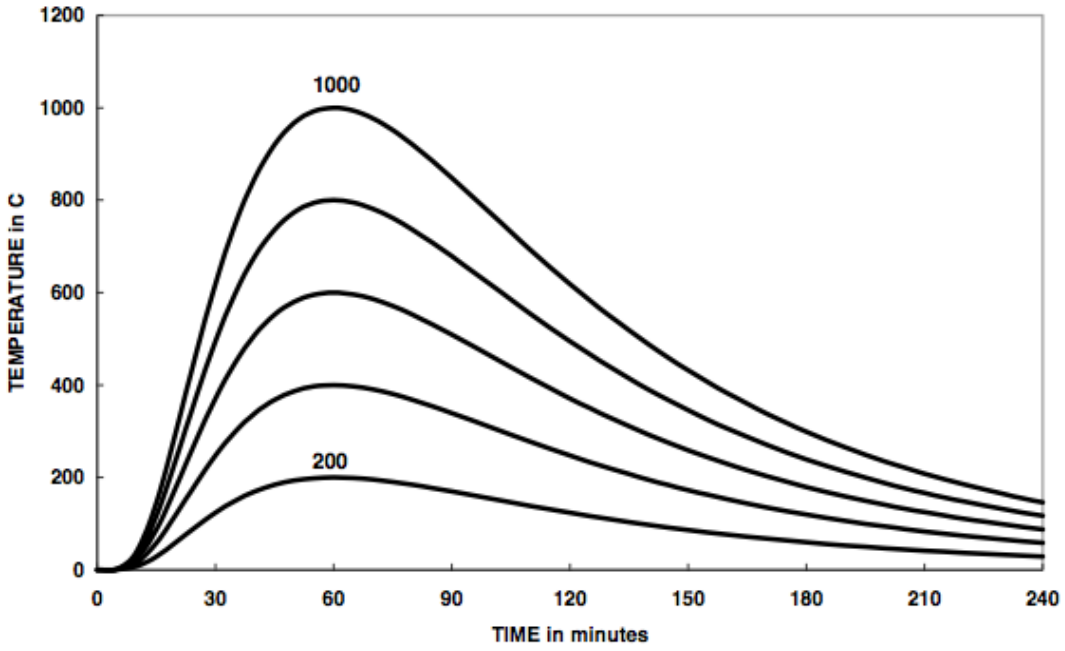

Figure 2.14. Impact of the maximum gas temperature T_m in the BFD curve [14]

In Figure 2.15 it is shown the effect of the shape constant of the curve S_c while maximum gas temperature and time to achieve it are considered constant.

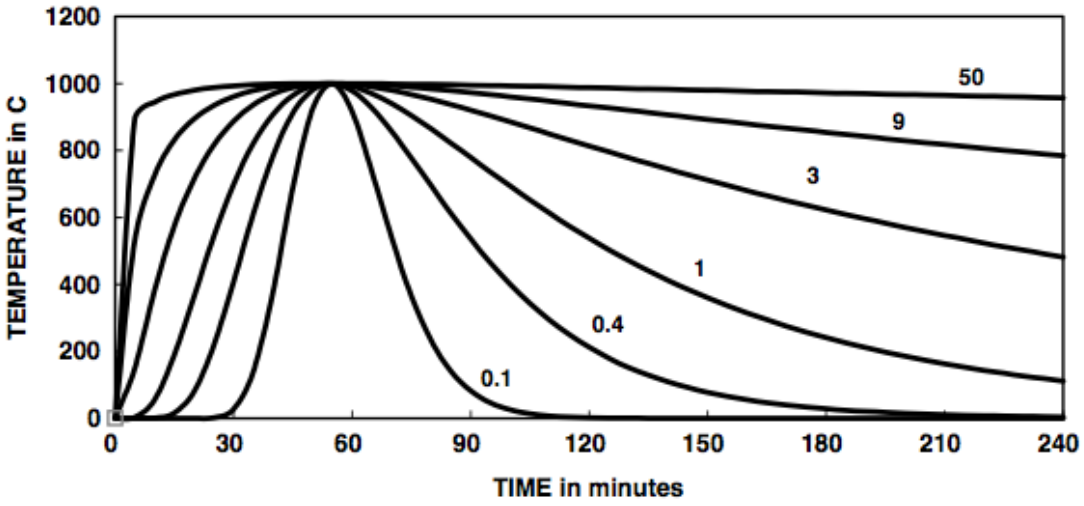

Figure 2.15. Impact of the shape constant of the curve S_c in the BFD curve [14]

2.3.3. Advanced design fire models

The design fire curves presented in the previous paragraphs are based on simple calculation approaches for determining fire response of structural members. These methods may not offer realistic response of structural members as they do not take into account some factors due to simplifications. With the rapid development in computer engineering, advanced models can be used to predict fire response of structures close to real situations. These advanced models are based on finite elements methods and in lieu of simple calculation models, they take into account such factors as material and geometrical nonlinearity, creep and transient strain, restraint effects, etc. [15]

Advanced design models can be used to trace fire response for single structural members, assembly of elements or the entire structure. These models can be applied for different fire curves as well as for any type of cross section. Because of their complexity, the application of advanced methods requires significant background knowledge and good software skills. [15]

There are two main categories of advanced fire models: zone models and Computational Fluid Dynamics (CFD) models also known as field models.

2.3.3.1. *Zone model*

The development of zone models has started since the early 60's to predict fire parameters in structures with several compartments (Janssens, 1992). As it can be noticed from the name, zone models divide rooms into one or more zones but the most commonly used model assumes the room is made up of two zones.

Two-zone model is applied for pre-flashover fires stage where there it is plenty of oxygen and the combustion is complete. According to this model, the room is split into two zones: an upper layer of heated gas and a lower layer of cooler air relatively free of heated gas. The connection between the upper and lower layers is made by the fire (Fig. 2.16).

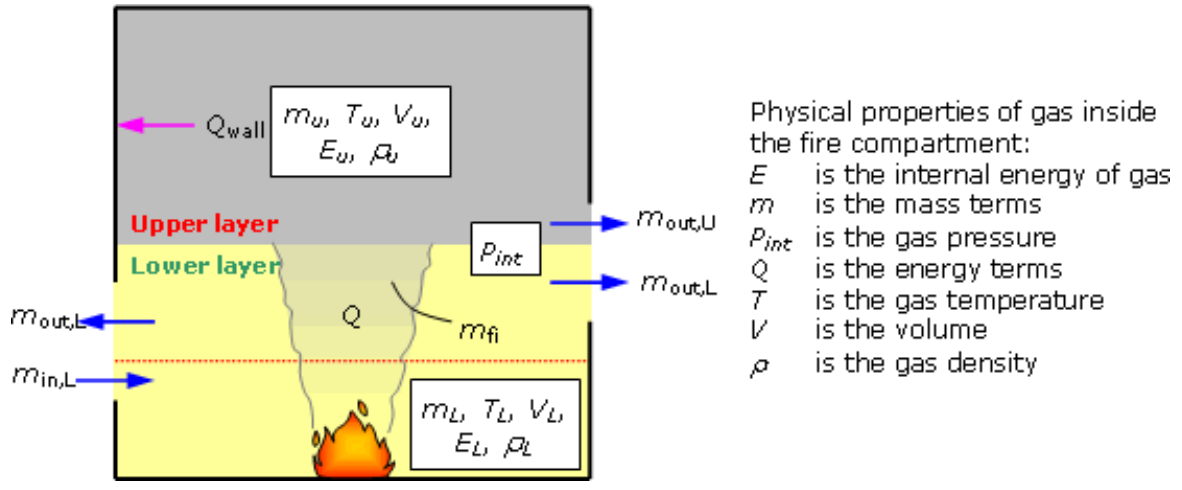

Figure 2.16. Schematic diagram for typical two-zone model using EN parameters [11]

The layers are assumed to be connected well and for each of them, physical parameters such as temperature and composition of gas are assumed to be constant. [16]

Some of the professional programs using two-zone models are:

- CCFM.VENTS from National Institute of Standards and Technology (NIST), US (Forney, Cooper & Moss 1990)
- CFAST from NIST (Peacock et al. 2000)
- OZone from the University of Liège, Belgium (Cadorin & Franssen 2003; Cadorin et al. 2003)

Oppositely from two-zone model, *one-zone model* should be applied for post-flashover fire conditions. As shown in Figure 2.17, in this model the room is taken as a single layer and gases inside the room are assumed to be well-mixed. The physical parameters of the layer are calculated by solving mass and energy equations for each layer. [17]

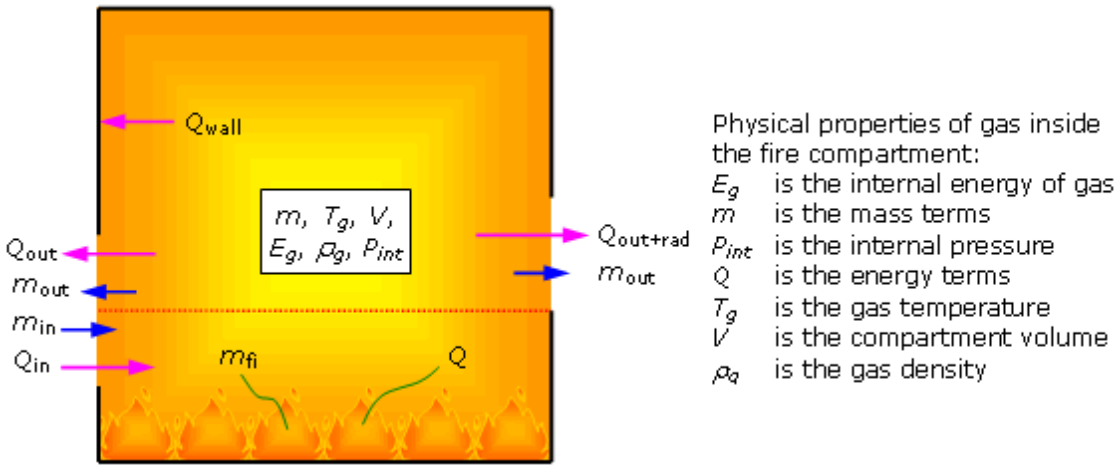

Figure 2.17. Schematic diagram for typical one-zone model using EN parameters [11]

Some of the professional programs using one-zone models are:

- COMPF2 from NIST, US (Babraukas 1979)
- OZone from the University of Liège, Belgium (Cadorin & Franssen 2003; Cadorin et al. 2003)
- SFIRE-4 from Lund University, Sweden (Magnusson & Thelandersson 1970)

In a fire compartment with uniformly distributed fire load, a pre-flashover fire may develop into a post-flashover fire under certain conditions. In Annex D of EN1991-1-2:2002 [10] the circumstances when a two-zone fire model may develop into a one-zone fire model are:

- if the gas temperature of the upper layer is higher than 500°C;
- if the upper layer is growing to cover 80% of the compartment height.

Beside fire parameters in the model, software input should also include compartment characteristics such as room dimensions and building materials, the sizes and locations of openings and room furnishing characteristics. [15]

Zone models are described in several codes and standards including North American codes or Eurocode. EN 1991-1-2:2002, Annex D shows the procedure of design, restrictions and recommendations for usage of one-zone and two-zone models.

2.3.3.2. *Computational Fluid Dynamics (CFD) model*

Huge developments in software engineering have led in the creation of advanced fire models very close to real situations. Computational Fluid Dynamics (CFD) models are among the most avant-garde and sophisticated fire methods that are used to predict fire behaviour and temperature of the compartment. These models have a large variety of usage and can be applied for modelling localised or pre-flashover fires in compartments with complex geometry or multi-compartments structures [18].

CDF models divide the whole or specific parts of the building into a three dimensional grid and material properties and furniture characteristics are also added to make the model closer to reality. Fire is modelled taking into account outer factors like possible door openings or window breakages to give output data similar to real case. In Figure 2.18 an example of a discretised compartment subjected to a CFD model is shown.

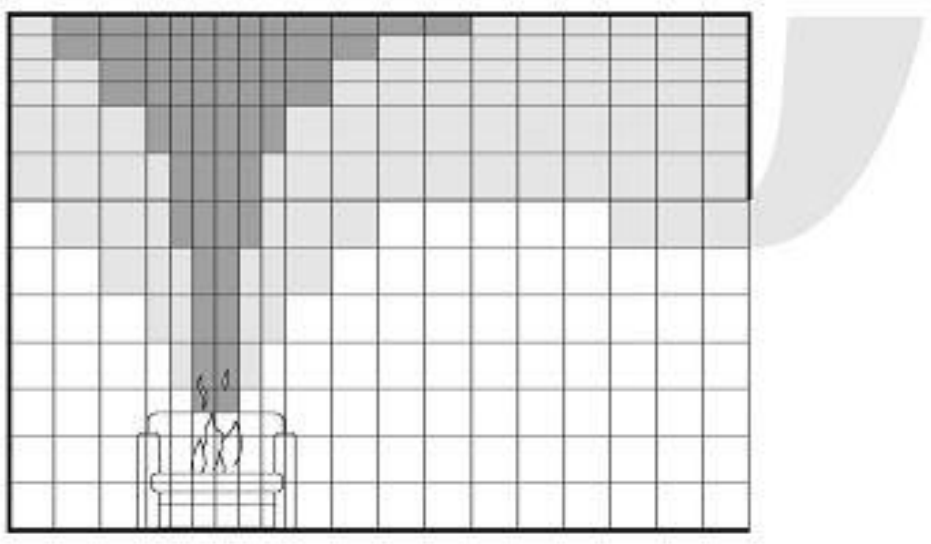

Figure 2.18. CFD model dividing the enclosure into sub-volumes [19]

Due to the detailed discretisation of the compartment in a CFD model, the partial differential equations of the thermodynamic and aerodynamic variables (Navier-Stokes equations) are solved for a very large number of points. Mainly CFD models are suitable for low-speed fires and thermally-driven flows with predominance of smoke and heat transport [18]. The usage of software based on CFD models is very demanding in defining the correct input fire parameters and also it requires high level of knowledge to interpret the calculated results after analysis. They need sufficient background knowledge in both chemistry and engineering field. For these reasons, CFD models are used mainly in research fields or in cases of very complicated structures. On the other hand, due to their complexity, the software output results are much various and given with details for all points of the compartments, such as temperature, velocity and chemical species concentration, three dimensional fluid flows, laminar and turbulent flow, heat release and transfer, phase change, etc. [20]

According to Annex D of EN1991-1-2:2002, typical CFD models analyse systems involving fluid flow, heat transfer and associated phenomena by solving the fundamental equations of the fluid flow. These equations represent the mathematical statements of the conservation laws of physics:

- the mass of a fluid is conserved;
- the rate of change of momentum equals the sum of the forces on a fluid particle – the Newton's second law;
- the rate of change of energy is equal to the sum of the rate of heat increase and the rate of work done on a fluid particle – the first law of thermodynamics.

Some of the professional programs using CDF models are:

- FDS from NIST, US (McGrattan et al. 2002)
- SMARTFIRE from the University of Greenwich, UK (SMARTFIRE 1998)
- SOFIE from Cranfield University, UK (Rubini 2000)

2.4. Travelling fire

Inspections of real accidental fires in large compartments or full scale compartment tests have shown that large and even middle open-plan compartment sizes do not burn uniformly throughout the entire area but the fire tends to move across the area of the compartment to consume fuel. These observations have directed to the concept of *travelling fire* which is a new dimension in the field of fire design engineering.

2.4.1. Advantages

Traditional methods mentioned in the previous paragraphs have their limitations of application regarding compartment dimensions, opening size or height of the floor. Due to the technological development, contemporaneous architecture is getting challenging and ambitious day by day. Complex compartment shapes or high storeys, usage of glass and new materials are becoming popular and traditional methods cannot be applied to these enclosures. These methods have been developed based on small scale tests and do not have validity for the new requests of complex structures. Integration of travelling fire methods with these modern structures has become necessary to calculate structural performance of them. [21]

Due to moving flames, mainly for post-flashover fires, experiments in large compartments have shown regions with big differences of temperature up to 400°C. These variance leads to limitations of many traditional methods since they are based on the assumption of homogenous temperature. Both standard temperature-time curve and parametric temperature-time curve use the same temperature distribution throughout the compartment. Also zone models described above, use homogenous temperature for each zone based on the laws of energy balance. Hence, it can be easily noticed that the methods using travelling fires are more comprehensive and innovative in comparison with traditional design methods that assume uniform conditions throughout a compartment for the entire duration of the fire. [21]

Another difference between these methods is that traditional ones assume that most severe cases are produced by ventilation controlled fires. However, tests conducted by Majdalani and Torero [22] show that ventilation controlled fires are not probable to occur in large compartments and therefore, they cannot be presumed to be the worst condition for fire design.

2.4.2. Travelling fire methods

To compensate the gap created by the limitations of traditional methods, new design methods applying travelling fires have been developed.

2.4.2.1. *Large Firecell Method (LFM)*

The first pioneering method named Large Firecell Method (LFM) was presented by Clifton (1996) as part of HERA programme in New Zealand. According to him, a firecell is one compartment of the building where the assumption of homogenous temperature cannot be applied, for example, an open plan office floor. Through this concept, he gave an approach to generate temperature-time curves for travelling fires.

In Clifton's model, the firecell is divided in design areas where fully developed fire is applied in each of them using a parametric temperature-time curve. [23] One of the following conditions must be fulfilled by each design area of the firecell at any certain time: fire, preheat, smoke logged, or burned out. Figure 2.19 shows the division of the firecell during a travelling fire according to LFM at a certain time.

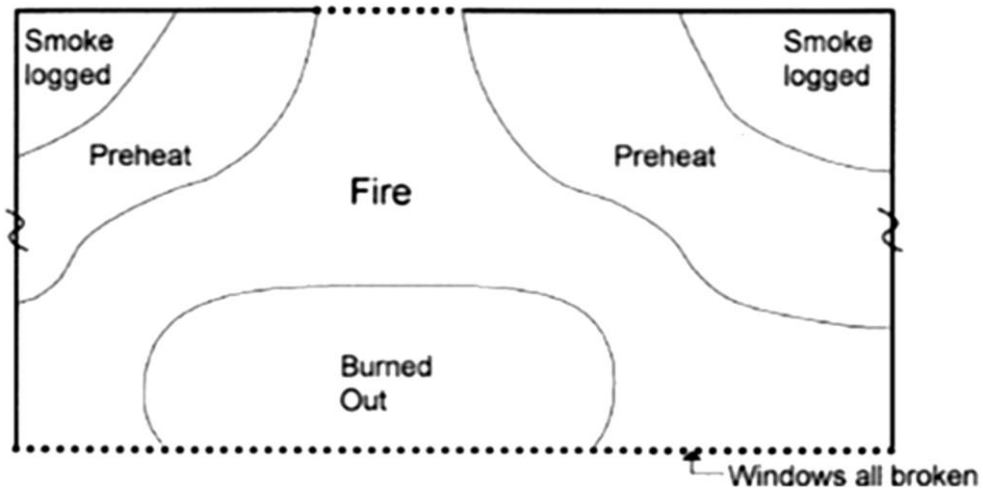

Figure 2.19. Division of a firecell during a travelling fire in the LFM [21]

Temperature-time curve was generated for ventilation controlled fires. In the last version of the model, preheat temperature was taken as 400°C and cooling phase temperature was equal to 800°C. Size of each design area was finally adjusted to 50 m^2 for all types of fuel loads. The breaking of the windows was assumed to occur when gas temperature in the room reaches 350°C. The opening factor of one design area was included in the model by the rate of the fire spread: 1 m/s for good ventilation conditions and 0.5 m/s for less ventilated. Finally, temperature-time curve is obtained by the combination of all these inputs and it can be used for any structural element. [21] Below, in Figure 2.20 a curve of one of the design areas of the model is shown.

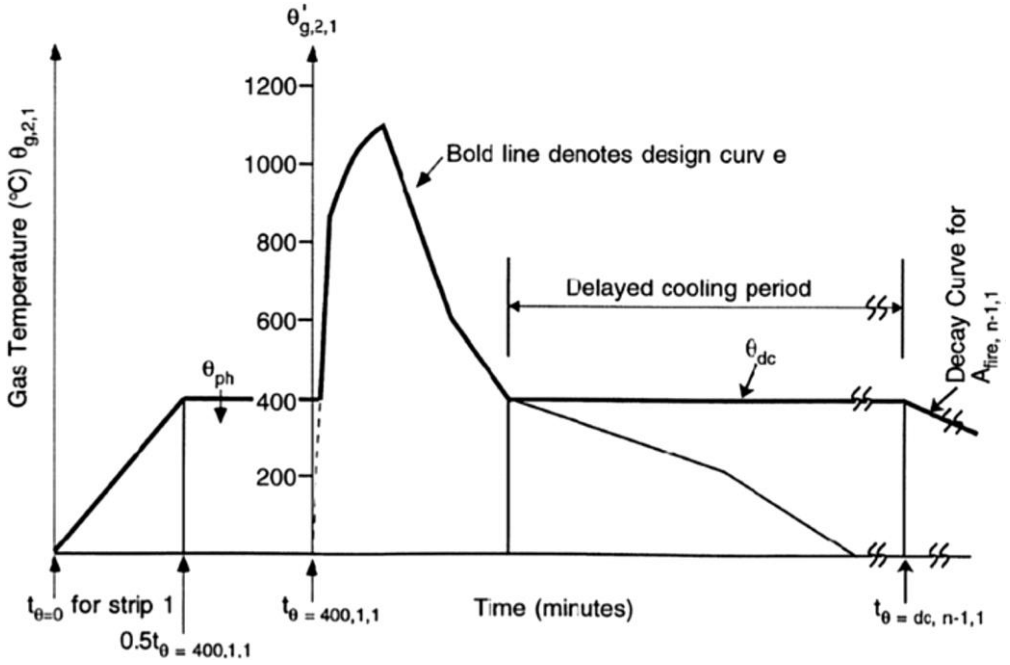

Figure 2.20. Temperature-time relationship of one design area according the LFM [21]

As it can be seen from the figure, the diagram consists of four phases: a growth from room to preheat temperature, phase in which fire is local, the delayed cooling phase until it reaches the preheat temperature and in the end, the decay phase.

Although it was an innovative method, the Large Firecell Method has many assumptions regarding fire size, ventilation, fire spread and fuel type. Due to these limitations and the lack of real large-scale tests, this method still is not applicable for real structures but it is a good base for research studies or for design of single elements. [21]

2.4.2.2. *Travelling Fires Methodology (TFM)*

In advantage with Large Firecell Method (LMF), Travelling Fires Methodology (TFM) can be applied in fire structural design. This method has been developed from Stern-Gottfried and Rein (2006) from University of Edinburgh, United Kingdom. The fire model suggested by them takes into account both spatial and temporal effects of the temperature field.

According to TFM, the fire-induced field is divided in two parts: the near field and the far field. Both regions are travelling with the fire within the enclosure. The near field is the burning region of the fire and the far field is the region distant from it. Structural elements exposed directly to the near field suffer the most severe heating from the flames meanwhile elements subjected to far field are exposed to the smoke and do not suffer intense heating. In Figure 2.21 the division of the compartment into near and far fields is shown.

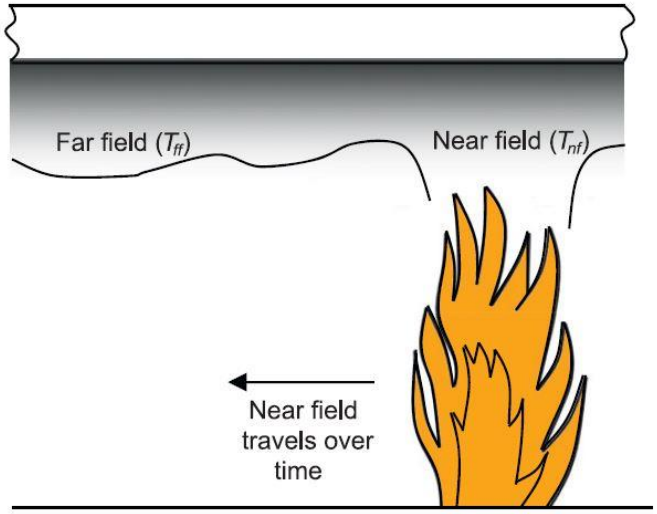

Figure 2.21. Display of the near and far field according to TMF [21]

TFM is a very comprehensive method. It does not take into account only one specific fire model but all possible fire scenarios, starting from small travelling fires with long duration and low temperatures to big fires with short duration and high temperatures. By using all the family of fire scenarios it is easy to determine the most severe combination to be used as input in structural design. [21]

The variable which characterises travelling fire is A_f which represents the burned surface area over the total floor area A. This parameter varies in percentage from 1% to 100% regarding the severity of the fire. For the value of 100%, the situation is the same with the other methods described above as they consider well distributed fires.

The assumption used in TFM considers that the release rate per unit area is constant and it depends on the characteristics of the building. According to this, the heat released from the fire can be calculated with the following expression:

$$\dot{Q} = A_f \cdot \dot{Q}'' \tag{2.39}$$

where:

$\dot{Q}$ is the total heat release of the fire [kW],

A_f is the floor area of the fire [m^2],

$\dot{Q}''$ is the heat release rate per unit area [MW/m^2].

The burning time over the fire area is determined by the following expression:

$$t_b = \frac{q_f}{\dot{Q}''} \tag{2.40}$$

where:

t_b is the burning time [seconds],

q_f is the fuel load density [MJ/m^2].

As it can be seen from the equation, the burning time t_b does not depend on the floor burning area A_f. This leads to the conclusion that the consumption of fuel over one defined area takes the same time for fires with 1% or 100% of burning area floor ratio. The reason why the total burning time is prolonged for travelling fires, is connected with the fact that fire moves from one burning area to the other inside the compartment. Typical value of the burning time from the applications of TFM is t_b = 19min, derived from values of fuel load density $q_f = 570\,MJ/m^2$ and heat release rate $\dot{Q}'' = 500\,MW/m^2$.

As stated above, some elements of the structure during a travelling fire will be subject to near field through flames and in the same time other elements will be subject to far fields through smoke. In the TFM, temperatures are determined for each of these fields. For the near field the temperature is assumed 1200°C as the highest temperature of flames measured during a compartment fire. In opposite, the determination of far field temperature is more complex as it is a function of other variables like distance from the centre of fire, the compartment height and the total heat release of the fire. [21] A simplified equation to obtain far field temperature was given according to Alpert:

$$T_{\max} - T_{\infty} = 5.38 \frac{\left(\dot{Q}/r\right)^{2/3}}{H} \tag{2.41}$$

where:

T_{max} is the maximum ceiling temperature [°C],

T_{∞} is the ambient temperature [°C],

r is the distance from the centre of fire [m],

H is the floor to ceiling height in [m].

Figure 2.22 shows the plot of a calculated far field temperature using TFM during a case study. The red vertical lines in the graph show the borders of the flame region (near field) with smoke regions (far field).

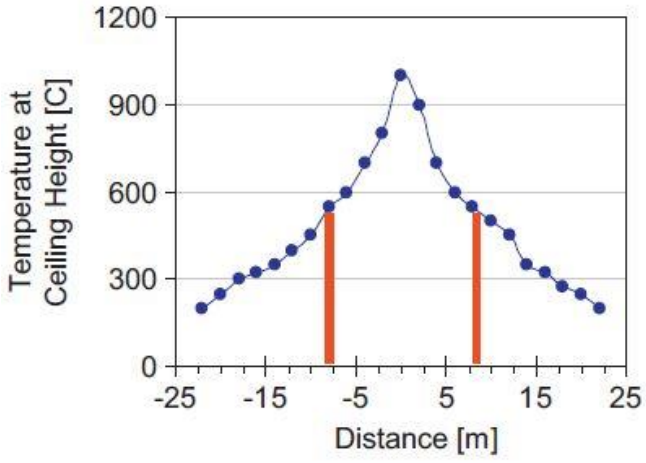

Figure 2.22. Example of a calculated far field temperature in the TFM [21]

In further studies, Stern-Gottfried et al. [21] described the procedure of determining temperature-time curve for different points as a function of the distance from the fire for both averaged and resolved far field temperatures. In Figure 2.23 an example of a temperature-time curve of a single point for both averaged and resolved far field temperatures is shown.

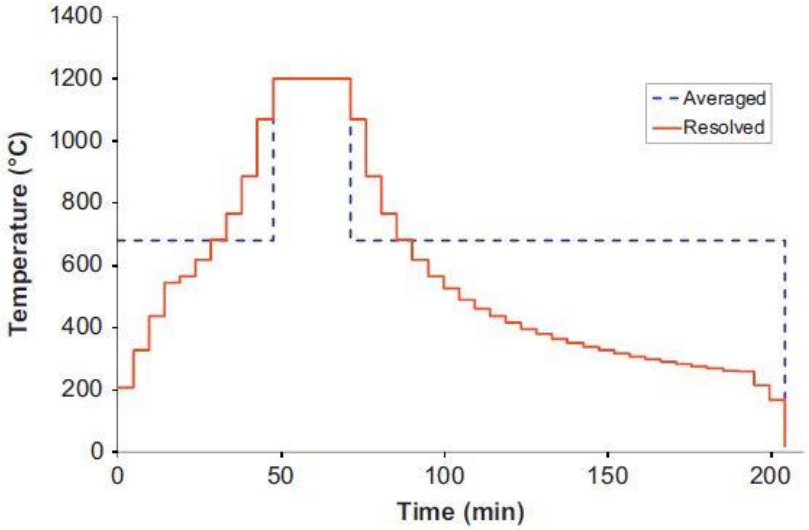

Figure 2.23. Temperature-time curve of a single point in the TFM for average and resolve far field temperature [21]

When average far field temperatures are used, an entire family of fires for different burned surface areas ranging from 1% to 100% can be built and used to determine the most severe case for the structure. Figure 2.24 shows an example of this family used during a case study of a steel structure in Edinburgh.

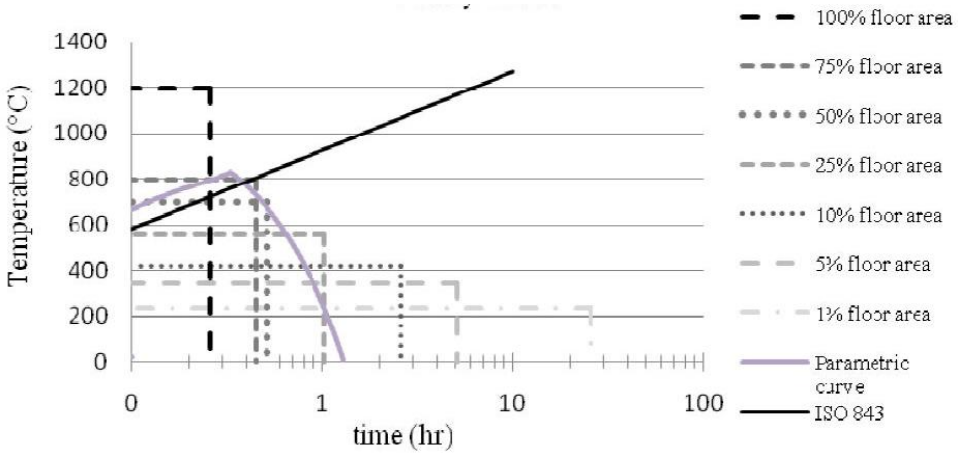

Figure 2.24. Example of an average far field temperature in the TFM [24]

Results of the study [24] show that the most severe situations for the structure are caused by medium size fires with ratio of burning area from 10% to 25% due to the combination of long duration and far field temperature.

2.4.3. Structural response of structures subjected to TFM

2.4.3.1. *Structural response of steel structures*

The first study to analyse the structural response of a building during a spreading fire was introduced by Bailey et al. (1996) [25]. The work consists in studying a simple two-dimensional steel frame of a structure which has three and five structural bays and comparing the results with those obtained by using a uniform fire. The effect of travelling fire is given by a natural curve which moves in time because it is assumed that when the curve of the first bay reaches maximum value, fire moves to the adjacent bay. The temperature-time curves used in the study are given in Figure 2.25. As it can be seen, the cooling and heating phases are taking place at the same time but in different zones.

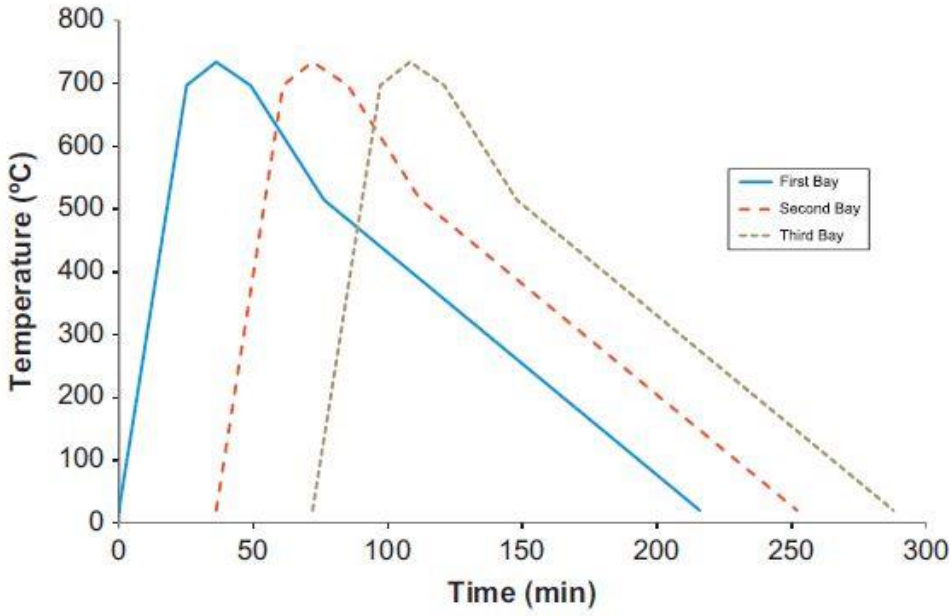

Figure 2.25. Temperature-time curve used to model travelling fire [25]

Results of the study show that the vertical displacements and internal forces are higher in case of travelling fire than traditional one. However, as the study was in the early stages, the method had neglected many factors. Ventilation, especially for structures with high number of bays, is not fully controlled as it is supplied by the air inside the building. Also, the far field temperature of the second bay cannot be equal to the ambient one as it is influenced by the fire of the previous bay. For these reasons, further studies have been done to improve the method. [21]

To concretise the effect of spreading fire in the structural response, TFM has been applied in two real buildings. The first application was made by Stern-Gottfried et al. in 2009 [24] to Mumbai C70 building project. Due to the complexity and special architecture, this structure cannot fulfil the requirements for applying traditional methods so the TFM was used to plot far field temperatures versus burning duration for a family of fire scenarios.

One year later, Jonsdottir et al. [24] did a comparison of steel temperatures by using traditional methods and Travelling Fires Methodology. The difference was evaluated for three different beams of Informatics Forum at the University of Edinburgh and their temperature-time curves are shown in Figure 2.26.

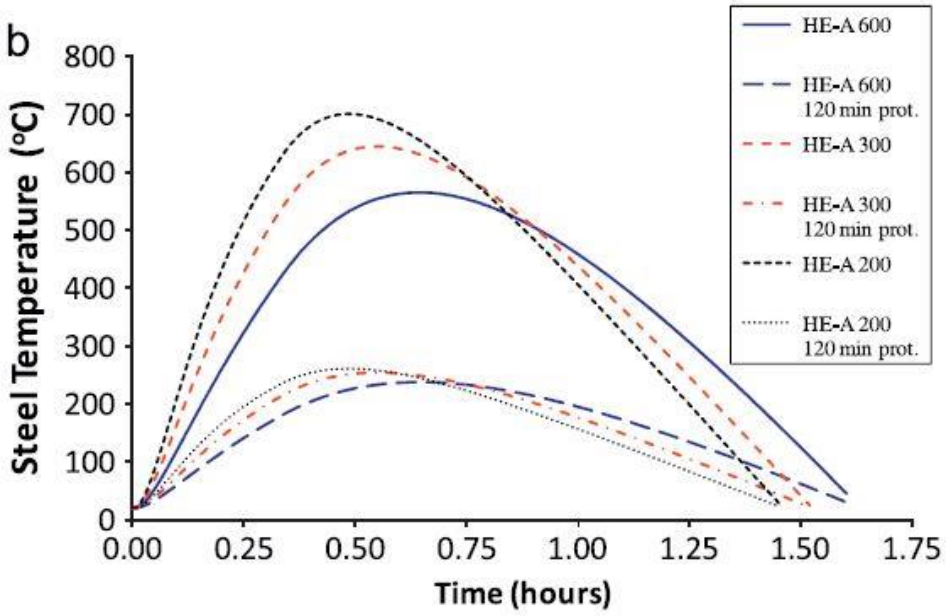

Figure 2.26. Temperature-time curves for three different steel beams [24]

This study was the first who provided results for steel elements subjected to travelling fire. The comparison shows that traditional methods underestimate the maximum steel temperature. In particular, small travelling fires give higher values of temperatures in comparison with uniform fires. For protected steel members, fire sizes with ration of burning area between 5 and 10%, give the maximum steel temperature. For unprotected steel, TFM predicts 65 to 95% higher steel temperatures in comparison with the traditional methods.

Application of the TFM in both of the above described cases has been done for simple structural elements. Structural behaviour of the entire structure is more complex, however these studies have shown the significance of travelling fires.

2.4.3.2. *Structural response of concrete structure*

Two papers regarding the effect of travelling fire on concrete structures have been carried out based on two different methods utilising travelling fire.

The first one was done by Ellobody and Bailey [26] who studied the effect of a horizontal travelling fire on a post-tensioned concrete floor. This study was done using a three-dimensional FEM but the fire input was similar with the one used by Bailey et al. [25] for steel structures. The base temperature-time curve was taken from Eurocode and it was shifted in time to provide heating and cooling scenarios. Inter-zone time delays were taken 64 min for the first fire scenario and 30 min for the second one. The parametric curves used are shown in Figure 2.27.

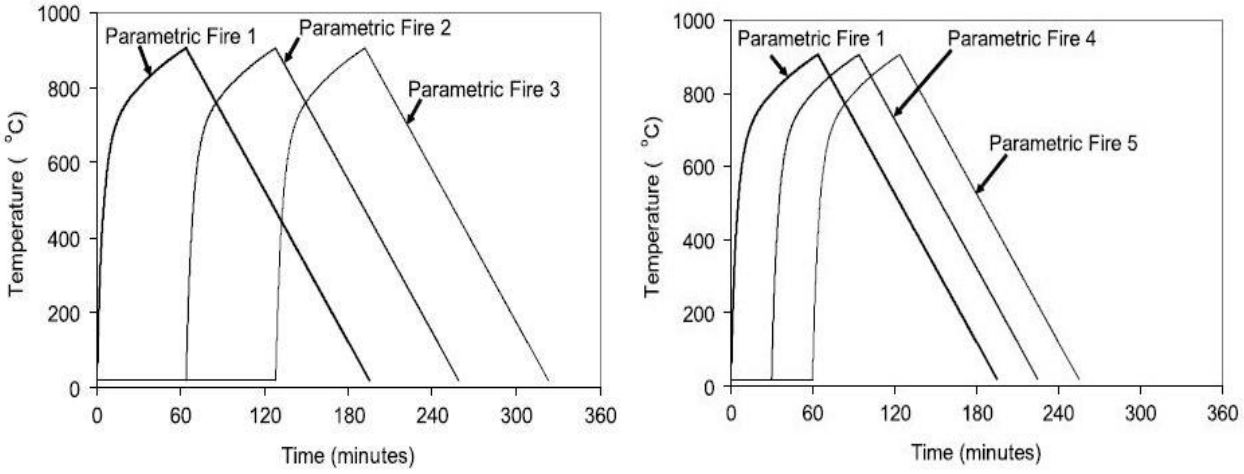

Figure 2.27. Parametric curves used with 64 and 30 min time shift [26]

The parameters examined were tendon temperatures, deflection and axial displacement. The results showed that these parameters were influenced by the time delay used for shifting temperature-time curves in comparison with classical design fire models. As a result, the authors concluded that travelling fire should be taken into account to find the most severe scenario in order to evaluate better the structural response.

This study was using similar curves with the one used by Bailey et al., therefore some parameters like ventilation and far field were still neglected. However, this negligence does not influence the recommendation for engineers to include travelling fire in design for a coherent structural response.

The second study was done by Law at al. [27] using TFM as described in paragraph 2.4.2.2 and the generated curve was applied to a FEM to study a concrete floor plan with dimensions 42 × 28 m as shown in Figure 2.28. Each column span in both directions is 7 m and the storey height 3.6 m. The fire occupies full width and moves alongside the longer wall.

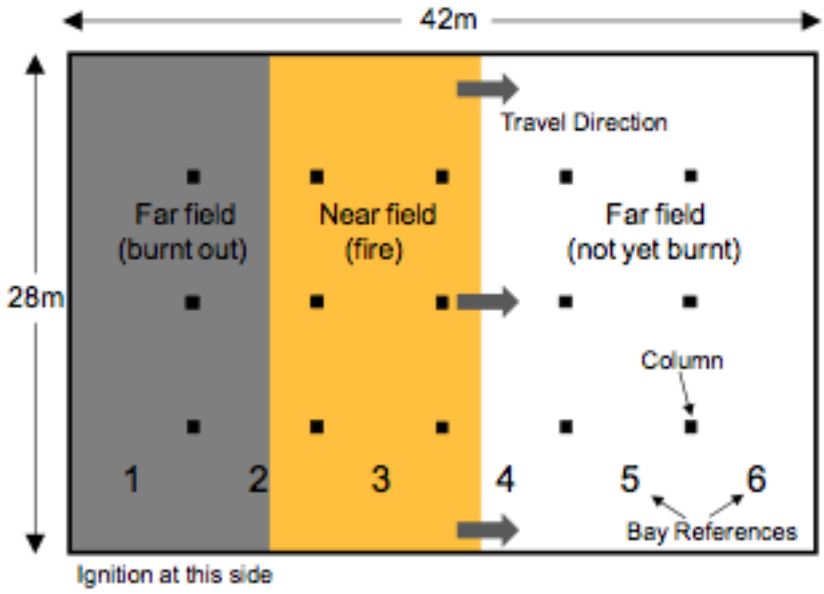

Figure 2.28. Plan of concrete structure where TFM is applied [27]

The structural response was viewed in terms of rebar temperature, tensile strain and deflections. Ratio of fire sizes between 10% and 25% of the floor area produced the most onerous results for rebar temperature. All travelling fire scenarios used, showed that they were the worst cases in comparison with parametric temperature-time curves taken from Eurocode.

To sum all findings, as shown at all the studies given, travelling fire concept allows a range of realistic fires to be considered and, thus, allows structural engineers to evaluate better the structural response of the elements. In all of the cases presented above, methods using spreading fire tend to be more comprehensive and innovative in comparison with traditional design methods that assume uniform conditions throughout a compartment for the entire duration of the fire.

3. BEHAVIOUR OF STRUCTURES SUBJECTED TO TRAVELLING FIRE

3.1. Introduction

Steel and concrete structural members like columns, beams, slabs, are commonly found in the construction industry. Behaviour of these members during a natural fire is very important to be studied as their structural performance influences directly the stability of the entire structure. In order to have an accurate assessment of the elements' behaviour, the thermal load applied in structural design should be as close as possible to the real natural fire. The scope of the study carried out in this chapter tends to show that the method of travelling fire aims to determine the true performance of a structure exposed to fire and applicative computational examples have been performed to realise this.

Material models of steel, reinforcement steel and concrete at elevated temperatures are referred respectively to Eurocode 2 [28] and 3 [29]. This study will examine first of all the effect of travelling fire in the mechanical behaviour of a structure by comparing results of analysis with two other fire models which are described in Eurocode 1. Afterwards, analysis for structures with different materials will be realised in order to evaluate the effect of travelling fire in steel and composite structures.

All the thermal analyses have been performed with the licenced commercial program Vulcan which is fully validated for real-size tests and capable to perform non-linear finite elements analyses of three-dimensional structures at elevated temperatures.

3.2. Material properties at elevated temperatures

3.2.1. Steel

3.2.1.1. *Mechanical properties*

The stress-strain relationship of steel *f-ε* at ambient temperature is essentially different from that of steel exposed at high temperature. Experimental tests show that this relationship at high temperatures is without a clear yield plateau but strain hardening occurs all the way in the plastic range. [11]

Eurocode EN1993-1-2 gives the stress-strain relationship for steel at high temperatures by defining stress and strain for each part of the curve, taking into account strain hardening for steel temperatures below 400°C. This relationship is given in Figure 3.1.

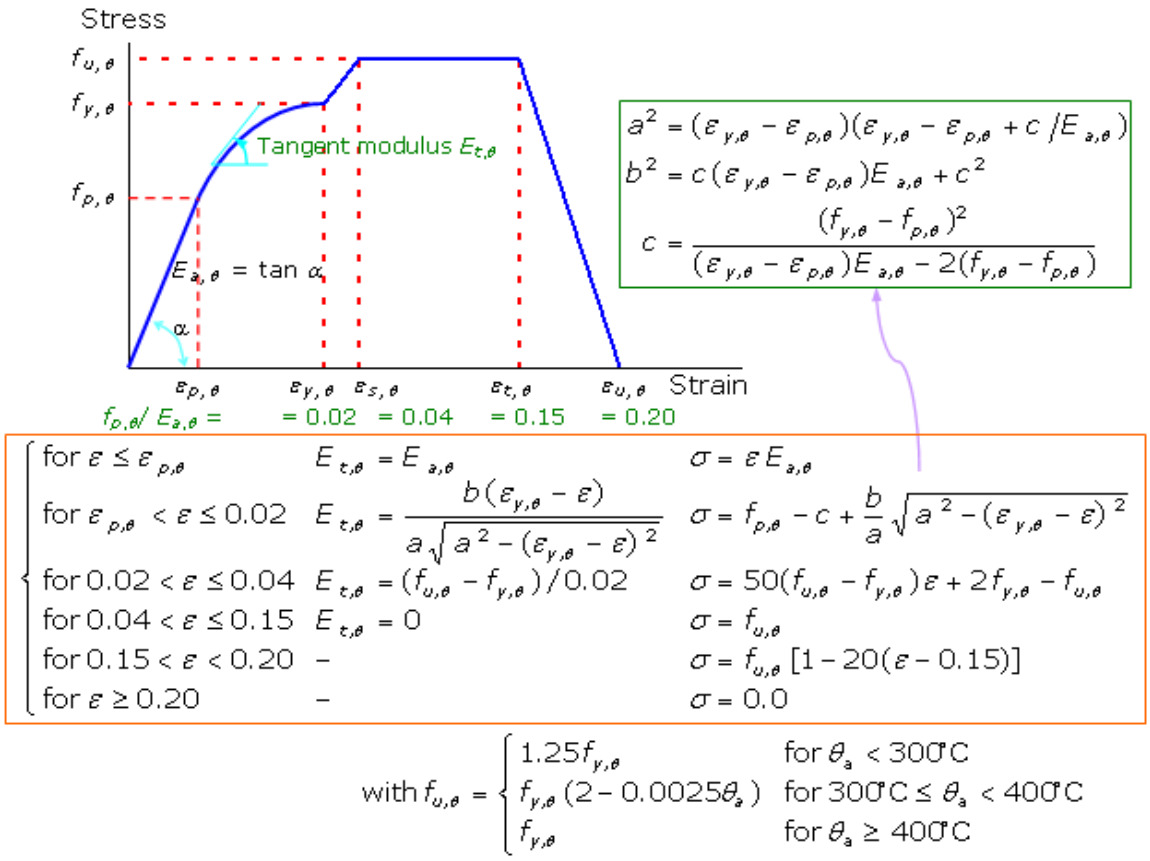

Figure 3.1. Stress-strain relationship for steel at high temperatures according to EN1993-1-2 [11]

As it can be seen from the figure, the curve is formed by five parts. The first part shows that the curve is linear progressing up to the proportional limit $f_{p,\theta}$ and the elastic modulus $E_{a,\theta}$ is the tangent of the slope of this straight-line segment. The second part of the curve depicts the transition from the elastic to the plastic range. The third part of the curve is a linear line up to the limit $f_{u,\theta}$ due to steel strengthening because of plastic deformation. The fourth part of the curve is a flat yield plateau up to a limiting strain for yield strength $\varepsilon_{t,\theta}$. The last part of the curve shows a linear line decreasing to zero stress at the ultimate strain $\varepsilon_{u,\theta}$. [11]

Using the expressions given by EN1993-1-2, a series of stress-strain curves for different temperatures have been drawn for S275 steel as shown in Figure 3.2.

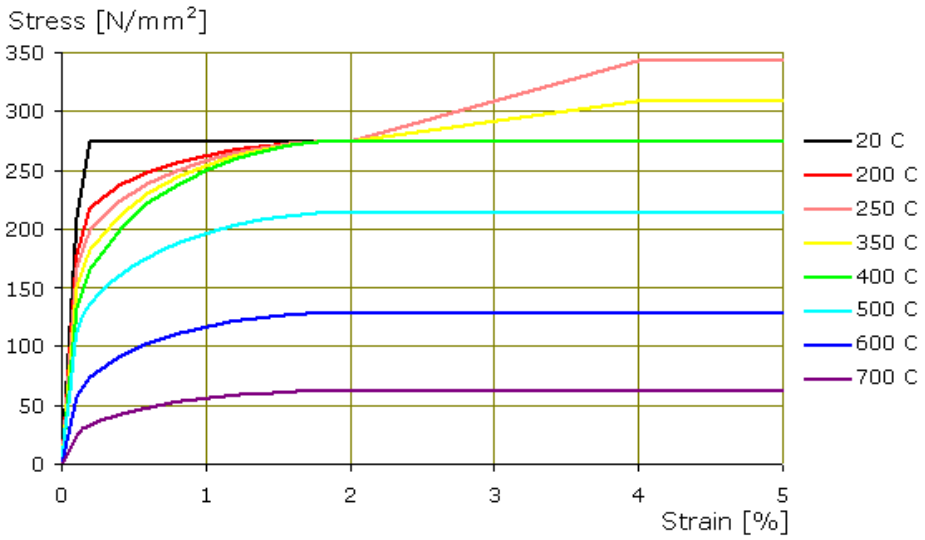

Figure 3.2. Stress-strain curves for S275 steel at different temperatures [11]

The above figure shows the stress-strain relationship for S275 steel at high temperatures, where for temperatures below 400°C, the steel continues strengthening because of plastic deformation.

3.2.1.2. *Thermal properties*

The properties that depend on steel temperature are thermal elongation, thermal conductivity and specific heat capacity of steel. Expressions given by Eurocode EN1993-1-2 describe how to determine these properties as a function of steel temperature.

Figure 3.3 shows the variation of the thermal elongation $\Delta l / l$ with steel temperature θ_a and the expression to determine the coefficient of thermal elongation of steel according to EN.

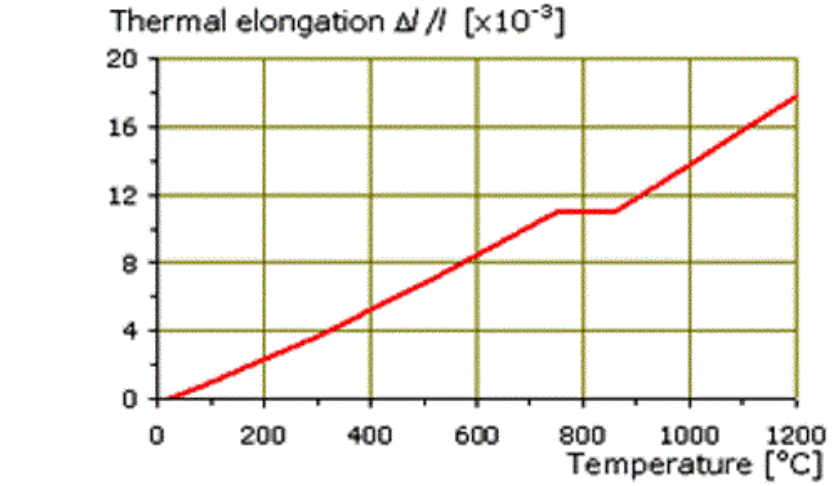

$$\Delta l / l = \begin{cases} 1.2\times10^{-5}\theta_a + 0.4\times10^{-8}\theta_a^{\,2} - 2.416\times10^{-4} & \text{for } 20^{\circ}C \le \theta_a < 750^{\circ}C \\ 1.1\times10^{-2} & \text{for } 750^{\circ}C \le \theta_a \le 860^{\circ}C \\ 2\times10^{-5}\theta_a - 6.2\times10^{-3} & \text{for } 860^{\circ}C < \theta_a \le 1200^{\circ}C \end{cases}$$

Figure 3.3. Thermal elongation of steel as a function of temperature [11]

Figure 3.4 shows the variation of the specific heat c_a with steel temperature θ_a and the expression to determine the specific heat according to Eurocode.

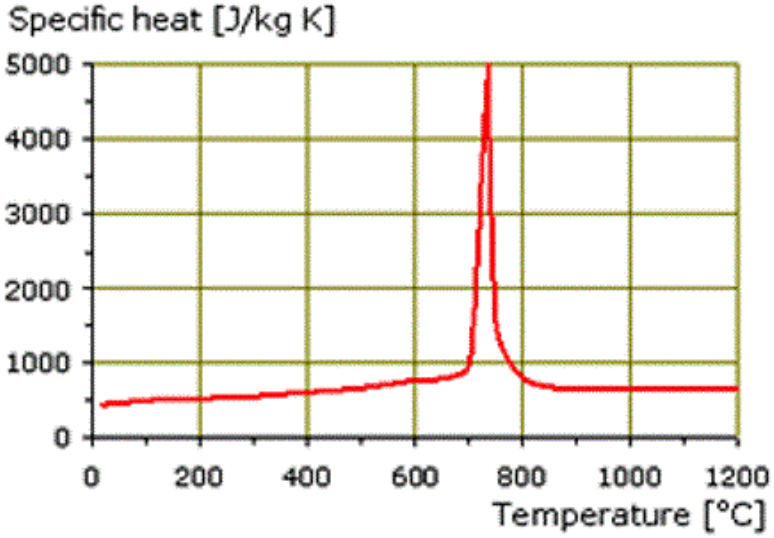

$$c_a = \begin{cases} 425 + 7.73\times10^{-1}\theta_a - 1.69\times10^{-3}\theta_a^2 + 2.22\times10^{-6}\theta_a^3 & \text{for } 20^\circ C \le \theta_a < 600^\circ C \\ 666 + 13002/(738 - \theta_a) & \text{for } 600^\circ C \le \theta_a < 735^\circ C \\ 545 + 17820/(\theta_a - 731) & \text{for } 735^\circ C \le \theta_a < 900^\circ C \\ 650 & \text{for } 900^\circ C \le \theta_a \le 1200^\circ C \end{cases}$$

Figure 3.4. Specific heat of steel as a function of temperature [11]

Figure 3.5 shows the variation of the thermal conductivity λ_a with steel temperature θ_a and the expression to determine the thermal conductivity according to Eurocode.

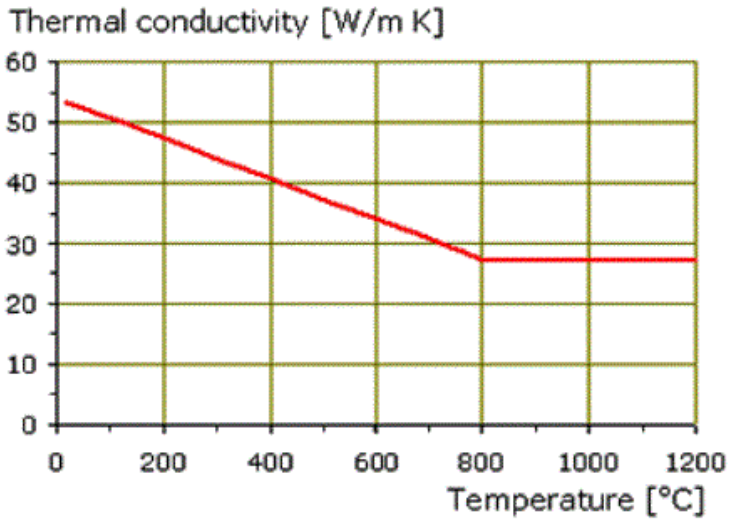

$$\lambda_a = \begin{cases} 54 - 3.33\times10^{-2}\theta_a & \text{for } 20^\circ C \le \theta_a < 800^\circ C \\ 27.3 & \text{for } 800^\circ C \le \theta_a \le 1200^\circ C \end{cases}$$

Figure 3.5. Thermal conductivity of steel as a function of temperature [11]

3.2.2. Concrete

3.2.2.1. *Mechanical properties*

According to Eurocode EN1993-1-2, the stress-strain relationship of concrete *f*-*ε* for temperatures higher than ambient is shown in Figure 3.6.

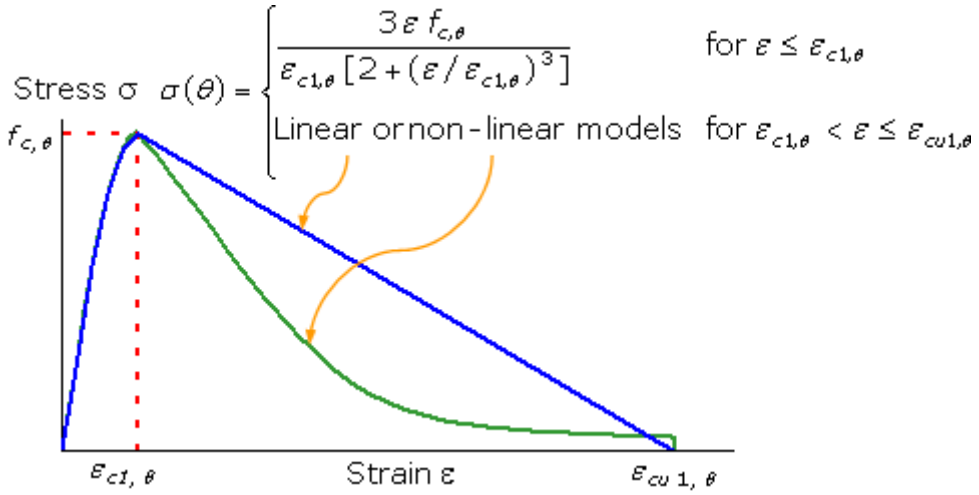

Figure 3.6. Stress-strain relationship for concrete at high temperatures according to EN1994-1-2 [11]

The values of each of the parameters used in the formula above are given in Eurocode tables for different temperatures. Replacing several values of temperature, a series of relative compressive stress-strain curves $f_{c,\theta}/f_{ck}$–ε are produced for normal-weight concrete as shown in Figure 3.7.

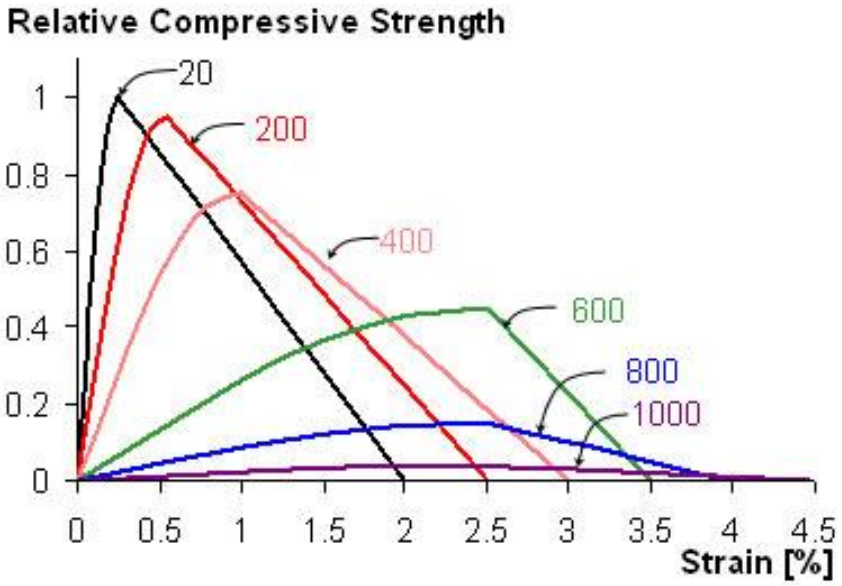

Figure 3.7. Stress-strain curves for concrete at different temperatures [11]

The above figure shows that when temperature is increased, the concrete compressive strength is reduced meanwhile the corresponding strain of concrete is increased.

3.2.2.2. *Thermal properties*

Concrete is a material more complex than steel, therefore there are more parameters of concrete which are influenced by the fire. The properties that depend on concrete temperature are thermal expansion of concrete, specific heat of dry concrete, density of concrete and thermal conductivity of concrete. Also thermal properties depends if the concrete is normal-weight concrete (NWC) or lightweight concrete (LWC). Eurocode EN1993-1-2 gives expressions to determine these properties in function of concrete temperature. In the applicative study, calcareous normal-weight concrete will be used.

Figure 3.8 shows the variation of the thermal expansion $\varepsilon_{c,\theta}$ with concrete temperature θ_c and the expression to determine thermal strain (expansion) of concrete according to Eurocode.

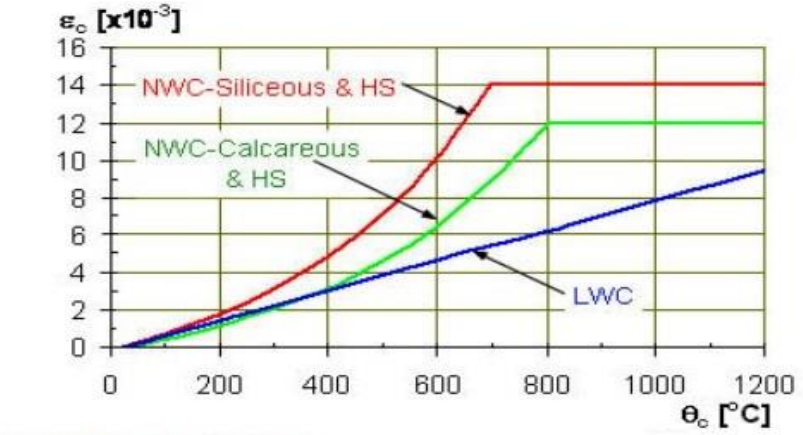

Figure 3.8. Thermal expansion of concrete as a function of temperature [11]

In Figure 3.9 the variation of the specific heat of dry concrete $c_{c,\theta}$ with temperature θ_c and calculation of the specific heat according to Eurocode for different water content is shown.

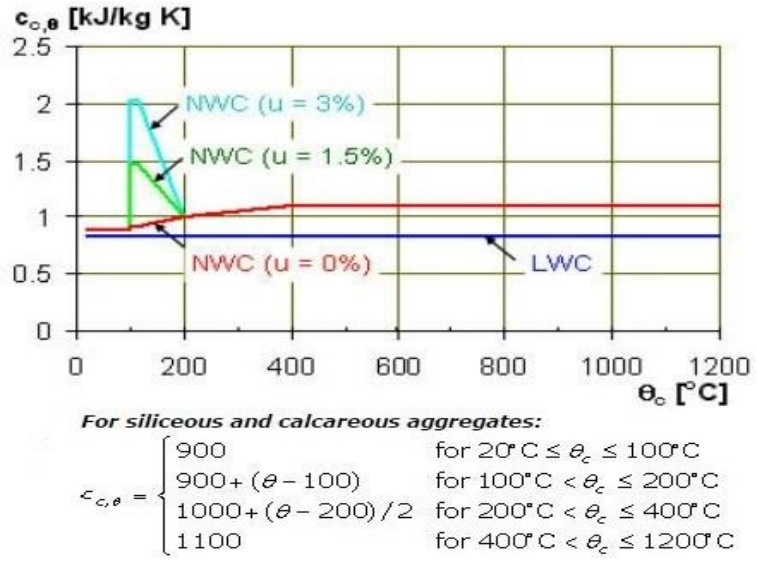

Figure 3.9. Specific heat of concrete as a function of temperature [11]

Figure 3.10 shows the curve of the relative density of concrete at fire with the density of concrete at ambient temperature $\rho_{c,\theta} / \rho_{c,20}$ and the expression to determine the density of concrete according to Eurocode.

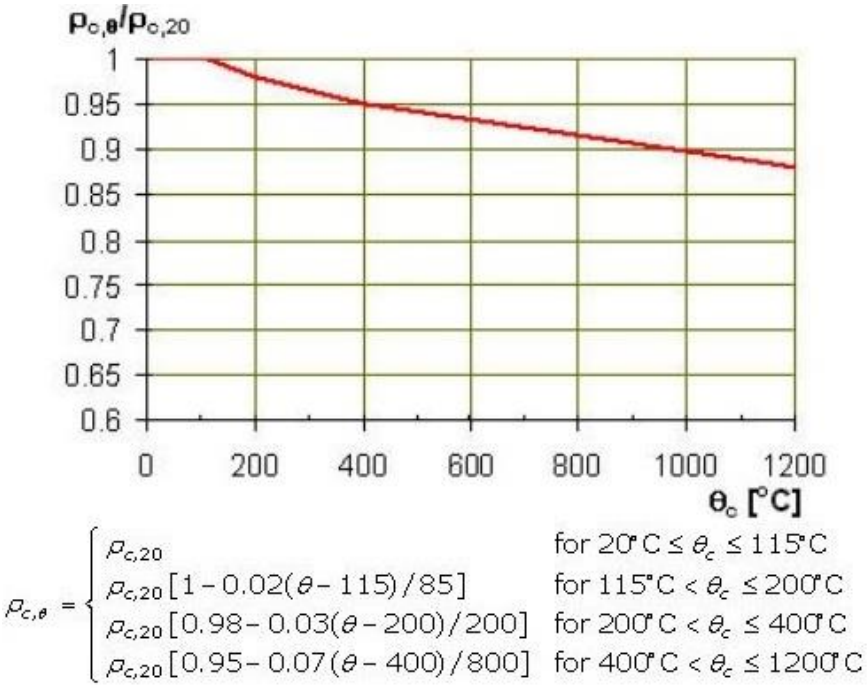

Figure 3.10. Relative density of concrete as a function of temperature [11]

Figure 3.5 shows the variation of the thermal conductivity λ_c with concrete temperature θ_c and the expression to determine the thermal conductivity according to Eurocode.

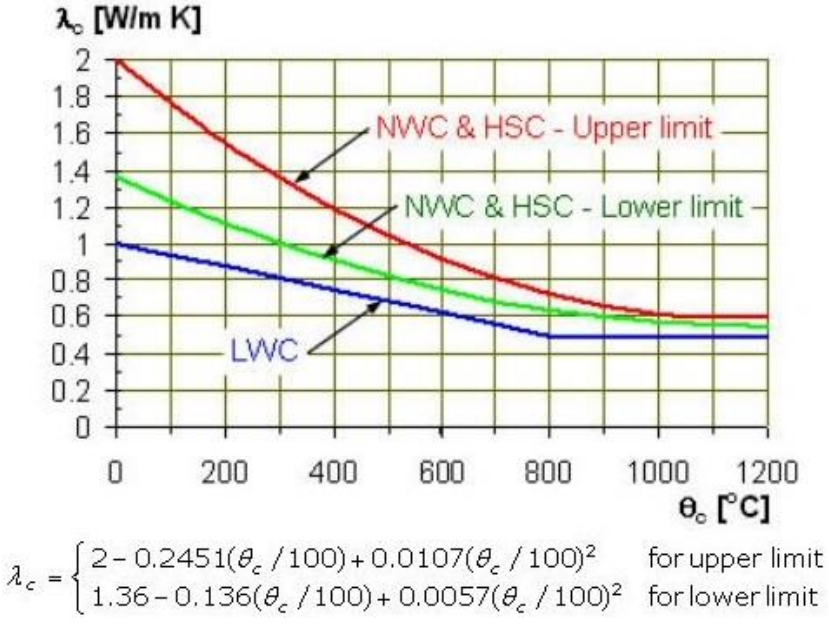

Figure 3.11. Thermal conductivity of concrete as a function of temperature [11]

3.3. Description of software

Full-scale fire experiments have relatively high cost in performing; therefore computer simulations are usually done. Using professional software, especially in research studies, has become more popular recently due to the increase of programs ability to perform several analyses and also the speed of obtaining the results. Once these analyses are fully validated with real-scale tests, the software can be used to perform parametrical analysis and to study in details the behaviour of different structures subjected to thermal loads. [30]

Nowadays there are several fully validated programs that are capable to perform non-linear finite elements analyses of three-dimensional structures at elevated temperatures. One of them is the commercial software Vulcan [31] which is used for the purpose of this master thesis. In this paragraph a brief description of software history, capabilities and limitations is presented.

3.3.1. Software history

The software Vulcan is originally based on software named Instaf, which was developed at the University of Alberta (Canada) in 1980 and was capable to accomplish two-dimensional non-linear finite element analysis. By 1990, the software has been improved further at the University of Sheffield (UK) by allowing three-dimensional structures to be analysed under fire conditions, taking also into account some effects missing in the previous version. After all these extensions, the software has been renamed Vulcan to emphasise the improvement from its predecessor Instaf.

Vulcan currently has two different versions, a research version written in FORTRAN programming language like Instaf was, and a commercial version written in C++ which is available from the company Vulcan Solutions [32]. For the analyses carried out in this master thesis, the commercial version is used.

3.3.2. General description

The computer software Vulcan is a three-dimensional frame analysis program, which has been developed to study the behaviour of steel and composite structures under fire conditions, also allowing the modelling of floor slabs. Stress-strain curves and material properties at elevated temperatures are taken into account in modelling concrete and steel elements. Also the distribution of temperature across the members is non-uniform which allows temperature, stress and strain to vary within the cross section. From the software library a wide range of cross-sections can be defined, allowing users to choose between different shapes and materials. The software also enables the usage of a range of fire curves so large parametric analyses can be performed quite easily.

As many engineering programs that use finite elements analysis, Vulcan takes an input file, performs the non-linear finite element analysis on the structure, and creates a corresponding textual output file of results like internal forces or deformations of elements.

The software Vulcan is well validated with full-scale test data, including six large scale fire tests at Cardington, UK. [31]

3.3.3. Capabilities and limitations

The structure in Vulcan is modelled as an assembly of finite beam-column, support, spring, shear connection and floor slab elements. The beam-columns are represented by 3-noded line elements with two Gaussian integration points along their length. The interaction of beam-column connections in a frame is represented using a 2-noded spring element of zero length, with the same nodal degrees of freedom as a beam-column element. To represent the characteristics of steel beams and concrete slabs within a composite floor, a 2-noded shear-connector element of zero length, with three translational and two rotational degrees of freedom at each node, is used. For composite floor elements it is assumed that their nodes are defined in a common fixed reference plane, which coincides with the mid-surface of the concrete slab element. All the nodes of springs and shear connectors are assumed to be in this plane as well. The model of a connection between a refined layered concrete slab with a steel beam in Vulcan is shown in Figure 3.12. [31]

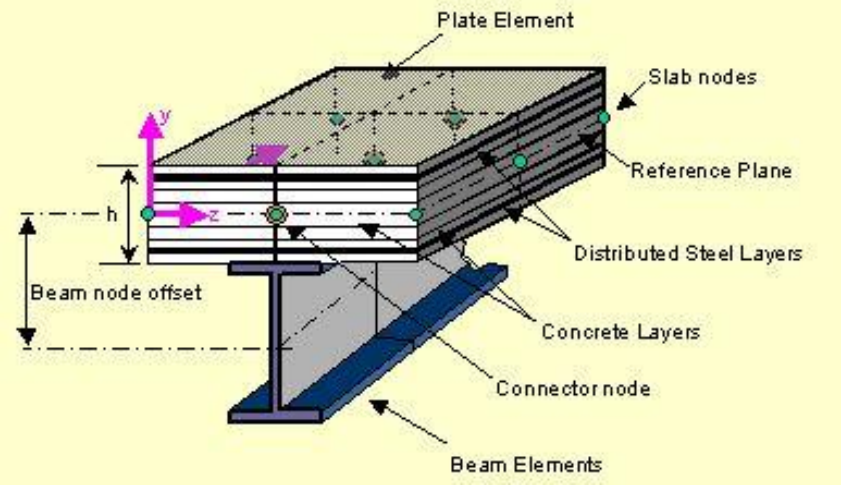

Figure 3.12. Refined layered slab element connected to steel beam element in Vulcan [31]

The cross section of a beam-column element is divided into a matrix of segments where each segment has its own temperature and its own mechanical and thermal properties at any stage of an analysis. This division makes possible the modelling of different temperature distributions across element's cross-sections and therefore, different stress-strain curves and material properties at any stage of analysis. The uniaxial properties of concrete and reinforcing steel at elevated temperatures have been adopted in the software.

The general assumptions for the elements defined in the software are: cross sections remain plane and undistorted under deformation and there is no slip between segments. They do not necessarily remain normal to their reference axis where they are originally located, as displacement occurs. The "small strain and large deformation" theory is adopted, i.e. the displacements and rotations can be arbitrarily large but strains remain small enough. [33]

3.3.4. Verification of the results

Full-scale fire tests have high cost and also the results need a lot of time to be obtained due to the time of building the structure, installing special measurement devices and processing the outputs. Therefore, the verification of the results achieved from the software will be done using previous verified numerical models. This can be done by modelling a previous structure studied with Vulcan and comparing the results among them. Objective evidence that the software meets all requirements for design is obtained when the design outputs of the new and existing model are found similar.

The structure, subject of this verification is taken from the paragraph 19.2.1.3 – Composite slab with columns (BMS_7) of the book "Benchmark studies – Verification of numerical models in fire engineering" [33]. 3D view of the structure modelled for verification of the software and the cross-sections of the elements are given in Figure 3.13.

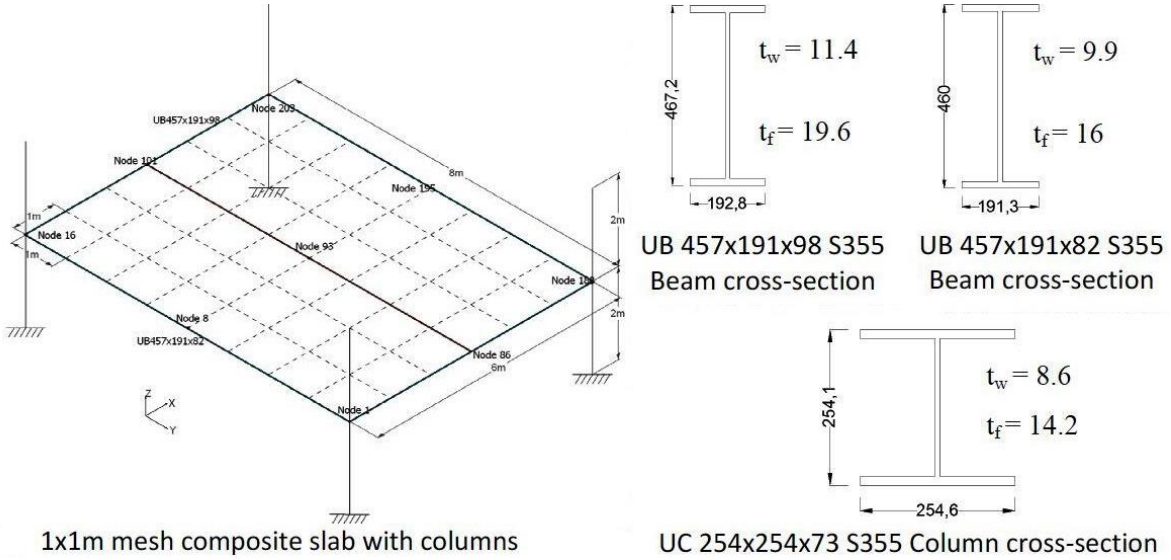

Figure 3.13. 3D view of the verification structure [33]

The structure consists of a 6 × 8m composite slab, four primary beams around perimeter with section UB457×191×98, S355 and one secondary beam parallel to the longest span with section UB 457×191×82, S355. At each corner of the structure there is a column with section UC 254×254×73, S355. The concrete slab is modelled with mesh 1×1m and a uniform area load of 5 KN/m^2 is applied. The structure is heated uniformly along its entire volume with thermal load according to BS476 Standard fire. Primary beams and columnn are protected while secondary beams are unprotected.

The results of the vertical displacements in the middle of each typical beam (Node 8, 86 and 93) from software analysis and from benchmark study are presented respectively in Figure 3.14 and 3.15.

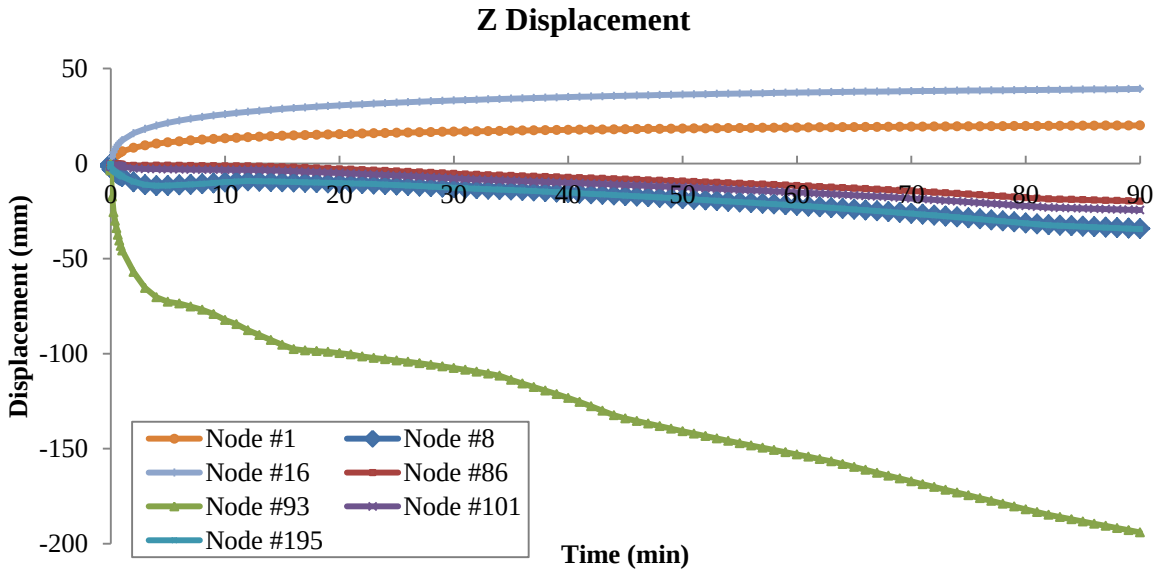

Figure 3.14. Vertical displacement at midpoint of the beams according to software analysis

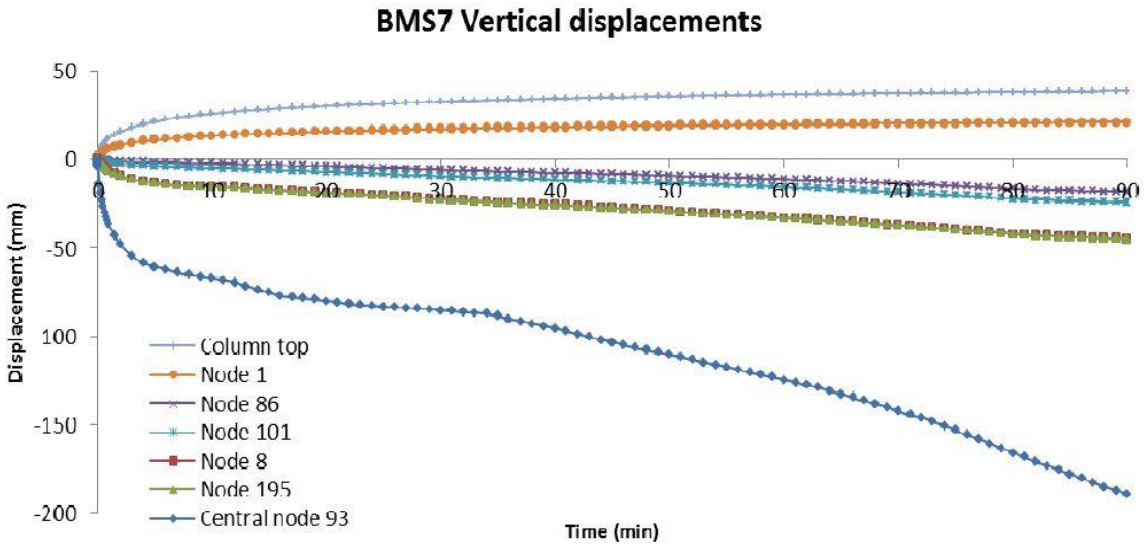

Figure 3.15. Vertical displacement at midpoint of the beams according to benchmark study [33]

As it can be seen from the above figures, the results obtained from software analysis are very close to the results shown in benchmark studies for verification of numerical models. From this comparison, the software results are verified and fully satisfy all the expected requirements; therefore the software can be used for designing different structures as the results obtained from the analysis accurately represents reality.

3.4. Description of the structure

3.4.1. Loading

The building is assumed to be situated in a non-seismic area therefore no seismic load was taken into account during the study. It is considered that the terrace would be accessible so the live load of it is taken according to Eurocode. In Table 3.1, design load and additional information regarding the materials used are presented. Thermal load is not displayed as it will be described in more details in paragraph 3.5.

Design Loading	
Slab dead load	2.0 kN/m^2
Imposed load	1.0 kN/m^2
Terrace live load (usable)	2.0 kN/m^2
Concrete class	
Columns, beams, floor	C30/37
Steel grade	
Columns and primary beam	S355
Other beams	S275
Reinforcement bars	S500

Table 3.1. Design loading and materials of the building

3.4.2. Structural scheme

In order to investigate the effect of different fire models in buildings, a simple structure was conceived and modelled in the software. The single storey office building is assumed to have steel-concrete composite construction with floor area 130 m^2. The structure has rectangular plan shape with dimensions 13.0 × 10.0 m and floor height 3.6 m. There are four equal openings with dimensions 1.2 × 3 m and parapet 1.5 m for ventilation of the compartment. Grade of steel used for columns and for primary beams is S355 while for secondary beams it is S275. Class of concrete used for composite slab is C30/37.

The cross-sections of beams and columns are defined with simple structural calculations for normal temperature applying loads and material properties shown in paragraph 3.4.1. According these calculations, the primary beams used are profile IPE 360 which are supported by HEA 300 steel columns. The secondary beams under the slab are IPE 240. The composite slab consists of trapezoidal sheets A55/P600 with thickness 0.8 mm, and concrete C30/37 with total height 120 mm over it. The concrete slab is reinforced by steel bars of area 190 mm^2/m placed 30 mm from the top of the slab in both directions.

The structural scheme studied in the software application is summarised in Figure 3.16.

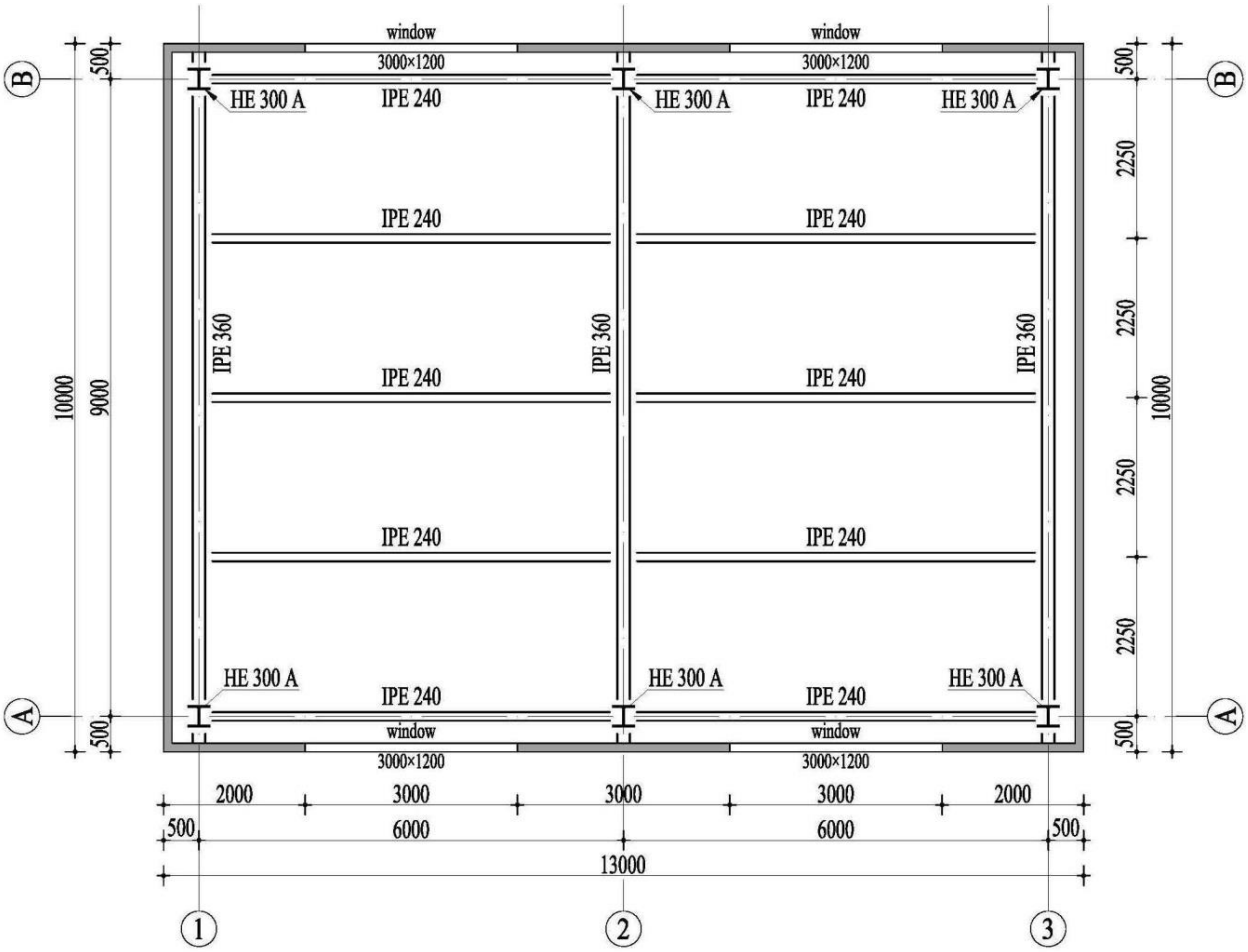

Figure 3.16. Structural scheme of the single storey building

As it can be seen from the figure, the structure consists of three steel frames with bay 6 m between them while the length of the frame is 9 m. Typically for steel structures, columns are assumed to be fixed in the ground while beam-column connections of the frames and secondary beams connections with primary beams are considered to be pinned. The secondary beams have axial distance 2.25 m to avoid big deflections at ambient temperature. The composite floor makes the floor infinitely rigid so no horizontal bracing system is used. For simplicity of the analysis, wind or other lateral loads are not taken into account at conceptual design; therefore no vertical bracing system has been inserted.

The initial structure is designed with steel beams and then, in the second case, with composite beams (shear connectors with diameter 22.5 mm and tensile strength 450 MPa are used). The two types of beams used are shown in Figure 3.17.

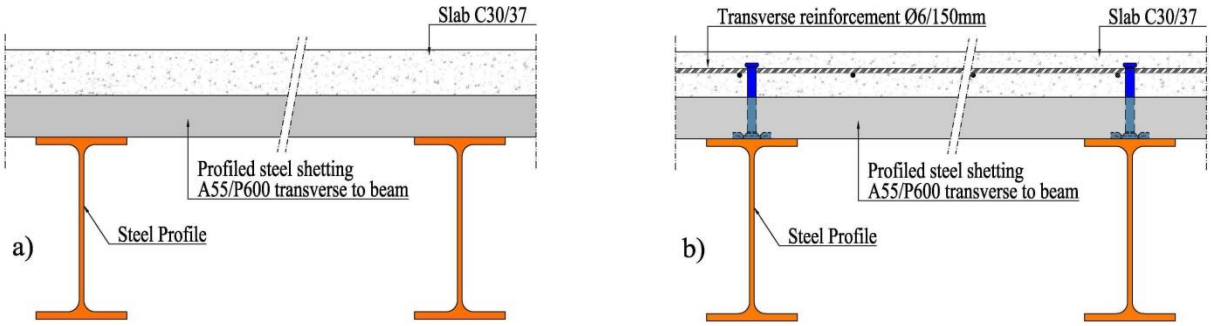

Figure 3.17. Type of beams used for analysis: a) steel beams; b) composite beams

All the structural elements are considered without fire protection and directly exposed to fire. The floor and ceiling are made from reinforced concrete and the walls from lightweight concrete. Mechanical behaviour of the structure is studied in terms of deflections and axial force of the primary beam in axis 2. For a better comparison of the results, the columns are assumed to be from steel and the same in all cases.

3.4.3. Finite Element Model

Geometrical 3D model of the structure has been incorporated within the software Vulcan which is suitable for such analyses. The accuracy and reliability of the software is shown by analyses of previous real experiment test fires executed in Cardington in The United Kingdom [31] or Veselí nad Lužnicí in the Czech Republic [1]. The structure was modelled in software according the geometric data described in the previous paragraph. Two different supporting beam systems have been applied. At the first case, steel beams are not connected with the composite slab considering zero interaction between them. In the second model, composite beams are modelled by using shear connectors to make a full connection. Composite slab has mesh range 1.0 × 0.75 m and it is subjected to a uniform area load of 5 kN/m^2.

In the analysis, the stress-strain relationship of steel and concrete at elevated temperatures and reduction factors of their material properties are in accordance with EC2 [28] and EC3 [29]. Creep analysis in Vulcan has been excluded in all models.

The structure modelled in the software including geometry, beam and column cross-sections and vertical loading applied in the structure is shown at Figure 3.18.

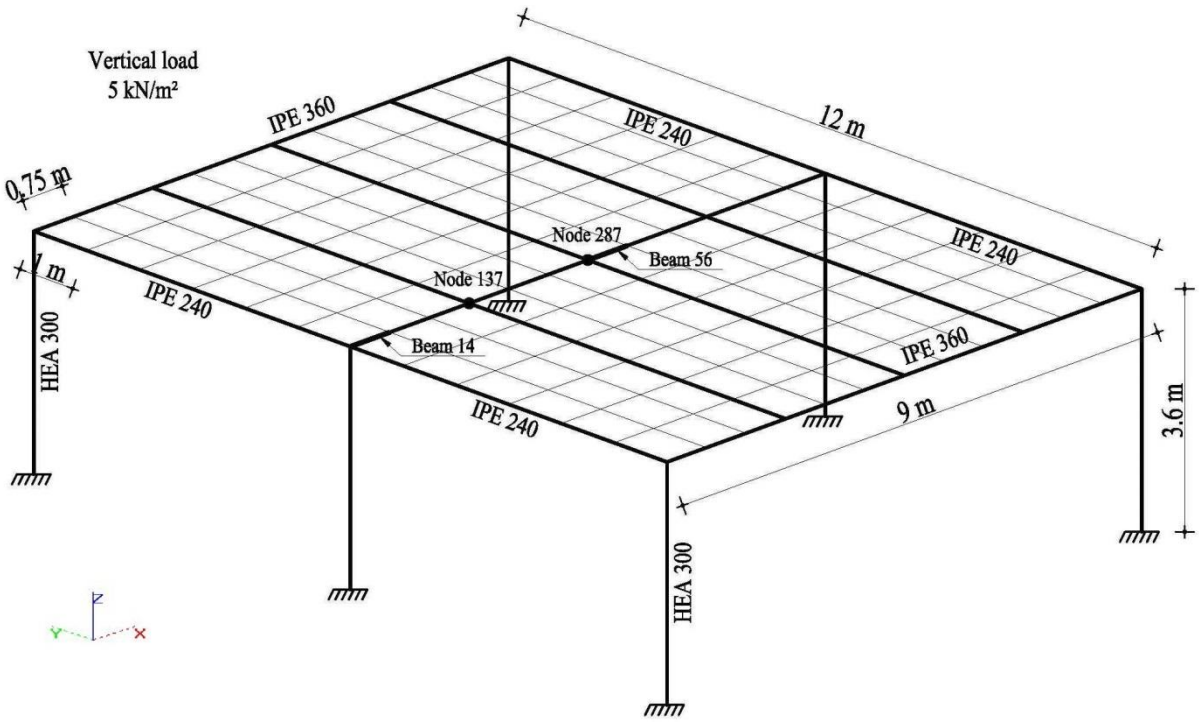

Figure 3.18. 3D view of the structure modelled in Vulcan

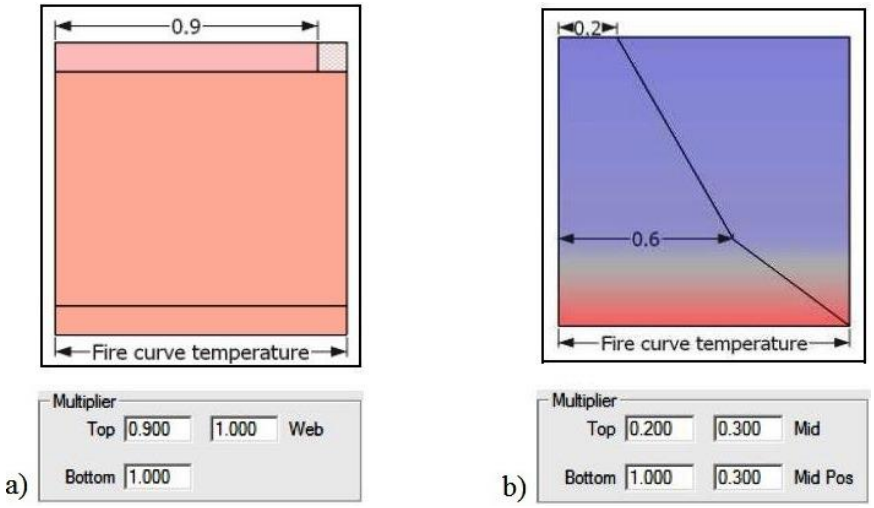

Figure 3.19. Temperature pattern applied to a) beams; b) slab [33]

All columns are considered protected while primary and secondary beams are considered not protected from fire. Temperature patterns regarding protection and function of the elements in the structure have been applied to each cross section. These temperature patterns which scale the controlling fire temperature curve by fixed factors for beams and slab are shown in Figure 3.19. Their values are defined for each structural element according the benchmark study that has been carried out using software Vulcan [33]. Uniform temperature factor of 0.7 across the entire cross-section of columns has been applied.

3.5. Description of fire models

Three different fire models have been applied as thermal loading in the structure described above. All the applied models are analytical for a better estimation of the structure behaviour and comparison of the results. In the second case, only the two parametrical models have been applied to the structure with composite beams to compare the mechanical behaviour of different materials. In this paragraph, a description for each of the fire models used is given in details.

3.5.1. Standard fire

The first fire scenario of the structure is created by applying standard temperature-time curve as outlined in EN 1991-1-2:2002 as thermal load. This curve, also referred as ISO834 curve, is general and depends only on the duration of fire, despite the characteristics of the compartment. The standard temperature-time curve obtained from Eurocode (paragraph 2.3.1.3) and applied in the software model is shown in Figure 3.20:

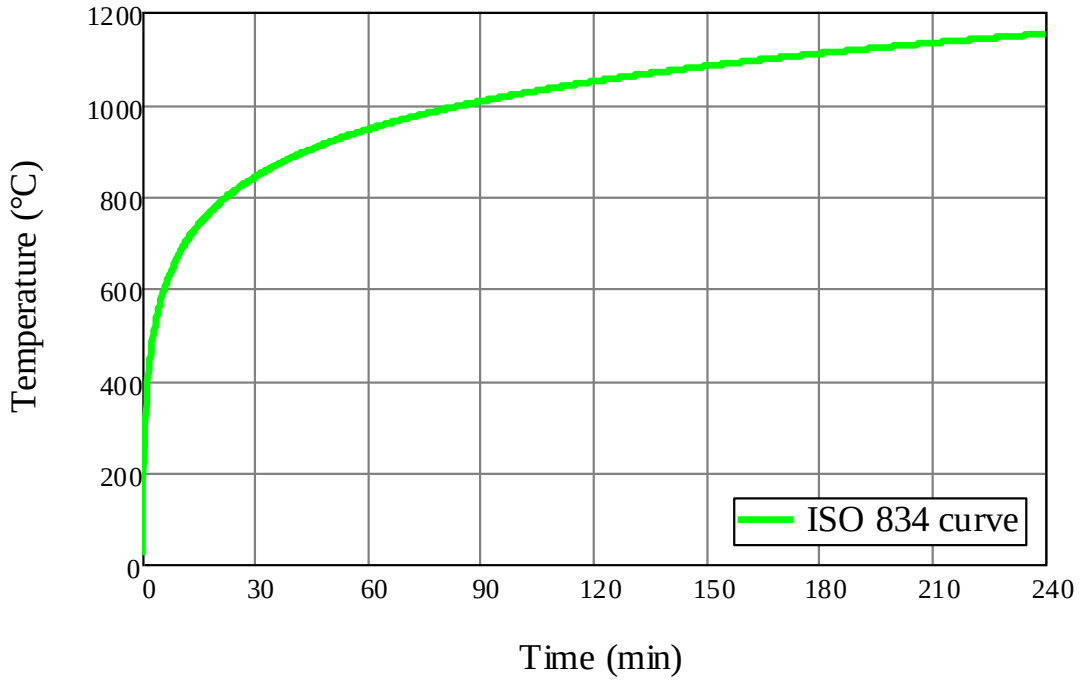

Figure 3.20. EN standard temperature-time curve

3.5.2. Parametric fire

The second fire load on the structure is applied by using parametric fire curve as specified in Annex A of Eurocode EN 1991-1-2:2002. As it can be seen from Figure 3.21, the heating phase of the curve reaches the post flash-over phase where the fire load density is completely burned out and after, due to ventilation, the cooling phase occurs.

As the name indicates, the parametric fire curve has been applied in the software model taking into account the following parameters:

- Compartment size is 10 × 13 = 130 m^2, height 3.6 m and ventilation area calculated as the sum of the four openings with the dimensions 1.2 × 3 m,
- Characteristic fire load density related to floor area, for office buildings for the 80% fractile case is taken $q_{f,k}$ = 511 MJ/m^2 (Table E.4 of Annex E of EN 1991-1-2:2002),
- The floor and ceiling are made from reinforced concrete and the walls from lightweight concrete (surface factor respectively $b = 2000\ J/(m^2s^{0.5}K)$ and $b = 1120\ J/(m^2s^{0.5}K)$).
- Medium fire growth rate is expected at $t_{lim} = 20\ min$. Fire is ventilation controlled because time to reach maximum temperature $t_{max} = 35\ min$ is bigger than t_{lim}.

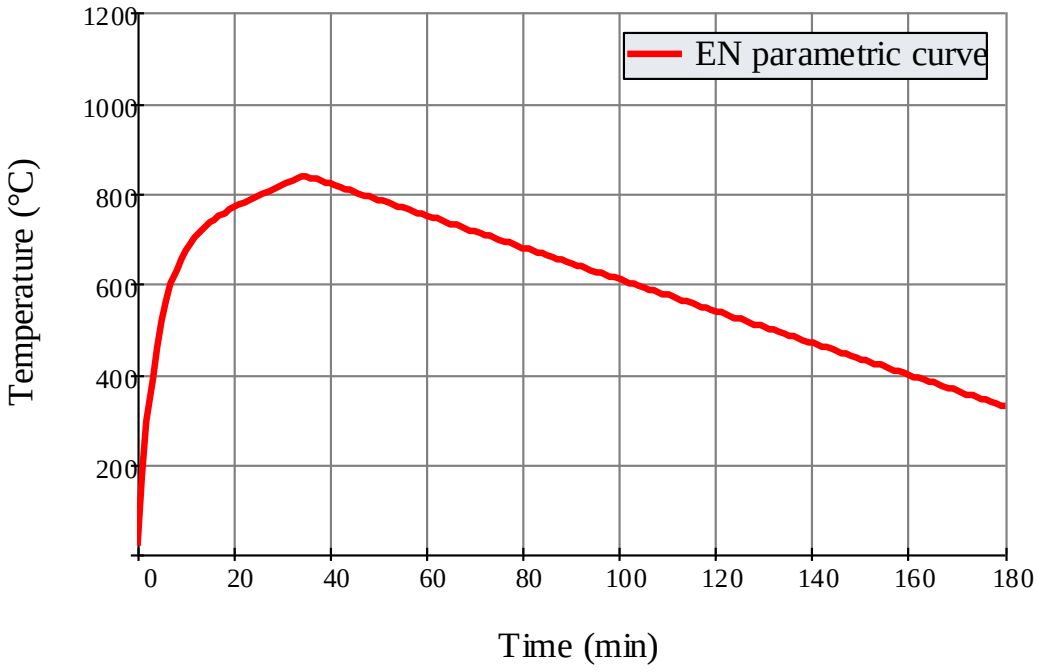

Figure 3.21. EN parametric temperature-time curve

3.5.3. Travelling fire

In order to find the most severe fire scenario for evaluating the mechanical behaviour of the structure, travelling fire model was applied as the third and last thermal load. For a better comparison of the results with the previous models, analytical inputs to simulate the travelling fire are used. The travelling fire model applied in the software is based on iBMB parametric fire curve (paragraph 2.3.2.2) which is developed by Zehfuss and Hosser (Germany, 2003) [13]. This curve takes also into account the boundary conditions. The build of parametrical iBMB curve is connected with the rate of heat release parameter which covers more clearly the description of fire than temperature-time curve.

The first step of building iBMB curve is defining rate of heat release curve according to Annex E of EN1991-1-2:2002. From it, three characteristic points of time t_1, t_2, t_3 which govern the change in the slopes for both curves are determined. Three temperature values T_1, T_2, T_3 are calculated for each of these time values and the graphs between each specified point are drawn according to Zehfuss functional description for ventilation-controlled fires. Both rate of heat release and temperature-time curves of the compartment are shown in Figure 3.22. Except the parameters which are used to define Eurocode parametric curve, data are taken also from Table E.5 of Annex E of EN 1991-1-2:2002 to determine the rate of heat release curve:

- Time needed to reach a rate of heat release of 1 MW is $t_\alpha = 300s$ and maximum rate of heat release $RHR_f = 250\ kW/m^2$ for office occupancy and medium fire growth rate.

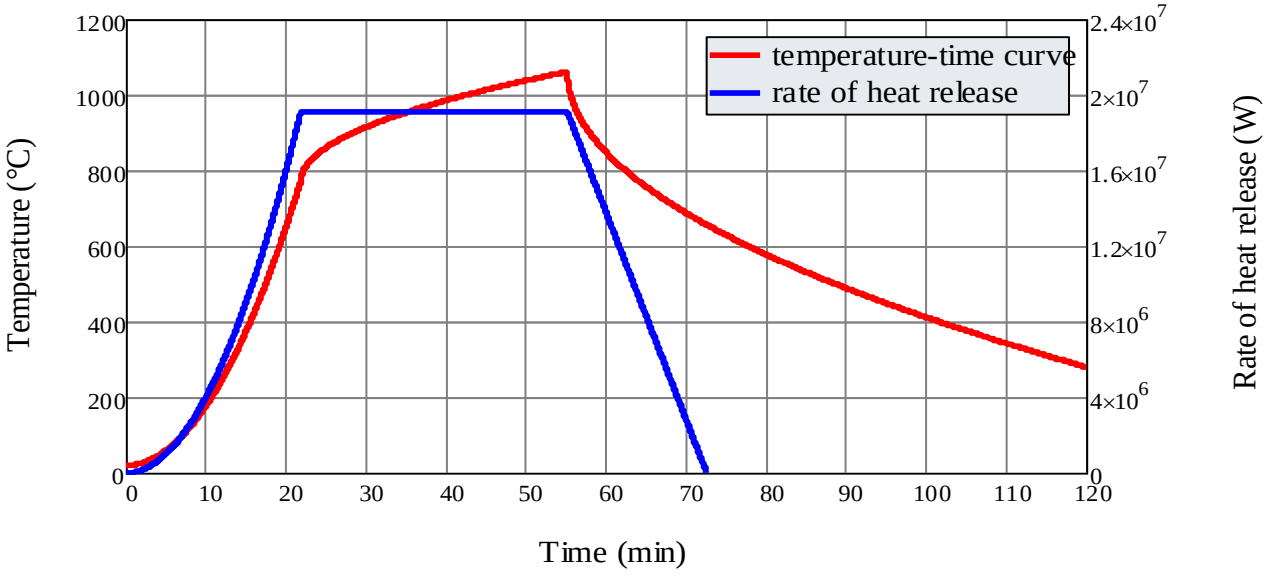

Figure 3.22. Relationship of heat release rate curve and iBMB temperature-time curve

In order to simulate travelling fire, principles of Travelling Fires Methodology (TFM) have been used. The enclosure is divided into three temperature fields and a iBMB parametric curve has been assigned to each of them taking fire load density shared equally between

fields. The assumption that the fire spreads in one horizontal direction within the enclosure and uniform temperature distribution in the second direction for each field is done. Each field is presented by one temperature-time curve. The first offset between curves is done for time t_1 which is the time when heat release rate reaches the maximum value. In reality, with only this shift, all the curves will start at ambient temperature which is not accurate because the pre-heating from neighbouring fields is not taken into account. Tests have shown that flames in small or medium compartments cause elevated temperatures also in other parts of the compartment which are not in flames yet. For this reason, the value of far field temperature T_{ff} according to Stern-Gottfried formulae (2.41) is defined and it is considered to be the second field temperature at time t_1. To realise this, the curve is shifted back so the field temperature at time t_1 will be T_{ff} and a linear line is drawn from the beginning of the fire till this point. The same procedure is repeated for the third field temperature considering the temperature of this field is influenced from the fire in first and second field. Described methodology of applying the travelling fire analytically was introduced by Horová [1].

In the analysis, four different types of travelling fires have been applied to the structure; two of them spreading horizontally in X and Y direction, one starting in the corner of the structure and spreading to the entire compartment and one starting in the centre of the structure and spreading to the sides. In the last case, although the fire does not spread linearly as the assumption is made, this method was applied because the same procedure was followed like all the other cases; the compartment is divided in three equal areas and the same fire load density was applied to all them. For each of the cases, different curves of travelling fire have been developed as far field temperature for second and third field depends on the distance from the centre of the fire. In Figure 3.23, the fire curve which is applied for travelling fire spreading in Y direction of the structure is shown.

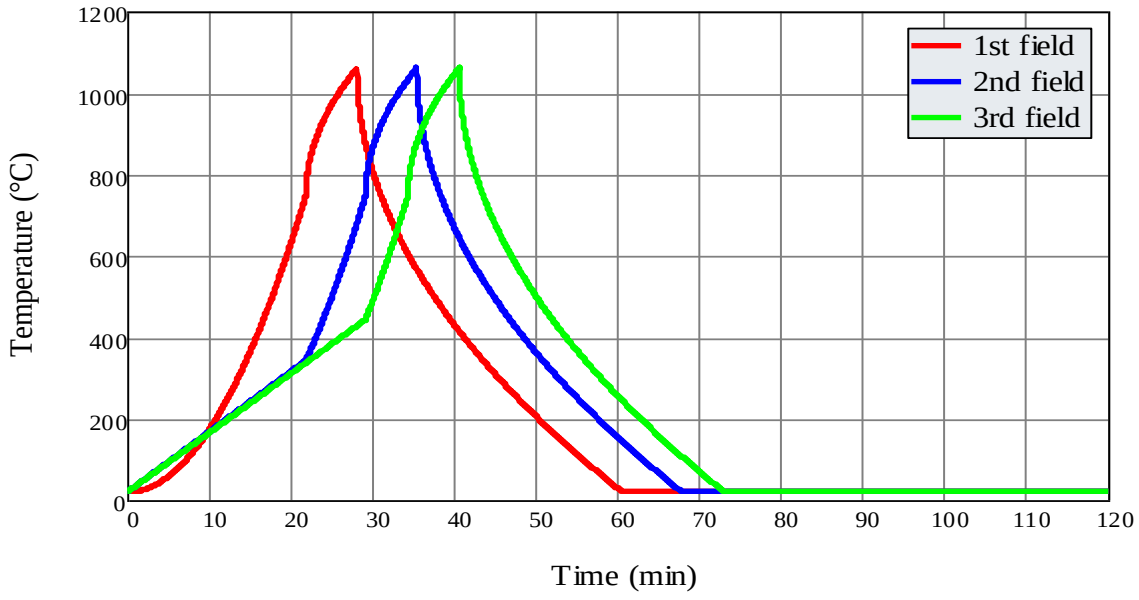

Figure 3.23. Travelling fire curve spreading in Y direction applied in the structure

From the figure it can be observed that the travelling fire curve reaches higher peak temperatures, however its growth is slower and decay period is faster comparing with EN parametric curve model.

3.6. Case study 1 - steel beams

All the analyses performed in the described structure with steel beams are listed in Table 3.2. Flame exposure period of 60 min for verification of R60 has been applied to all the cases. Except EN standard and parametric fire curves, four possible ways of travelling fire have been modelled; two according X and Y direction, one for fire starting to the corner of the structure and spreading to the other parts and one for fire starting in the centre of the structure and spreading to the sides.

Name	Material model	Load [kN/m^2]	Heating regime		Beam-slab connectors
Str_1a	EC2, EC3	5	EN 1991-1-2	Standard fire curve	No
Str_2a	EC2, EC3	5	EN 1991-1-2	Parametric fire curve	No
Str_3a	EC2, EC3	5	Travelling fire curve	Spread in X-direction	No
Str_4a	EC2, EC3	5	Travelling fire curve	Spread in Y-direction	No
Str_5a	EC2, EC3	5	Travelling fire curve	Spread from corner to all str.	No
Str_6a	EC2, EC3	5	Travelling fire curve	Spread from centre to sides	No

Table 3.2. Table list of performed analysis for steel beams

Results of the analyses for vertical displacements at ¼ and ½ length of the primary beam in axis 2 (node 137 and 287) and axial force of this beam at the support and mid-span (beams 14 and 56) in different times of fire are given for each fire case in the subparagraphs below.

3.6.1. EN standard fire curve

The EN standard fire curve was generated automatically from the software (Figure 3.24) and applied to the entire structure. This curve is general and depends only on the duration of fire, despite the characteristics of the compartment.

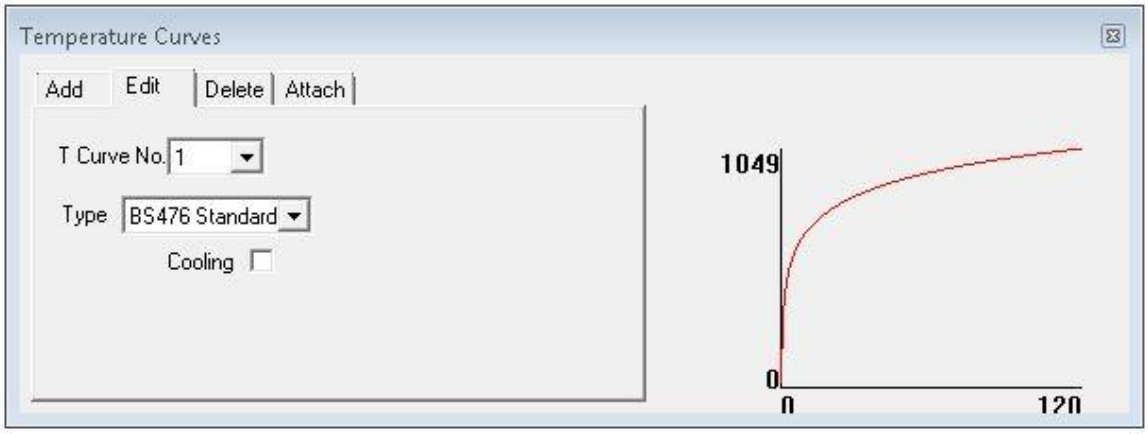

Figure 3.24. Standard fire curve (ISO 834) applied to the structure

The results of the analysis for deflections of the primary beam for EN standard fire curve are given in Figure 3.25.

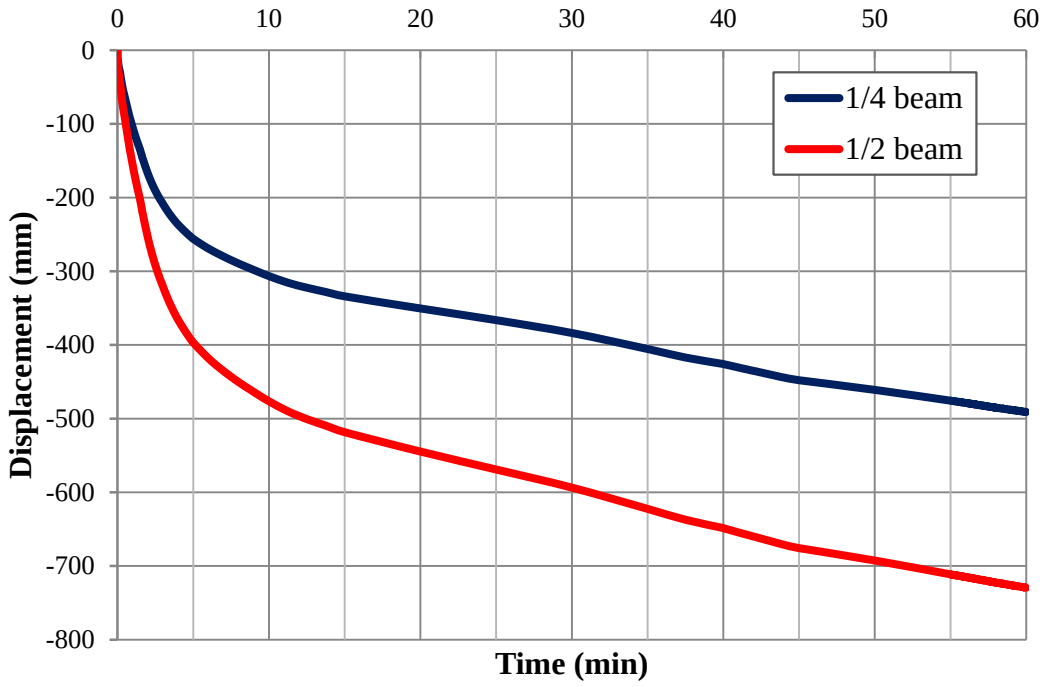

Figure 3.25. Deflection of the beam on axis 2 (Str-1a)

The results of the analysis for axial forces of the primary beam for EN standard fire curve are given in Figure 3.26.

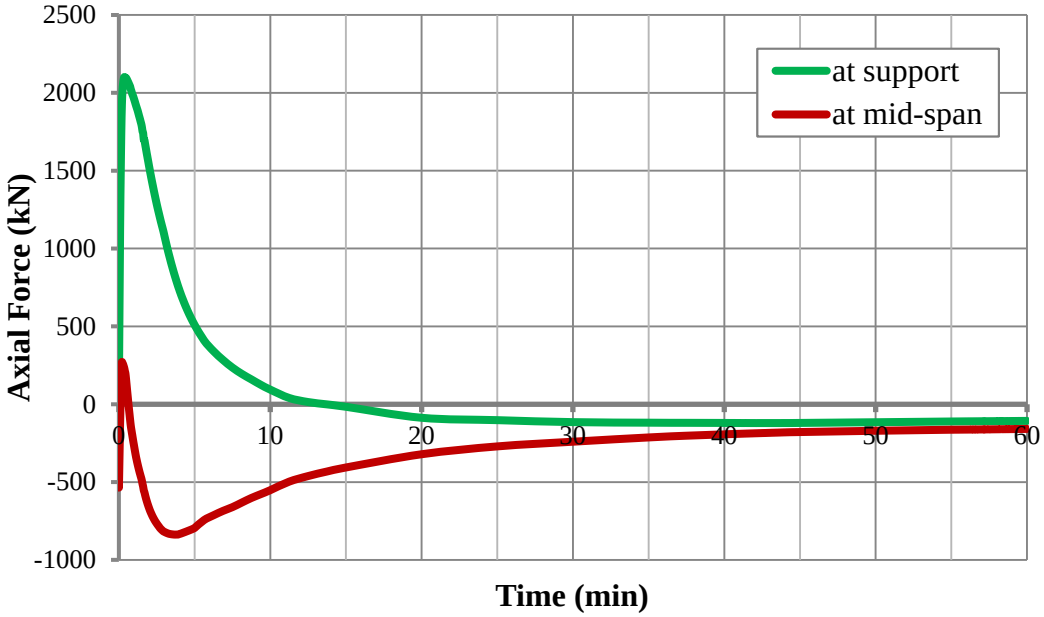

Figure 3.26. Axial force of the beam on axis 2 (Str-1a)

3.6.2. EN parametric fire curve

The EN parametric fire curve was also generated directly from the software by inserting the compartment parameters shown in Figure 3.27. Also this curve is based on homogenous temperature which is applied uniformly to the structure.

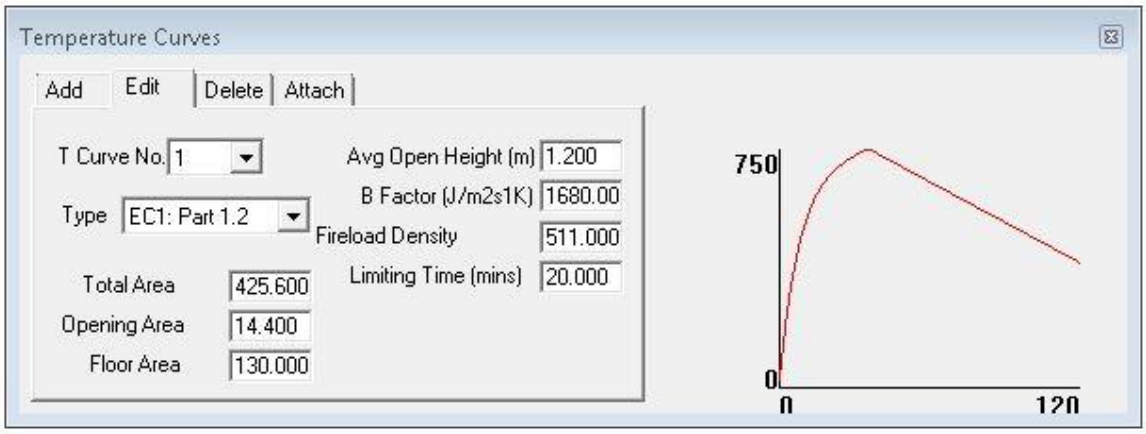

Figure 3.27. Parametric fire curve (EN1991-1-2) applied to the structure

The results of the analysis for deflections of the primary beam for EN parametric fire curve are given in Figure 3.28.

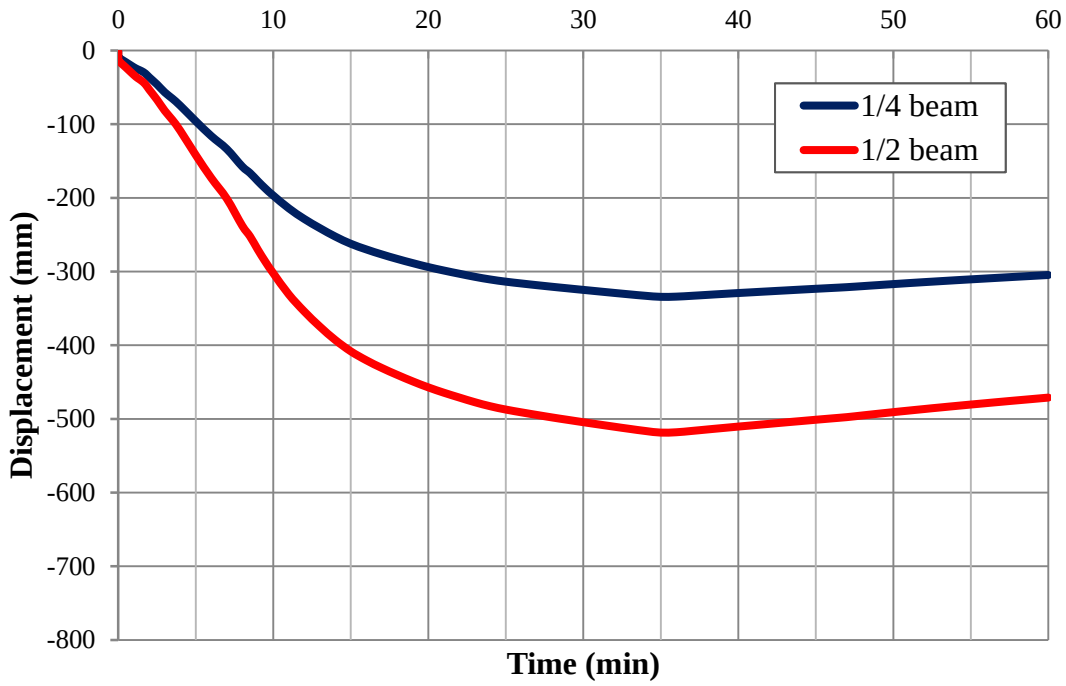

Figure 3.28. Deflection of the beam on axis 2 (Str-2a)

The results of the analysis for axial forces of the primary beam for EN parametric fire curve are given in Figure 3.29.

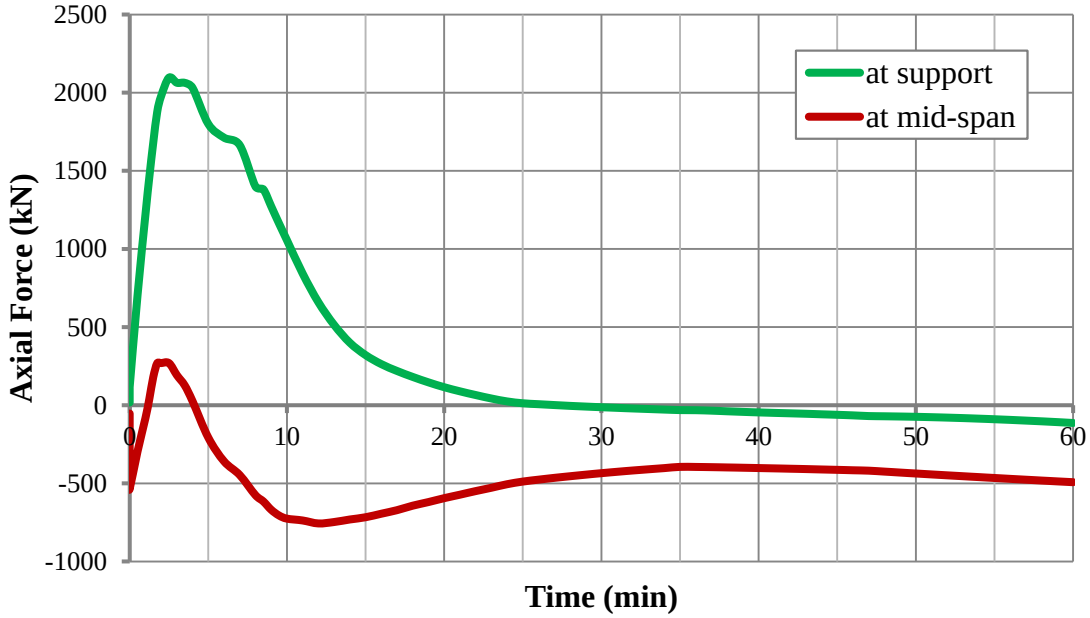

Figure 3.29. Axial force of the beam on axis 2 (Str-2a)

3.6.3. Travelling fire curve in X direction

The travelling fire curve was built using the procedure described in paragraph 3.5.3. Three component temperature-time curves have been created for each compartment field and have been applied manually to each beam and slab that lies in that field. The three component curves of travelling fire in X direction and the fields where these curves are applied are shown in Figure 3.30. It is assumed that the fire occupies full length of the compartment and moves alongside the width.

Note: Peak temperature for the three curves should be the same but in the figures they are slightly different because the time discretisation in creating the curves is in every 1 minute.

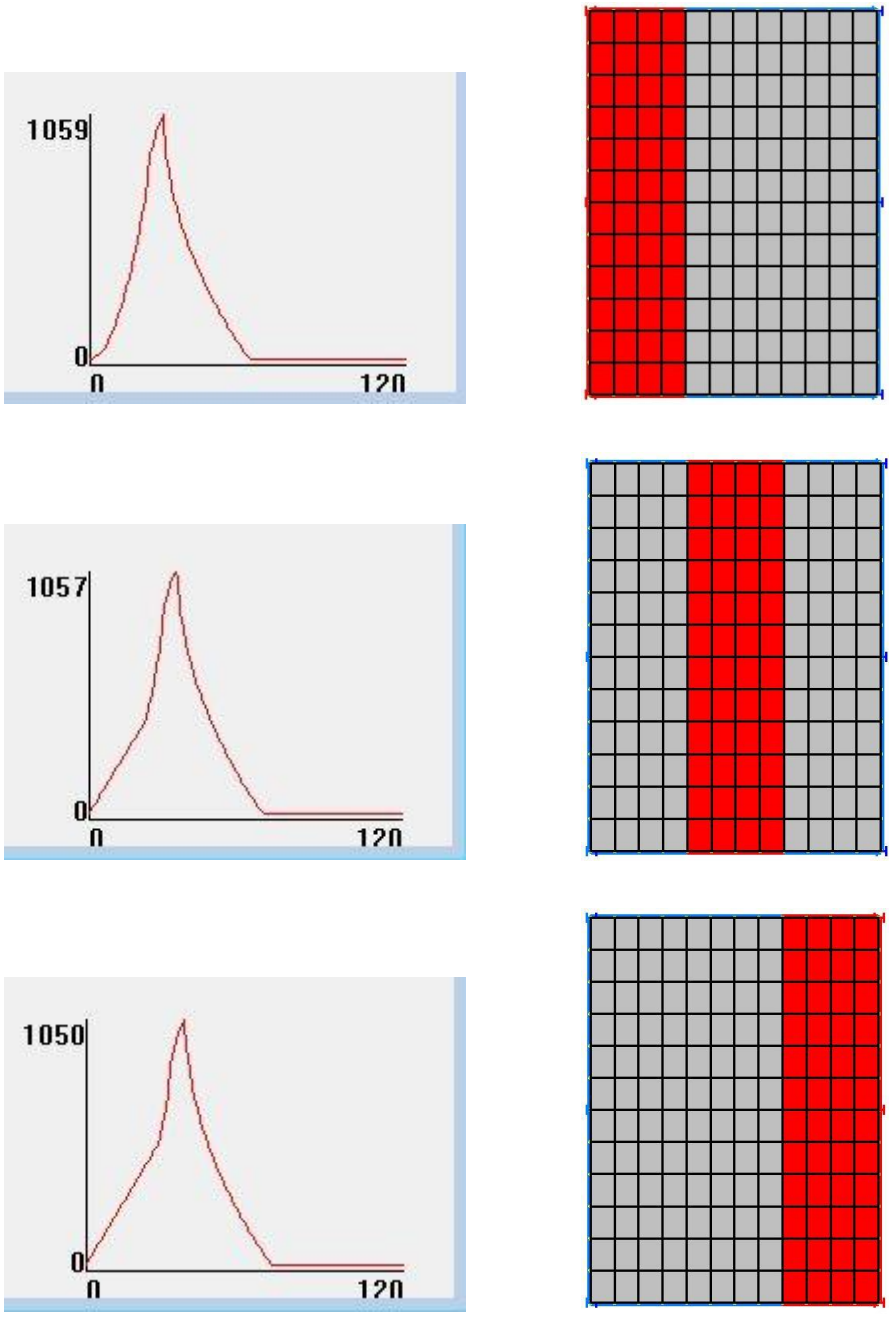

Figure 3.30. Three fire curves and respective fields for fire spreading in X direction

The results of the analysis for deflections of the primary beam for fire spreading in X direction are given in Figure 3.31

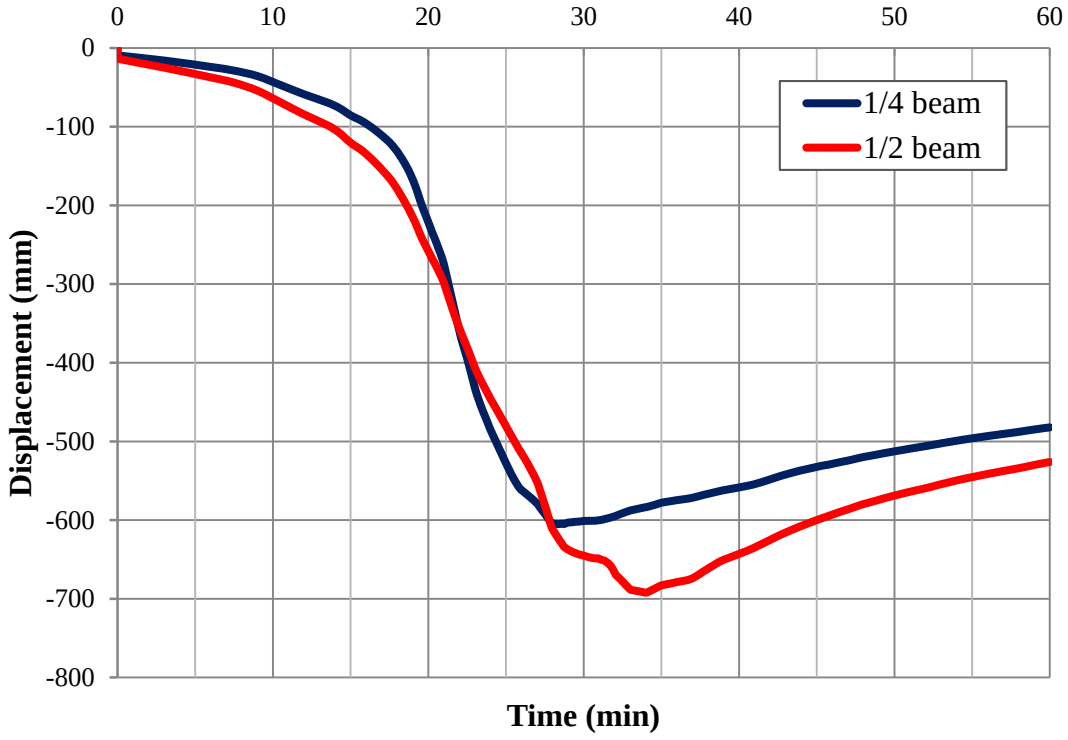

Figure 3.31. Deflection of the beam on axis 2 (Str-3a)

The results of the analysis for axial forces of the primary beam for fire spreading in X direction are given in Figure 3.32

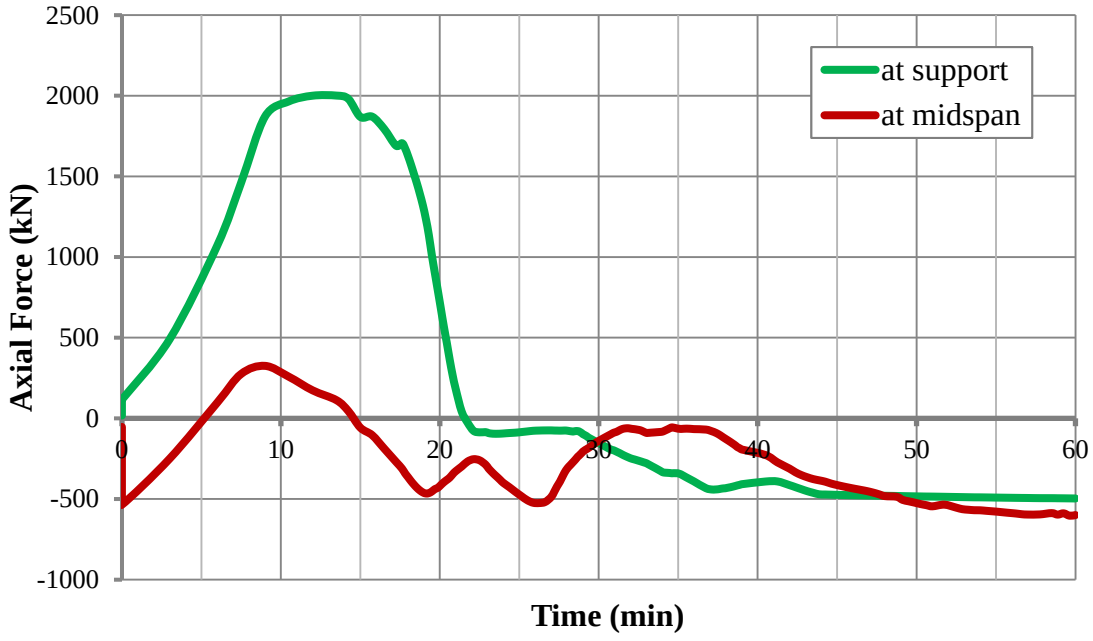

Figure 3.32. Axial force of the beam on axis 2 (Str-3a)

3.6.4. Travelling fire curve in Y direction

The same procedure was followed to apply the travelling fire at the structure in Y direction. The curve applied to the first field is identical with the first curve applied in X direction as the field area and fire load density are the same. The difference appears in building fire curves for second and third field where the distances of these fields from the centre of fire are different. The three component curves of travelling fire in Y direction and the fields where these curves are applied are shown in Figure 3.33.

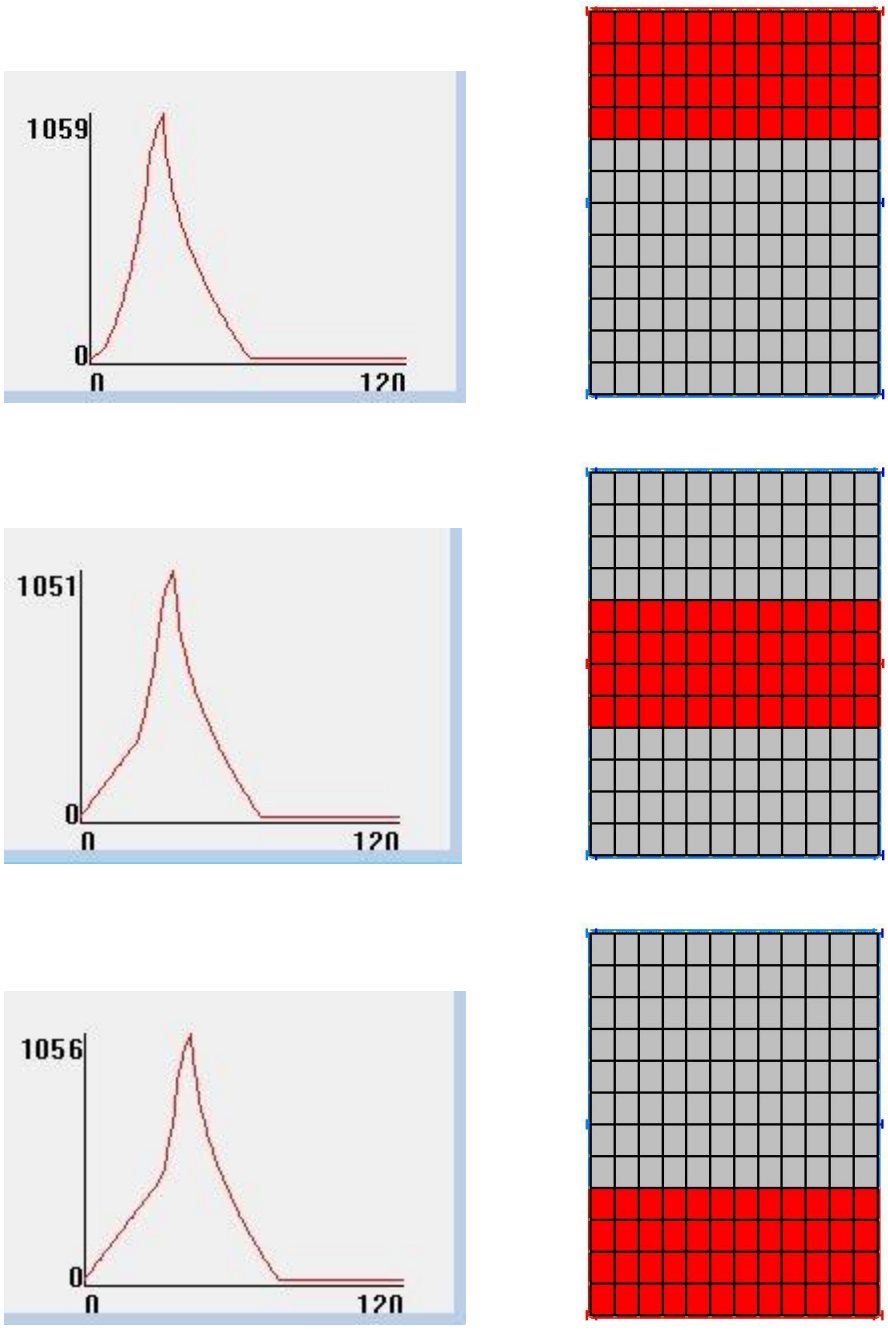

Figure 3.33. Three fire curves and respective fields for fire spreading in Y direction

The results of the analysis for deflections of the primary beam for fire spreading in Y direction are given in Figure 3.34.

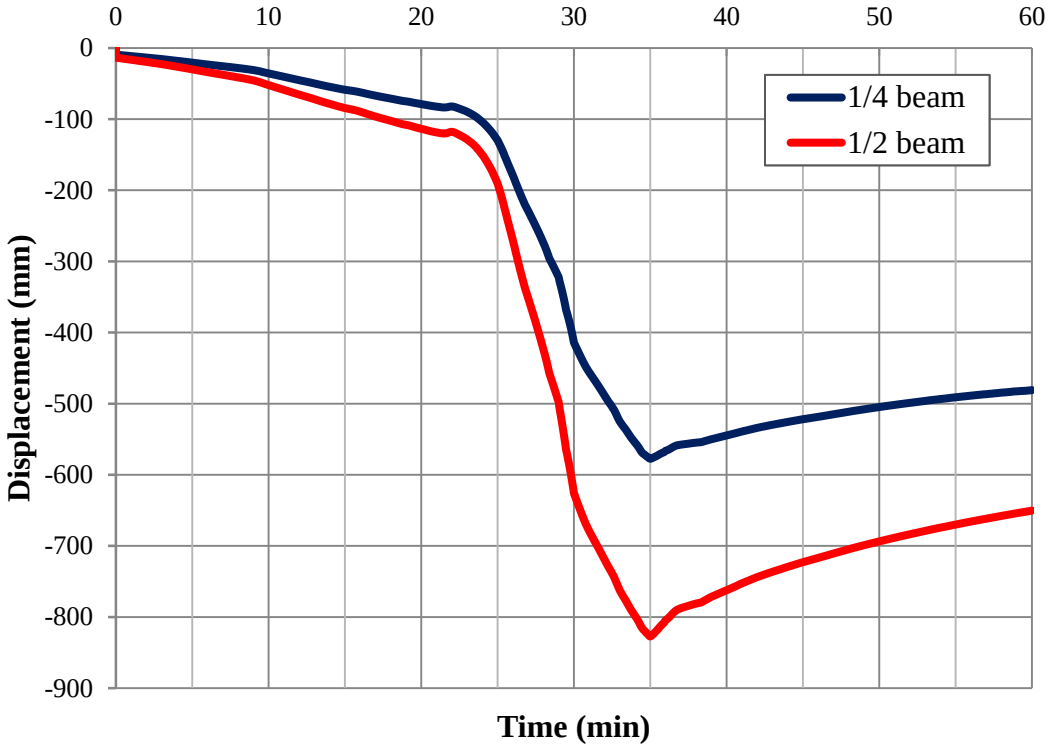

Figure 3.34. Deflection of the beam on axis 2 (Str-4a)

The results of the analysis for axial forces of the primary beam for fire spreading in Y direction are given in Figure 3.35.

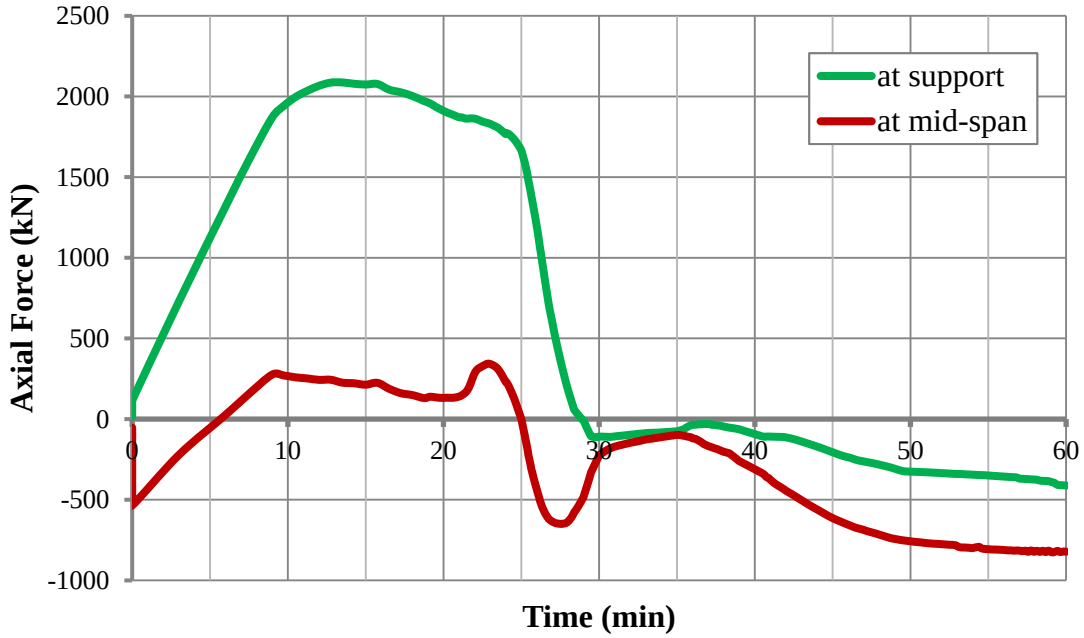

Figure 3.35. Axial force of the beam on axis 2 (Str-4a)

3.6.5. Travelling fire curve from corner to all structure

The same procedure was followed to apply travelling fire that starts at the corner of the compartment and spread all over it. Like in previous spreading fire cases, the compartment has been divided in three fields with equal areas. The curve applied to the first field is identical with the other first curves applied in all previous cases while the second and third field curves differ because their distances from the centre of fire differs as well. The three component curves of travelling fire for this case and the fields where these curves are applied are shown in Figure 3.36.

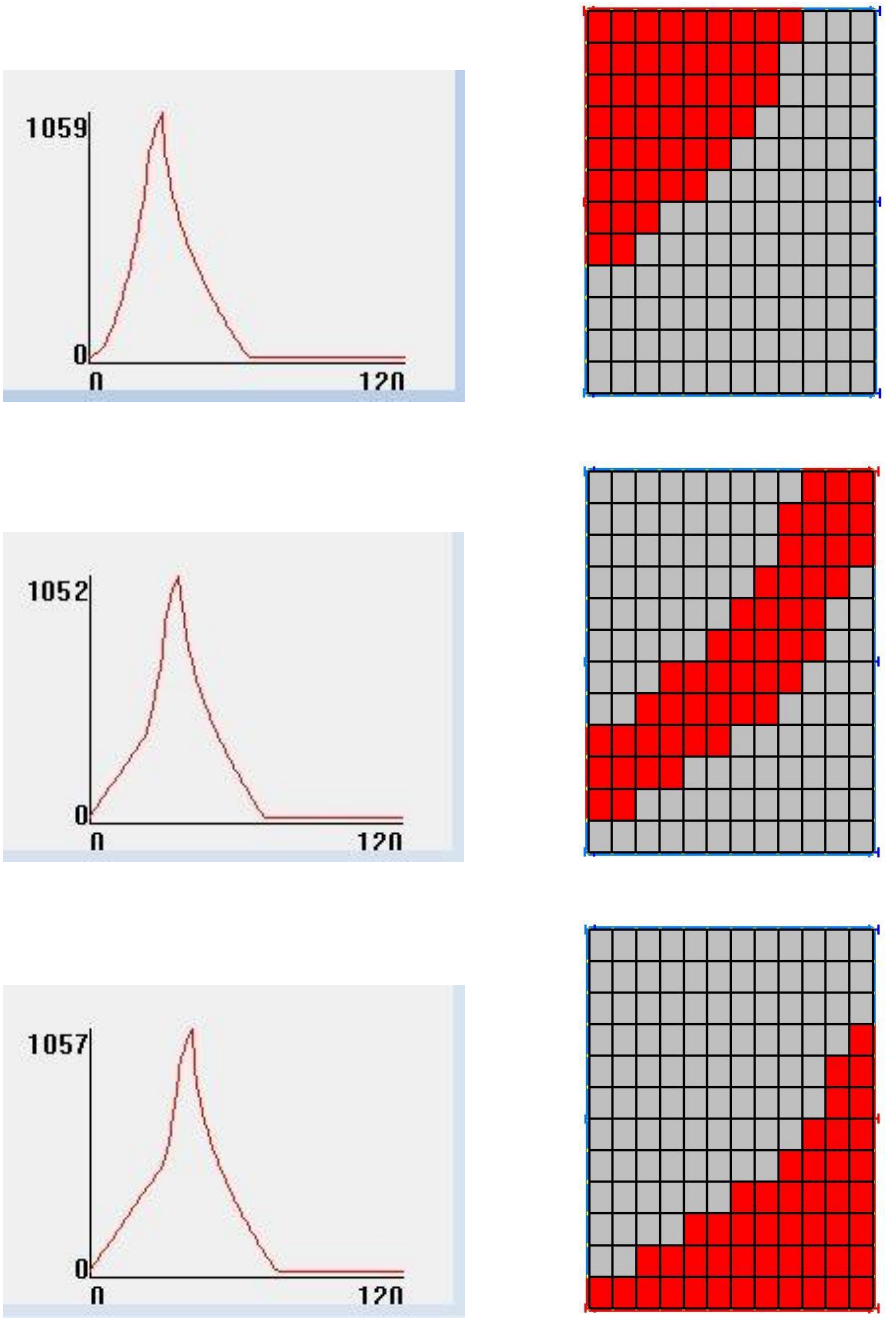

Figure 3.36. Three fire curves and respective fields for fire spreading from corner to all structure

The results of the analysis for deflections of the primary beam for fire spreading from corner to all structure are given in Figure 3.37.

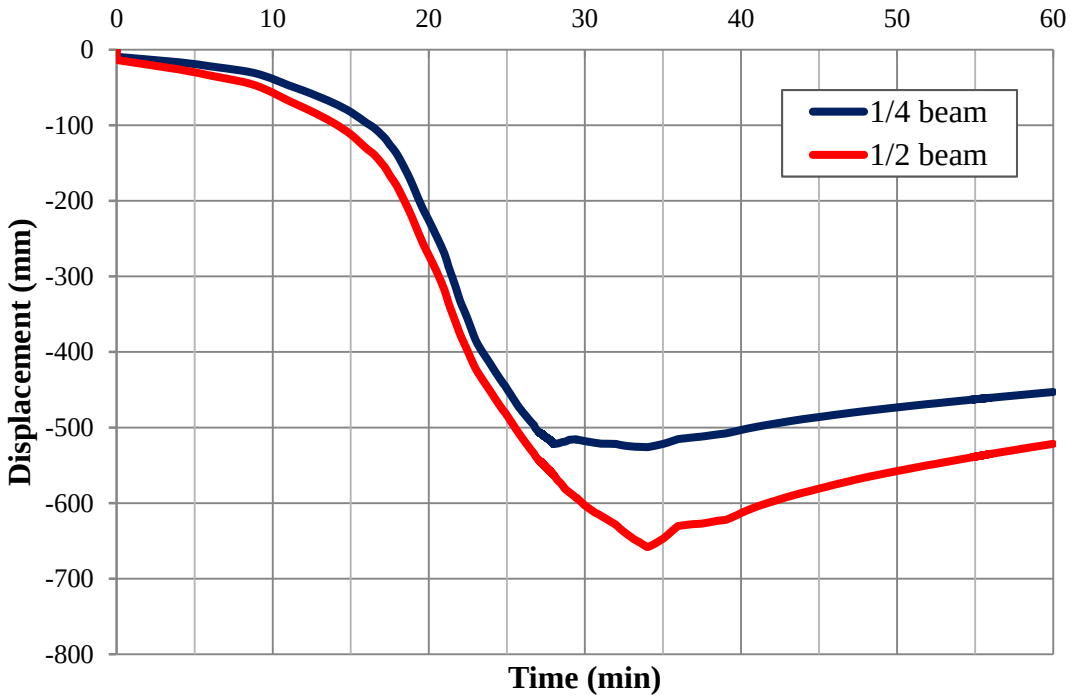

Figure 3.37. Deflection of the beam on axis 2 (Str-5a)

The results of the analysis for axial forces of the primary beam for fire spreading from corner to all structure are given in Figure 3.38.

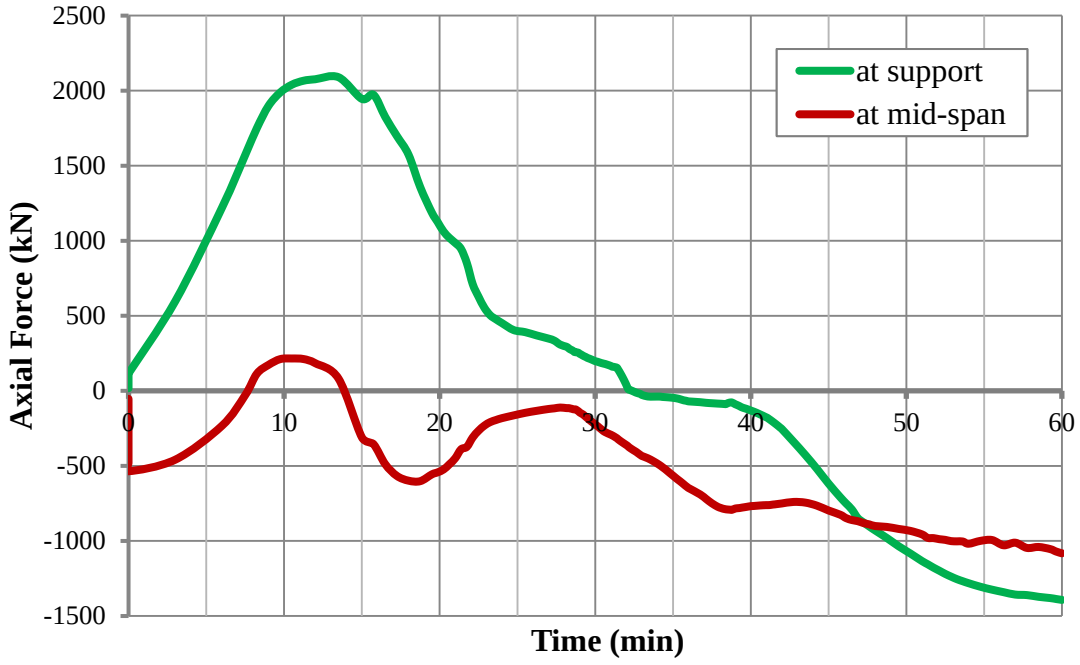

Figure 3.38. Axial force of the beam on axis 2 (Str-5a)

3.6.6. Travelling fire curve from centre to the sides

The last model of travelling fire applied to the structure is the one that starts at the centre of the compartment and spreads to the sides of it. The division of the compartment in fields is done with the principle of having the same area for each of the fields. The curve applied to the first field is similar with the other first curves applied in previous cases. To build the second and third curve, the shortest distance from the centre of the fire is taken into account to achieve higher values of far field temperatures. The three component curves of travelling fire for this case and the fields where these curves are applied are shown in Figure 3.39.

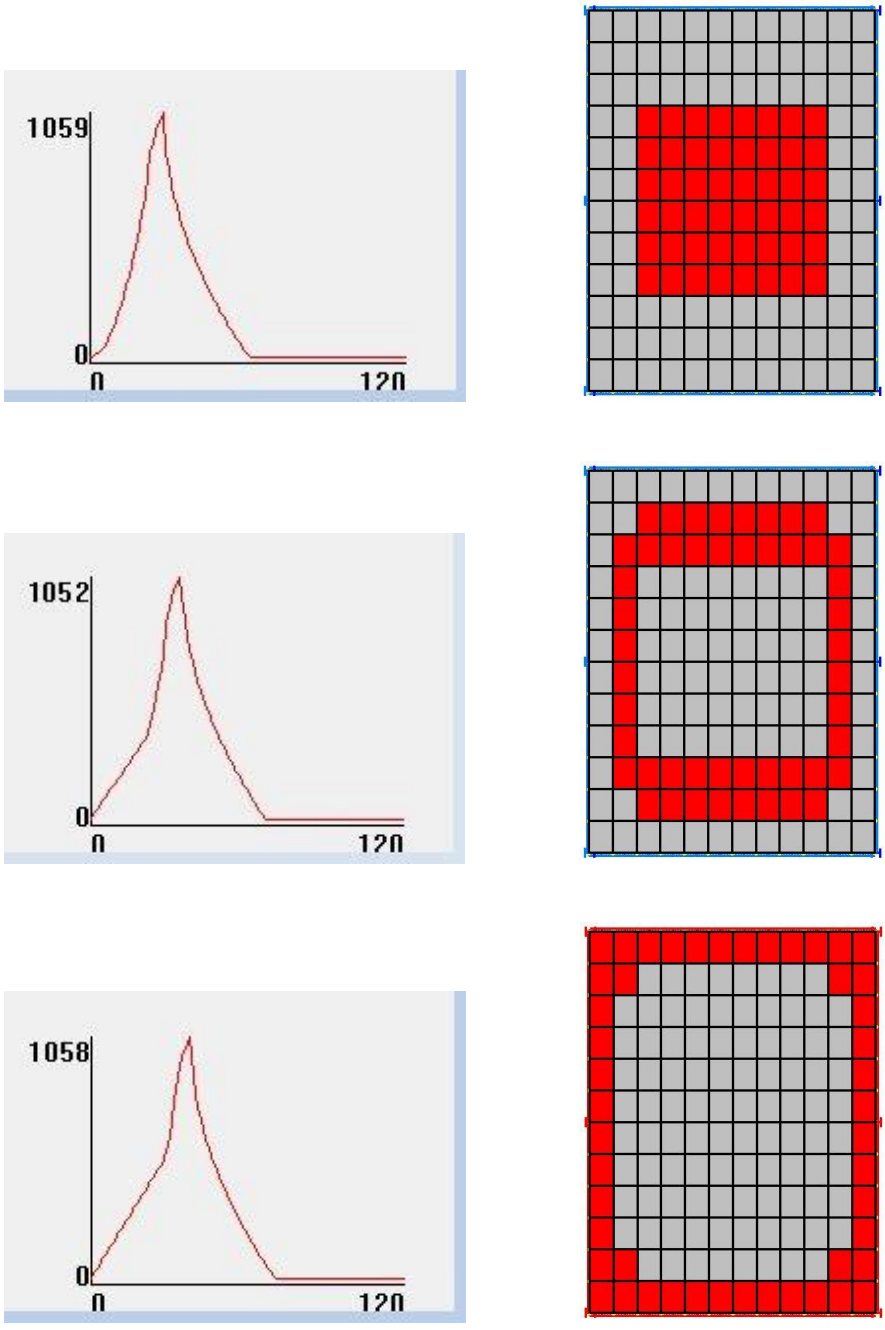

Figure 3.39. Three fire curves and respective fields for fire spreading from centre to sides

The results of the analysis for deflections of the primary beam for fire spreading from centre into sides are given in Figure 3.40.

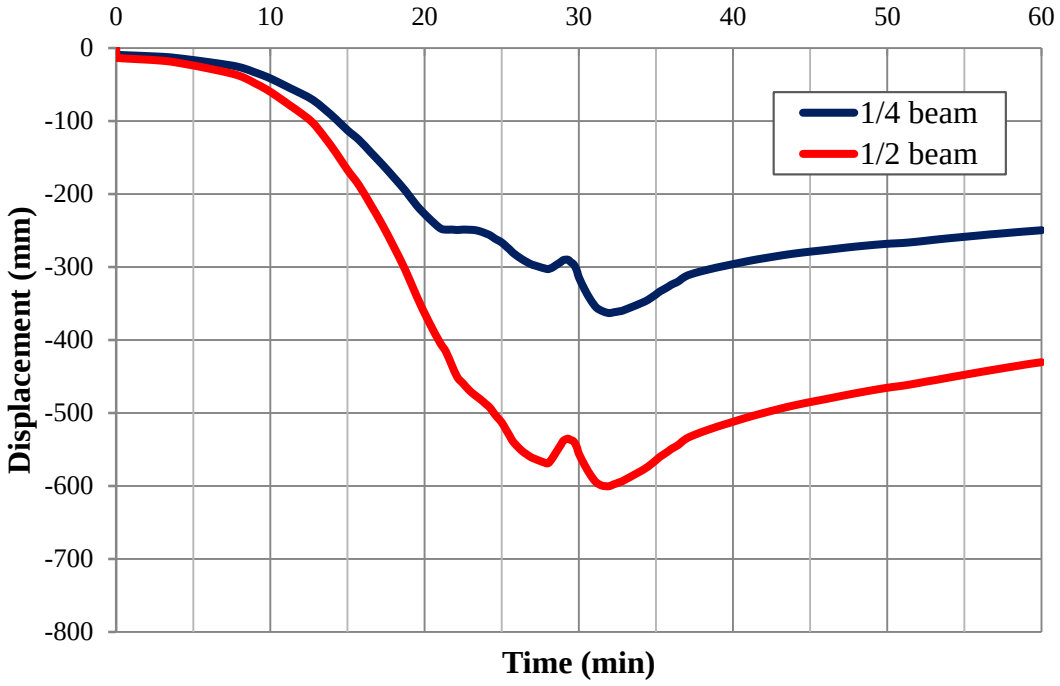

Figure 3.40. Deflection of the beam on axis 2 (Str-6a)

The results of the analysis for axial forces of the primary beam for fire spreading from centre into sides are given in Figure 3.41.

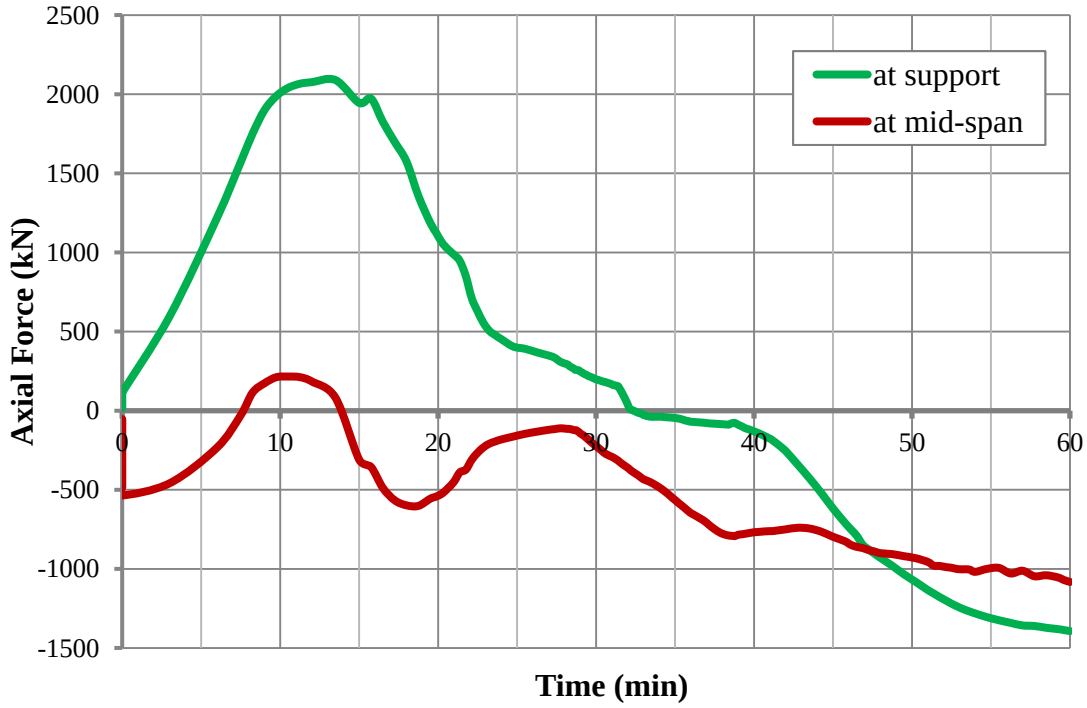

Figure 3.41. Axial force of the beam on axis 2 (Str-6a)

3.6.7. Comparison of results

3.6.7.1. *Deflections at 1/2 length of the beam*

The curves of deflection, measured in the mid-span of the primary beam on axis 2 during the cases of travelling fire are presented in Figure 3.42.

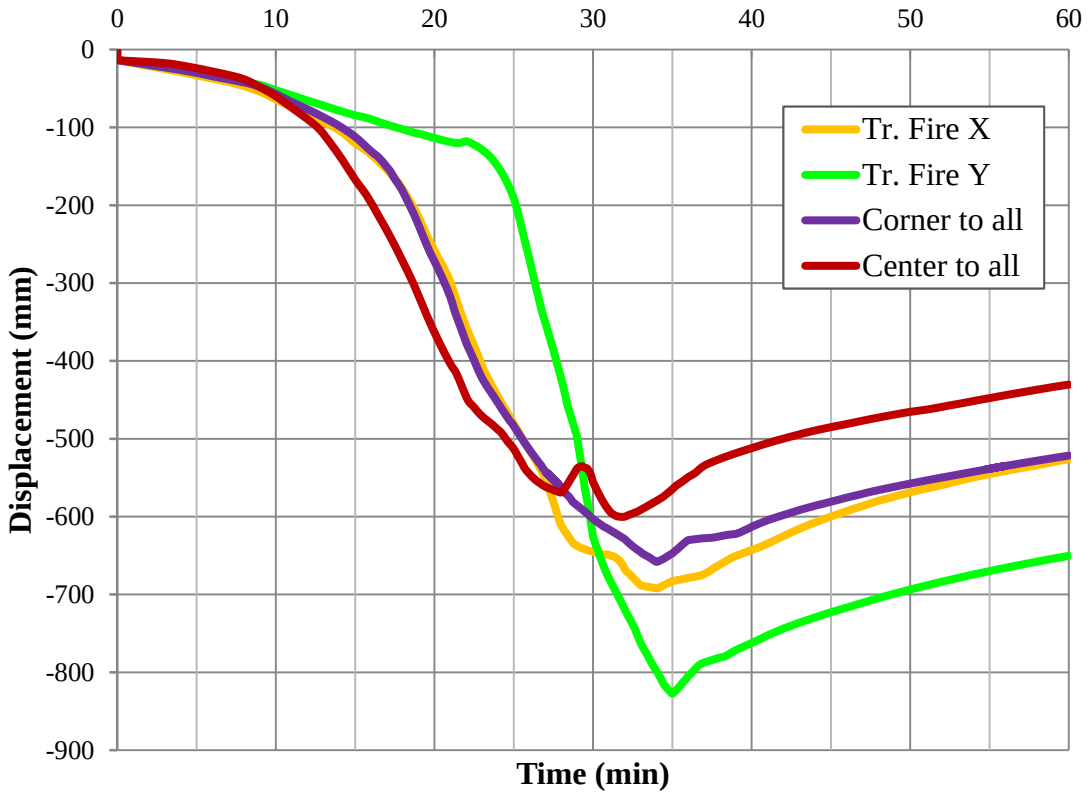

Figure 3.42. Deflections in the midpoint of the beam during travelling fire cases

At the first sight, it can be noticed from the figure that the deflection curve for each travelling fire case has three phases: at the beginning deflections increase moderately and afterwards their values increase rapidly. After reaching the maximum value, deflections decrease similarly in the four cases due to the start of cooling phase in the three fields. The residual deflections at the time of 60 minutes are about 170 mm smaller than the peak temperature values. All four travelling fire cases reach the peak values between 30 and 35 min which is the interval of time when the second field reaches the peak temperature value. From the curves it can be noticed that the highest value of deflection is 820 mm and it is obtained from the fire spreading in the Y direction. This result is predictable because the beam lies in Y direction and it is heated uniformly among all his length at this fire scenario. Because of this fact, the rapid increase of deflection value during fire spread in Y direction is shifted more in time (at minute 22) in comparison with other cases.

Figure 3.43 shows the deflections in mid-span of the beam for three thermal loading cases: EN standard temperature-time curve, EN parametric curve and travelling fire case with highest value of deflection.

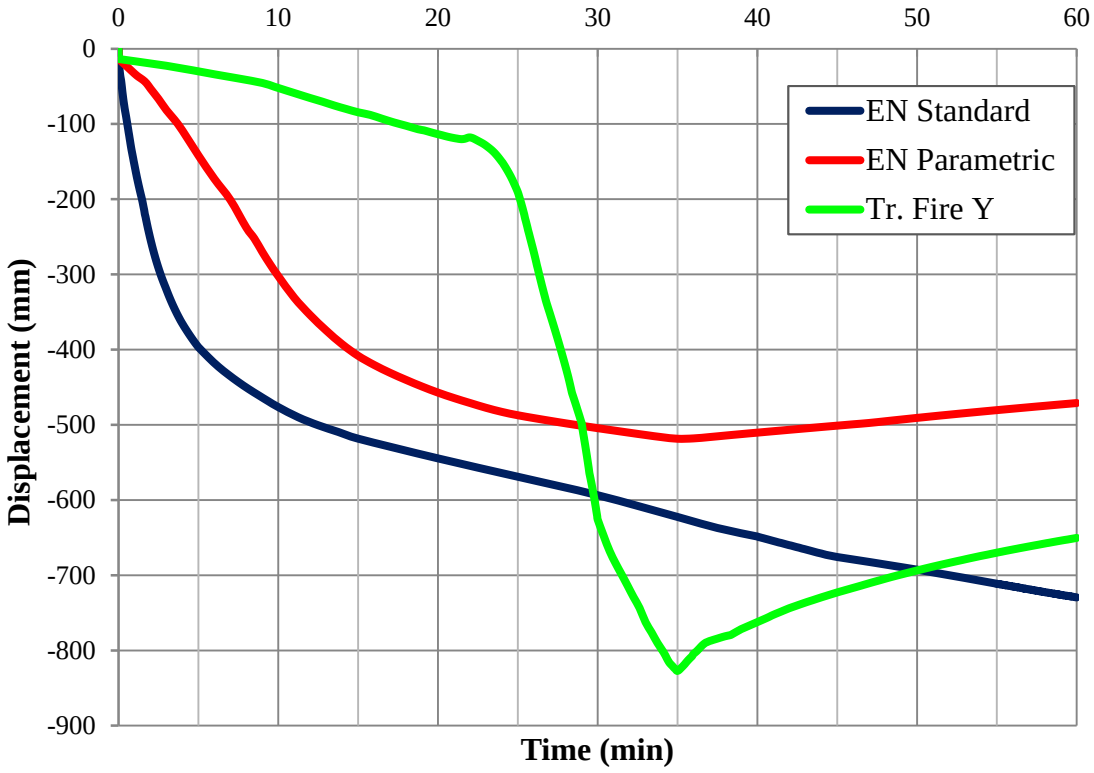

Figure 3.43. Deflections in the midpoint of the beam during different fire models

As it can be seen from the figure, the highest value of deflection is registered during travelling fire case. This result is very important because it shows that the travelling fire model presents the most severe fire scenario case in comparison with the other parametric model presented by Eurocode. The deflection difference between the two models is around 300 mm which is a very significant value. Also peak deflection value measured during travelling fire is higher than the value obtained by applying standard curve. This conclusion cannot be generalised because standard curve is universal and does not depend on compartment parameters but this case is a good example to show that travelling fire gives more severe results than both methods described in Eurocode. At the end of the exposure period of 60 min, the residual deflection obtained from standard curve is higher than the other cases as it has no cooling phase. Residual deformation caused by parametrical model is around 200 mm smaller than residual deformation caused from travelling fire. By comparing the continuity of the curves, it can be easily noticed that both Eurocode models have faster increase of deflections at the start of the fire while deflections during travelling fire increase moderately in the first minutes and rapidly after minute 22. At this time, deflection value during travelling fire is significantly smaller than the other methods. In case of requested fire resistance of short period, for example 15min, Eurocode models are recommended to be used.

3.6.7.2. *Deflections at 1/4 length of the beam*

The curves of deflection, measured in the 1/4th of the length of the beam on axis 2 during the cases of travelling fire are presented in Figure 3.44.

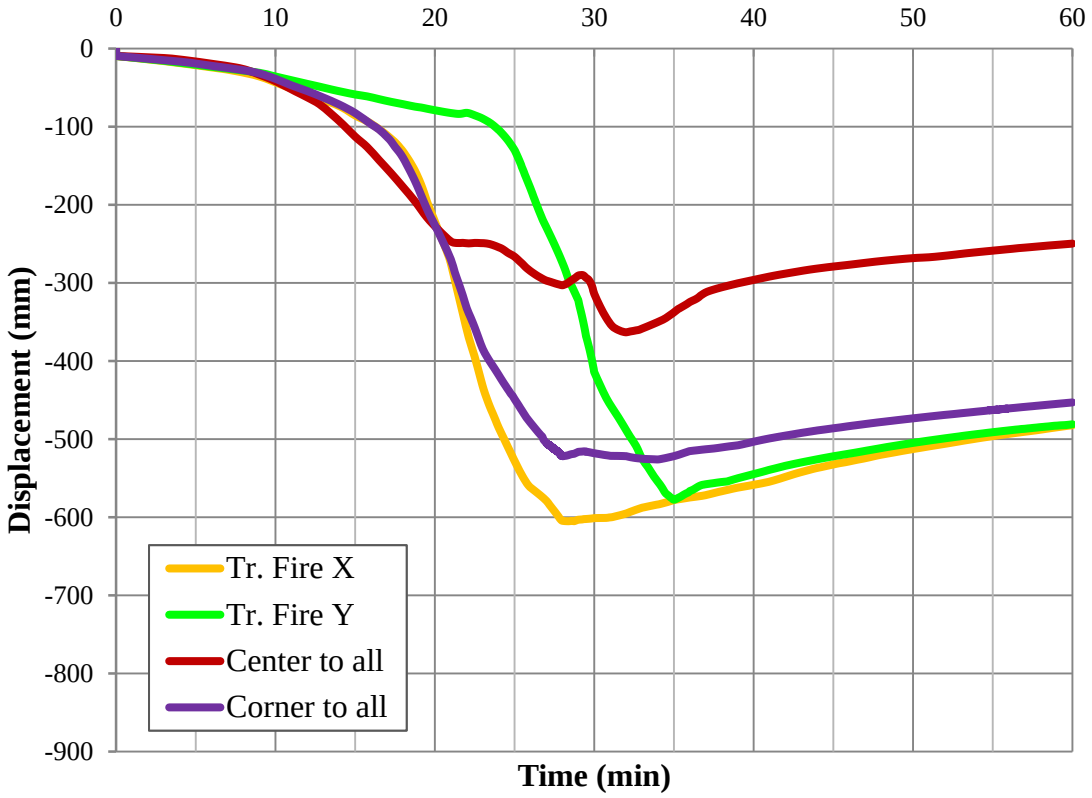

Figure 3.44. Deflections at the 1/4th of the beam length during travelling fire cases

From the figure it can be noticed that the deflection curve for the node at 1/4th of the length follows the same continuity as the mid-point of the beam; firstly the deflections are moderate, then increase rapidly and after reaching the peak value, the deformations get smaller at the end of the 60 min due to cooling phase. The deflection peak value for this point is obtained from the travelling fire in the X direction as in this case, it is situated at the first field affected from fire. Meanwhile for the midpoint, the peak deflection was obtained from travelling fire in Y direction. From the observation that different travelling fire scenarios gives the most severe results for different points of the structure, it can be concluded that multiple travelling fire scenarios have to be taken into account. The same as for midpoints, the rapid increase of deflection when travel spreads in Y direction is shifted in time in comparison with other cases as the entire beam is situated in the second field and not influenced significantly at the start of the fire.

Figure 3.45 shows the deflections in 1/4th of the length of the primary beam for three thermal loading cases: EN standard temperature-time curve, EN parametric curve and travelling fire case with highest value of deflection.

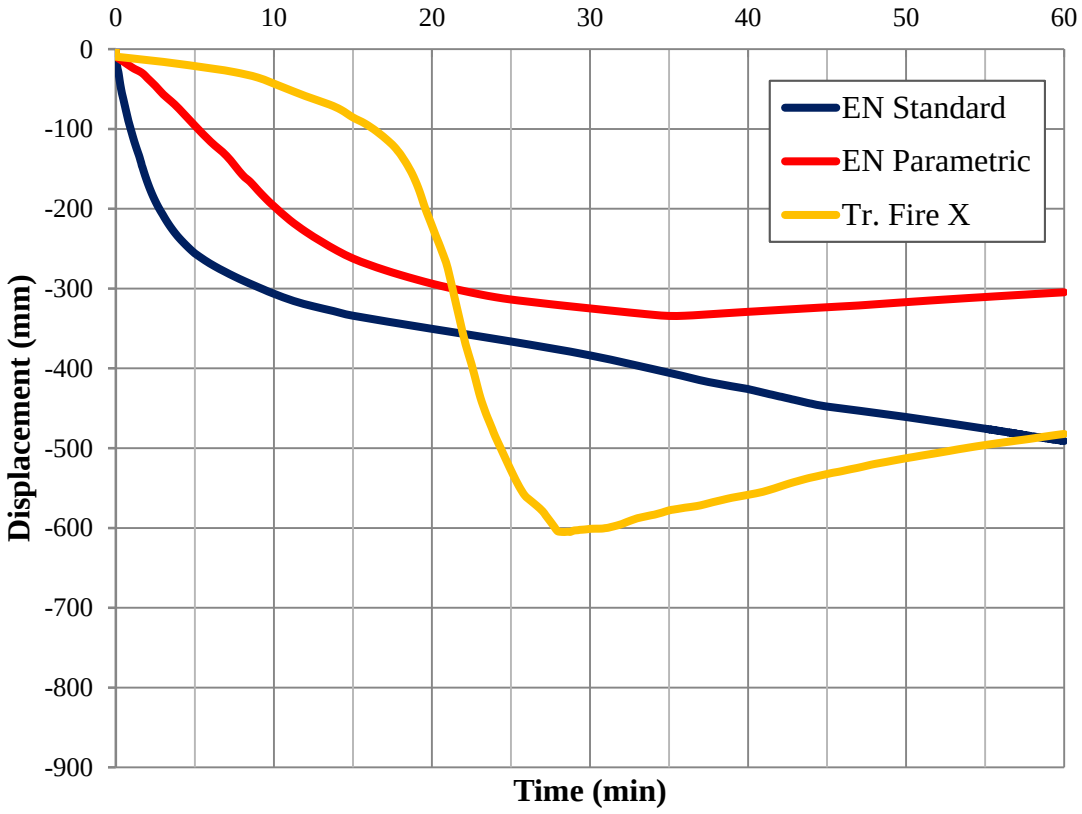

Figure 3.45. Deflections at the 1/4th of the beam length during different fire models

Also at this comparison of values, maximum deflection is presented during travelling fire scenario. The peak value is obtained during fire travelling at X direction and the time of reaching this value is the time when the first field reaches maximum temperature (the node is situated in the first field). Also during fire spreading in X direction, the difference in peak deflection values between nodes situated at 1/4th and 1/2nd of the length of the beam is very small (less than 100 mm) and at a certain time, deflections on quarter of the length exceed deflection in the middle. The observation that the deflection curvature is not symmetrical to the centre of the beam during travelling fire leads to the conclusion that several spreading fire cases should be taken into account to determine the worst scenario. The same resultss are observed as for the midpoint: at start of the fire, deflection increases more rapidly by applying traditional models. For small period of requested fire resistance, traditional models give the most severe cases in comparison with travelling fire scenarios. The difference in deflections between parametrical model and travelling fire is significant regarding the curve shape and also the residual values which differ 180 mm at the end of the fire.

3.6.7.3. *Axial forces at the edge beam*

The obtained diagrams of axial force in the edge beam, measured at different time of fire during the cases of travelling fire are presented in Figure 3.46.

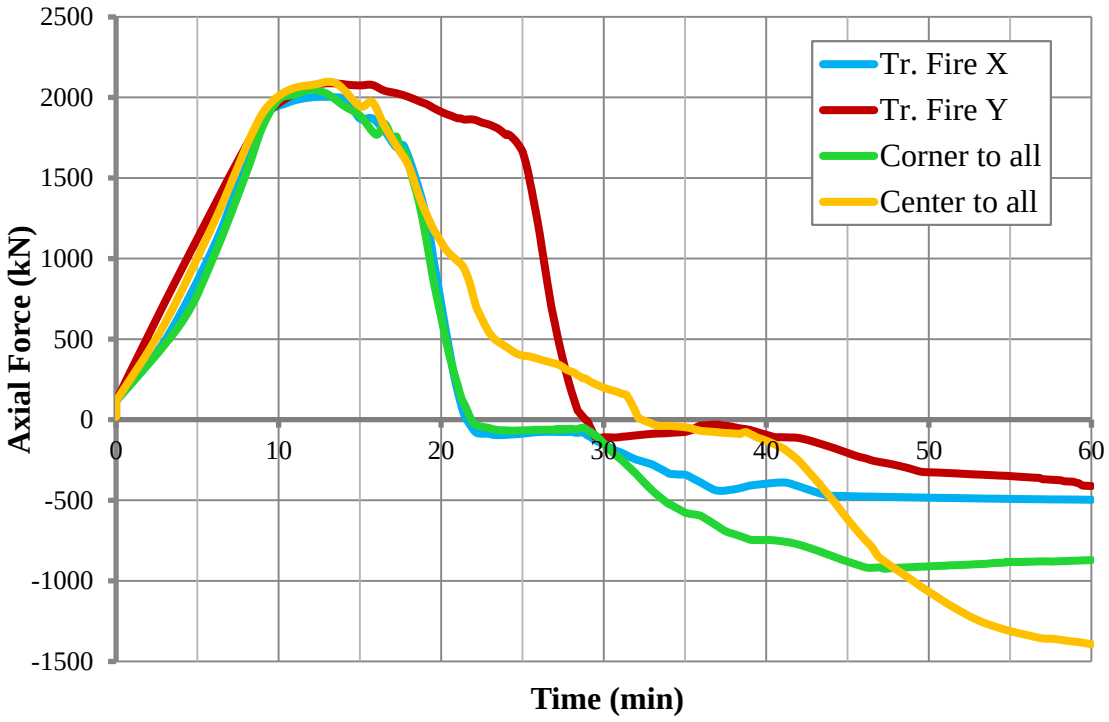

Figure 3.46. Axial force at the edge of the beam during travelling fire cases

As it is observed in all the cases of travelling fire, the initial values of horizontal reactions in the support are in compression and the rising parts of the curves look the same in all cases. With the increase of the temperatures, this support force lowers due to steel expansion, deflection of the beam and stiffness reduction. For fire travelling in Y direction, this decrease starts later in time in comparison with other fire scenarios. Characteristic for all the cases is that when the values of axial force reach negative value (tension), a flat plateau continues in each case (about 8 minutes) and then the values start decreasing again due to decrease of the temperature. This constant plateau occurs faster in time when the edge beam is situated is the first field (like fire travelling in X direction or from corner to all structure). When the plateau stops and tension grows in the section, the law of changing is different for each scenario and the residual value of axial force is diverse for each case. As a conclusion, each of spreading fire scenarios presents different way of axial force distribution during the time of fire so all cases must be taken into account to determine the most unfavourable travelling fire scenario.

Figure 3.47 presents the axial force at the edge element of the beam for three thermal loading cases: EN standard temperature-time curve, EN parametric curve and the case of fire spreading from the corner of the compartment to the entire structure.

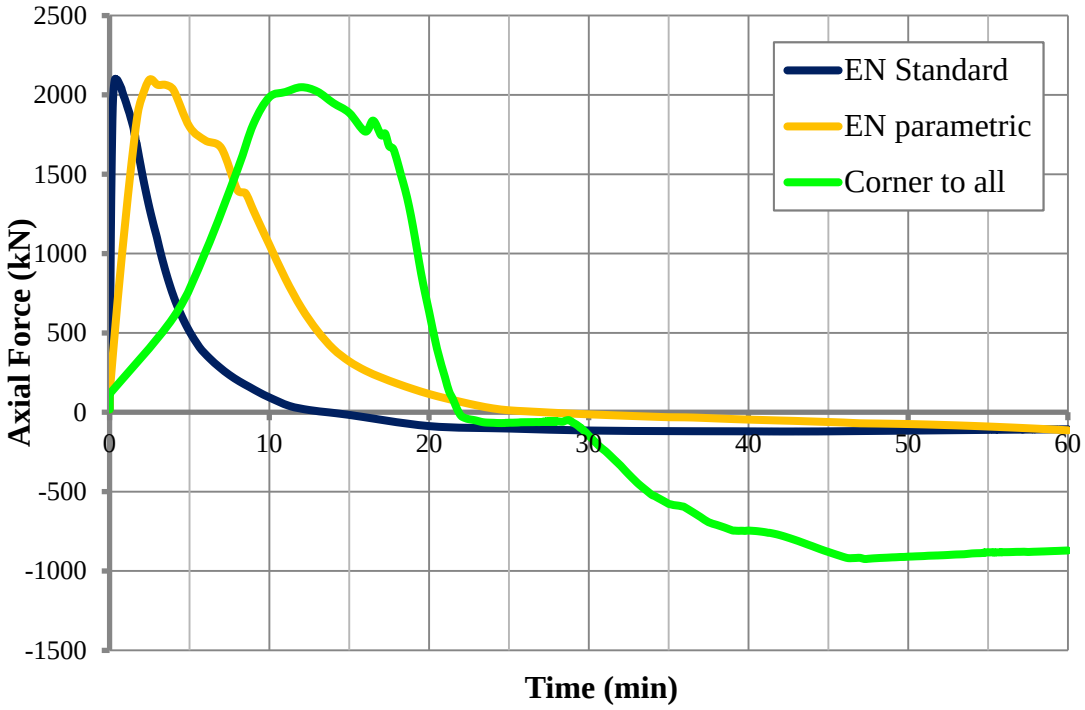

Figure 3.47. Axial force at the edge of the beam during different fire models

As it can be noticed from the graphs, axial force has different distribution along time for these different fire scenarios. For EN standard fire model, axial force reaches immediately top compression value due to fast increase of the temperature and then the value slows despite the temperature continues to increase. This decrease of value occurs because of steel expansion, deflection and stiffness reduction. Similar behaviour is noticed also for EN parametric fire curve; top value of axial force is reached in a later time because of the curve function and then the decrease starts to happen. The cooling phase of this curve is very moderate and slow, thus the residual value of axial force is approximately the same as for standard fire. The axial force distribution along time during travelling fire is more different. Firstly, the peak value is reached around minute 10 due to slow growth phase in comparison with other models and then it starts to decrease. Secondly, after the force reaches negative value, it continues constant for some minutes and then starts to decrease again due to the temperature decrease. Residual value of axial force during travelling fire has a significant value in comparison with other models prescribed in Eurocode.

3.7. Case study 2 – composite beams

In this case, shear connectors have been applied in the structure to make interaction between steel beams and concrete slab in order to model composite beams. The results of the analysis are compared with the results of previous case to determine the difference between steel and composite beams in elevated temperatures. In Table 3.3 all the analyses performed for flame exposure period of 60 min are listed. Two different thermal loadings have been applied; EN parametric fire curve and travelling fire case according X direction.

Name	Material model	Load [kN/m^2]	Heating regime		Beam-slab connectors
Str_2b	EC3, EC4	5	EN 1991-1-2	Parametric fire curve	Yes
Str_3b	EC3, EC4	5	Travelling fire curve	Spread in X-direction	Yes

Table 3.3. Table list of performed analysis for composite beams

Results of the analysis for vertical displacement at ¼ and ½ length of the primary beam in the axis 2 (node 137 and 287) in different times of fire are given in the subparagraphs below. Afterwards, comparison of the results has been done with previous case analysis where steel beams have been used.

3.7.1. EN parametric fire curve

In the model of the structure, shear connectors are inserted in both primary and secondary beams to achieve interaction between steel beams and concrete slab. The EN parametric curve applied is the same as described in the paragraph 3.5.2. The results of the analysis for deflections of the primary beam for EN parametric fire curve using shear connectors are given in Figure 3.48.

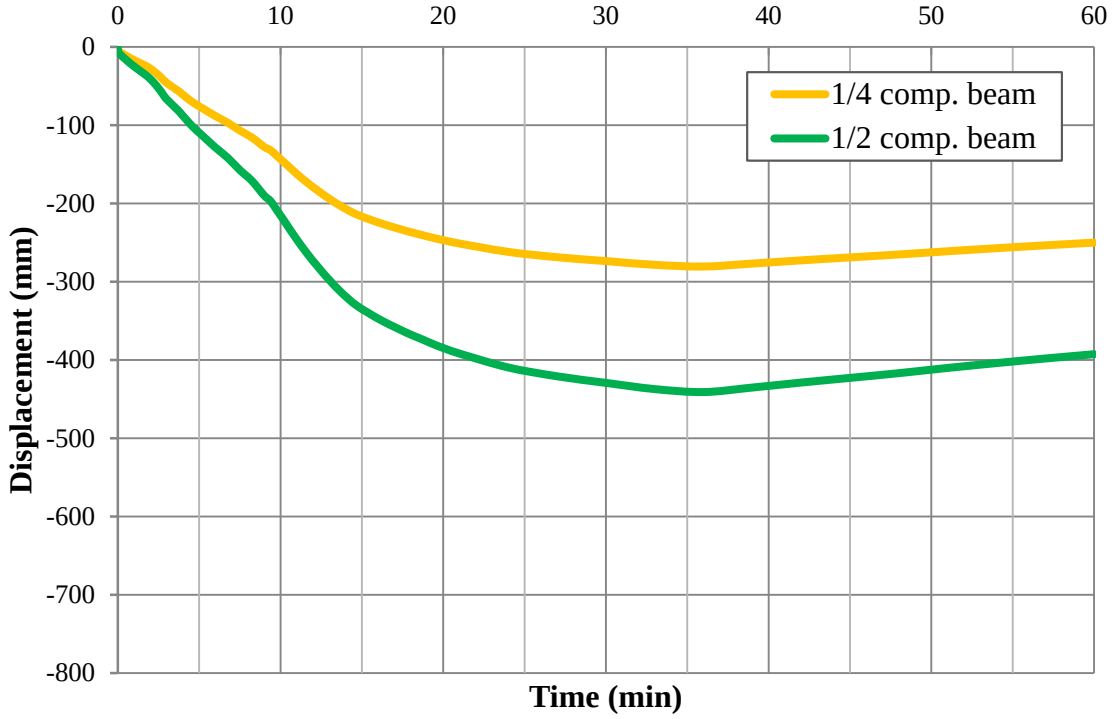

Figure 3.48. Deflection of the beam on axis 2 (Str-2b)

3.7.2. Travelling fire curve in X direction

The results of the analysis for deflections of the composite beam for fire spreading in X direction are given in Figure 3.49.

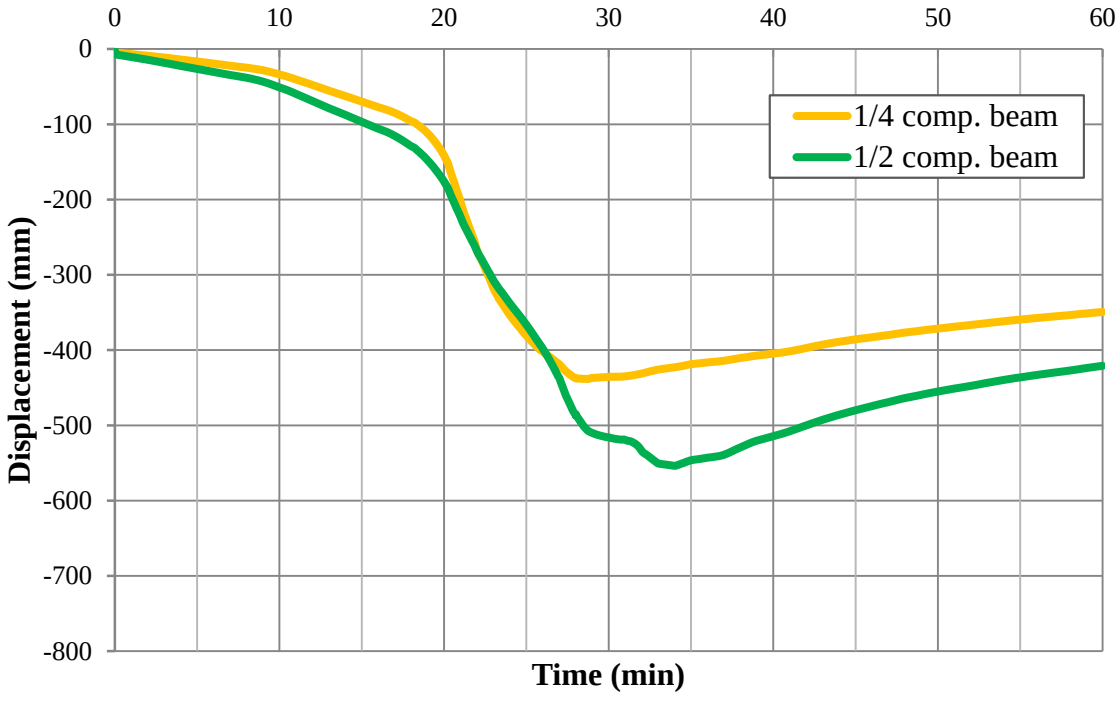

Figure 3.49. Deflection of the beam on axis 2 (Str-3b)

3.7.3. Comparison of results

Comparisons of the deflections for steel and composite beam when applying EN parametric and travelling fire curve are given respectively in Figure 3.50 and 3.51.

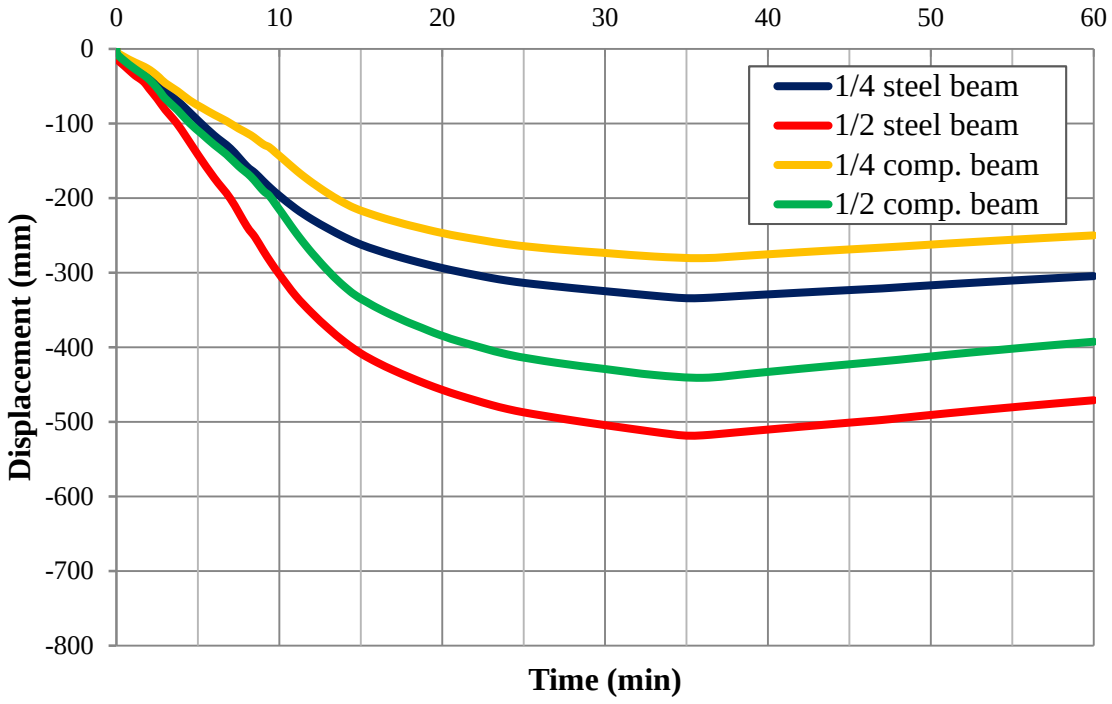

Figure 3.50. Deflection of steel and composite beam during EN parametric heating

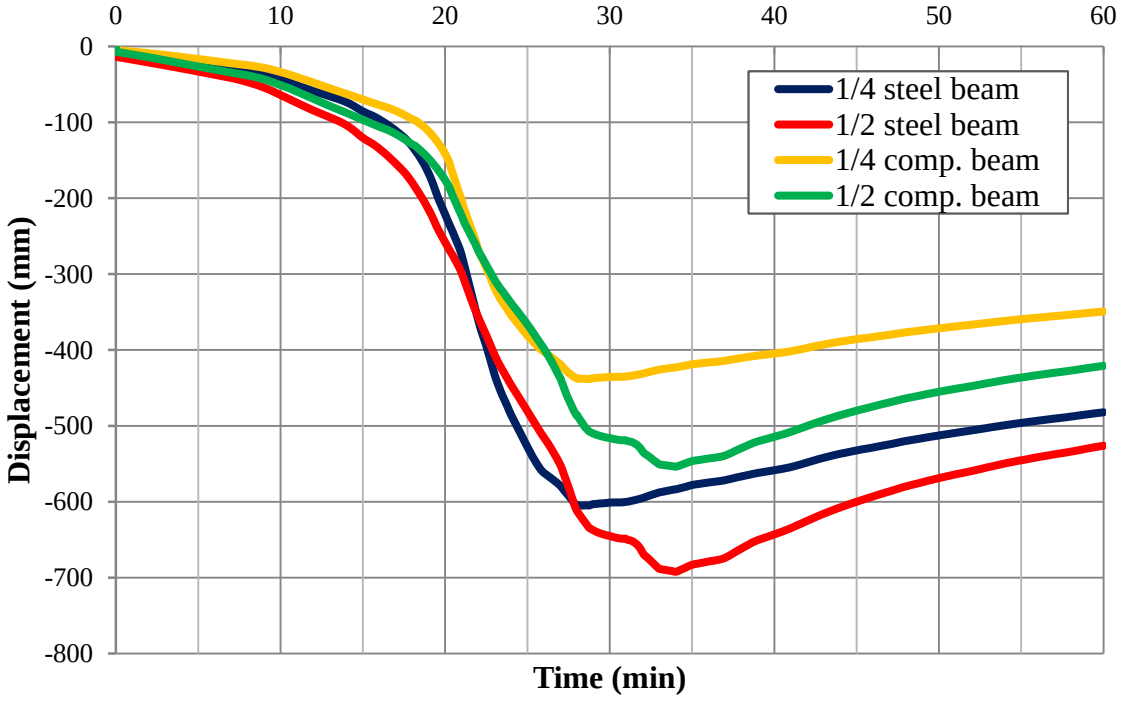

Figure 3.51. Deflection of steel and composite beam during travelling fire in X direction

As it is expected, the deflections in the structure with composite beams are smaller than the structure with steel beams in all fire models. From the comparison of deformation during parametric fire curve it can be observed that the ratio between the deflections of two structures tends to be constant throughout the duration of the fire. Also this ratio remains the same for the two points of the beam, at quarter of the length and at midpoint of the beam. In this structure, deflections in steel beam are about 20% higher than in the composite one.

When applying travelling fire in X direction, deflections of the composite beam at the first minutes of fire do not differ significantly from those of steel beam. Until 15 min their values have less than 20% of difference. With increase of the temperatures, differences between steel and composite beams start to be more significant. The peak deflection in the mid-span of composite beam is 25% smaller in comparison with steel beam. The difference can be noticed more in the $1/4^{th}$ of the beam length when the maximum deflections of this point differ approximately 38% between two models. In the case of structure with composite beams, the difference of residual deflections between these points is bigger comparing with steel beams. It can be concluded that the behaviour of the structure with composite beams is more complex during travelling fire so this method should be taken into account especially for this type of structures to determine a better response of the elements.

4. CONCLUSIONS AND FUTURE WORKS

4.1. Conclusions and final recommendations

To reach the objectives of this thesis, a simple structure was modelled in the software Vulcan. Standard and parametric fire models prescribed in Eurocode and different possible scenarios of spreading fire have been applied as thermal loads. Travelling fire curves have been built by applying iBMB parametric fire curve to each of the divided compartment fields. Essential results of mechanical behaviour of steel and composite steel-concrete beam have been observed through comparison with fire models described in Eurocode and through different models of travelling fire.

Results of the analysis show that the thermal load using travelling fire gives the most unfavourable conditions on the structure; during this case the structure has the maximum value of deflection in comparison with parametric fire prescribed in Eurocode. On the other hand, by applying traditional models deflection starts directly with rapid increase even in the first minutes of fire. Hence, traditional models are recommended to be used in case of fire resistance requested for a short time (e.g. R15).

Differences have been noticed between travelling fire models with different direction of flame spread. When the fire is travelling parallel to the beam, the maximum value of deflection is noticed but this is registered in a later time in comparison with other cases. When the fire is travelling perpendicular to the beam, peak value of deflection is not always measured in the middle of the beam but in different points along the beam length. During this case, the deflection of the beam has not the classic symmetrical shape with maximum value in the middle but it is irregular and peak deflection is not always in the mid-span during duration of fire.

Application of travelling fire gives important results regarding axial force which develops in the element during fire. At the support of the beams, the residual axial force has a significant tension value due to fast cooling phase while in other models of Eurocode the residual value of axial force in supports is negligible. These residual forces and stresses are very important when the structure is reconstructed after fire and travelling fire scenarios give higher values for them.

Travelling fire models also lead to interesting conclusions regarding comparison of steel or steel-concrete composite beams. When applying parametric curve, the ratio of deflections between the two types of beams stays approximately the same during the entire duration of fire and in different parts of the beam. When applying travelling fire, the ratio of deflections between steel and composite beam is bigger and it changes significantly with time and with location in the beam.

To summary all findings, travelling fire models are recommended to be implemented in design codes and used by structural engineers as these models examine a more realistic structural response and they show the most unfavourable results in comparison with models prescribed in design codes. All possible directions of travelling fire must be taken into account from engineers to ensure better structural safety.

4.2. Future works

This master thesis studied mechanical behaviour of different beams during multiple Eurocode models and travelling fire scenarios. Further studies may include the effect of spreading flames in other structural elements of the building like columns, slabs and connections in order to have a better understanding of the structure as a whole. Also inclusion of other common building materials like reinforced concrete would give a full view of the impact of spreading fire on structures.

This interesting topic should be undertaken to next studies which will verify it with the help of real experimental tests. Following experimental research, travelling fire models may be developed and validated, in order to perform parametrical studies for structures with different geometrical and material arrangements.

For each travelling fire case used, the compartment has been divided in three temperature fields. This number is chosen randomly to obtain results of the analysis in shorter time. It would be interesting to compare the results of the analysis if the compartment would be divided in higher number of fields and with the help of some real scale experiment, to determine the maximum size of the field where homogenous temperature can be applied.

The implemented travelling fire model is suitable for fire spreading in linear horizontal direction. From this on, studies must be enlarged to find suitable analytical curves which cover a wider range of possible spreads of fire including linear and radial in order to consider all potential scenarios of fire.

Furthermore, Eurocode standards, especially fire structural design parts are in continuous modification and improvement. The results of the studies can be suggested for implementation in Eurocode standards in order to apply to the structures a thermal load that is closer to the reality and to have an exact estimation of mechanical behaviour of the structure.

5. BIBLIOGRAPHY

[1] K. Horová, "Modelling of fire spread in structural fire engineering," Ph.D. Thesis, CTU in Prague, Prague, 2014.

[2] W. D. Walton and P. H. Thomas, "Estimating Temperatures in Compartment Fires (Chapter 3-6)," in *SFPE Handbook of Fire Protection Engineering, 4th edition*, 2008.

[3] J. A. Purkiss, Fire Safety Engineering: Design of Structures, Butterworth-Heinemann Ltd., 2nd edition, 2007.

[4] E. Hartin, "Fire Development and Fire Behavior Indicators," 2008. [Online]. Available: www.cfbt-us.com/pdfs/FBIandFireDevelopment.pdf.

[5] M. Gillie, "Heat Transfer in Structures - Lecture," 2008. [Online]. Available: http://civil.iisc.ernet.in/~manohar/Fire/Part-22_heatrannotes.pdf.

[6] K. A. Collette, "Comparisons of Structural Designs in Fire," M.Sc. Thesis, Worcester Polytechnic Institute, 2007.

[7] A. H. Buchanan, Structural Design for Fire Safety, Wiley, 1st edition, 2001.

[8] ASTM International, ASTM E119-12a, Standard Test Methods for Fire Tests of Building Construction and Materials, West Conshohocken, PA, 2012.

[9] International Standards Organisation, ISO 834-1: 1999, Fire-resistance tests - Elements of building construction - Part 1: General requirements, BSI, 1999.

[10] European Comittee for Standardization, EN 1991-1-2: Eurocode 1: Actions on structures - Part 1-2: General actions - Actions on structures exposed to fire, CEN Brussels, 2002.

[11] C. Bailey, "One Stop Shop in Structural Fire Engineering, University of Manchester," [Online]. Available: http://www.mace.manchester.ac.uk/.

[12] R. Zaharia, "Fire and mechanical loading - SUSCOS Lecture," 2014. [Online]. Available: http://www.ct.upt.ro/suscos/files/2013-2015/2C10/L2%20-%20Fire%20and%20mechanical%20loading.pdf.

[13] J. Zehfuss and D. Hosser, "A parametric natural fire model for the structural fire design of multi-storey buildings," *Fire Safety Journal*, vol. 42, p. 115–126, 2007.

[14] C. R. Barnett and G. C. Clifton, "Examples of fire engineering design for steel members, using a standard curve versus a new parametric curve," *Fire and Materials*, 2004.

[15] J.-M. Franssen, V. Kodur and R. Zaharia, Designing Steel Structures for Fire Safety, CRC Press, 2009.

[16] W. D. Walton and P. H. Thomas, "Estimating Temperatures in Compartment Fires," in *SFPE Handbook of Fire Protection Engineering*, Massachusetts, USA, National Fire Protection Association, 1995.

[17] T. Z. Harmathy and R. J. Mehaffey, "Post-flashover Compartment Fires," *Fire and Materials*, vol. 7, no. 2, pp. 49-61, 1983.

[18] J. Thiyagarajan, J. Vengadesan and S. Padmanathan, "Computational Fluid Dynamics in Fire and Life Safety," in *Advances in Mechanical Engineering*, New Dehli, Allied Publishers, 2010, pp. 242-247.

[19] B. Karlsson and J. G. Quintiere, Enclosure Fire Dynamics, CRC Press, 1999.

[20] Y. Wang, I. Burgess, F. Wald and M. Gillie, Performance-Based Fire Engineering of Structures, CRC Press, 2013.

[21] J. Stern-Gottfried and G. Rein, "Travelling fires for structural design–Part I: Literature review," *Fire Safety Journal*, vol. 54, p. 74–85, 2012.

[22] A. H. Majdalani and J. L. Torero, "Compartment Fire Analysis for Modern Infrastructure," in *1st Congresso Ibero-Latino-Americano sobre Segurança contra Incêndio*, Natal, Brasil, 2011.

[23] K. Horová and F. Wald, "Teplotní odezva ocelových a spřažených konstrukcí vystavených požáru," *CIDEAS Integrovaný návrh při mimořádných situacích,* 2011.

[24] A. M. Jonsdottir, J. Stern-Gottfried and G. Rein, "Comparison of Steel Temperatures using Travelling Fires and Traditional Methods: the Case Study of the Informatics Forum Building," in *Proceedings of the 12th International Interflam Conference*, Nottingham, UK, 2011.

[25] C. G. Bailey, I. W. Burgess and R. J. Plank, "Analyses of the effects of cooling and fire spread on steel-framed buildings," *Fire Safery Journal 26*, p. 273–293, 1996.

[26] E. Ellobody and C. G. Bailey, "Structural performance of a post-tensioned concrete floor during horizontally travelling fires," *Engineering Structures*, vol. 33, no. 6, p. 1908–1917, 2011.

[27] A. Law, J. Stern-Gottfried, M. Gillie and G. Rein, "The influence of travelling fires on a concrete frame," *Engineering Structures*, vol. 33, no. 5, p. 1635–1642, 2011.

[28] European Comittee for Standardization, EN 1992-1-2: Eurocode 2: Design of concrete structures - Part 1-2: General rules - Structural fire design, CEN Brussels, 2004.

[29] European Comittee for Standardization, EN 1993-1-2: Eurocode 3: Design of steel structures - Part 1-2: General rules - Structural fire design, CEN Brussels, 2005.

[30] P. Shepherd, "The performance in fire of restrained columns in steel-framed constrictions," Ph.D. Thesis, University of Sheffield, 1999.

[31] I. Burgess, R. Plank, M. Green, P. Shepherd and Z. Huang, Vulcan Solutions, [Online]. Available: http://www.vulcan-solutions.com/.

[32] P. Shepherd and Z. Huang, "Vulcan rewriting and re-validation," University of Sheffield, 2003 - 2004.

[33] F. Wald, I. Burgess, L. Kwasniewski, K. Horová and E. Caldová, Benchmark studies - Verification of numerical models in fire engineering, Prague: CTU - Publishing House, March 2014.